Simulated Water Sources and Effects of Pumping on Surface and Ground Water, Sagamore and Monomoy Flow Lenses, Cape Cod, Massachusetts

By Donald A. Walter and Ann T. Whealan

In cooperation with the Massachusetts Department of Environmental Protection
Drinking Water Program

Scientific Investigations Report 2004-5181

U.S. Department of the Interior
U.S. Geological Survey

U.S. Department of the Interior
Gale A. Norton, Secretary

U.S. Geological Survey
Charles G. Groat, Director

U.S. Geological Survey, Reston, Virginia: 2005
For sale by U.S. Geological Survey, Information Services
Box 25286, Denver Federal Center
Denver, CO 80225

For more information about the USGS and its products:
Telephone: 1-888-ASK-USGS
World Wide Web: http://www.usgs.gov/

Suggested citation:
Walter, D.A., and Whealan, A.T., 2005, Simulated Water Sources and Effects of Pumping on Surface and Ground Water, Sagamore and Monomoy Flow Lenses, Cape Cod, Massachusetts: U.S. Geological Survey Scientific Investigations Report 2004-5181, 85 p.

Contents

Figures

Tables

CONVERSION FACTORS, DATUMS, AND ABBREVIATIONS

Multiply	By	To obtain
cubic foot per second (ft^3/s)	0.02832	cubic meter per second (m^3/s)
foot (ft)	0.3048	meter (m)
foot per day (ft/d)	0.3048	meter per day (m/d)
foot squared per day (ft^2/d)	0.0929	meter squared per day (m^2/d)
inch (in.)	25.4	millimeter (mm)
inch per year (in/yr)	25.4	millimeter per year (mm/yr)
mile (mi)	1.609	kilometer (km)
million gallons per day (Mgal/d)	0.04381	cubic meter per second (m^3/s)
square mile (mi^2)	2.590	square kilometer (km^2)

Vertical cooordinate information is referenced to the National Geodetic Vertical Datum of 1929 (NGVD 29). Horizontal coordinate information is referenced to the North American Datum of 1927 (NAD 27).

AFCEE	Air Force Center for Environmental Excellence
APCC	Association for the Preservation of Cape Cod
CCC	Cape Cod Commission
IRP	Installation Restoration Program
MDCR	Massachusetts Department of Conservation and Recreation
MDEP	Massachusetts Department of Environmental Protection
MMR	Massachusetts Military Reservation
NGB	National Guard Bureau
USGS	U.S. Geological Survey

Simulated Water Sources and Effects of Pumping on Surface and Ground Water, Sagamore and Monomoy Flow Lenses, Cape Cod, Massachusetts

By Donald A. Walter and Ann T. Whealan

Abstract

The sandy sediments underlying Cape Cod, Massachusetts, compose an important aquifer that is the sole source of water for a region undergoing rapid development. Population increases and urbanization on Cape Cod lead to two primary environmental effects that relate directly to water supply: (1) adverse effects of land use on the quality of water in the aquifer and (2) increases in pumping that can adversely affect environmentally sensitive surface waters, such as ponds and streams. These considerations are particularly important on the Sagamore and Monomoy flow lenses, which underlie the largest and most populous areas on Cape Cod.

Numerical models of the two flow lenses were developed to simulate ground-water-flow conditions in the aquifer and to (1) delineate areas at the water table contributing water to wells and (2) estimate the effects of pumping and natural changes in recharge on surface waters. About 350 million gallons per day (Mgal/d) of water recharges the aquifer at the water table in this area; most water (about 65 percent) discharges at the coast and most of the remaining water (about 28 percent) discharges into streams. A total of about 24.9 Mgal/d, or about 7 percent, of water in the aquifer is withdrawn for water supply; most pumped water is returned to the hydrologic system as return flow creating a state of near mass balance in the aquifer. Areas at the water table that contribute water directly to production wells total about 17 square miles; some water (about 10 percent) pumped from the wells flows through ponds prior to reaching the wells. Current (2003) steady-state pumping reduces simulated ground-water levels in some areas by more than 4 feet; projected (2020) pumping may reduce water levels by an additional 3 feet or more in these same areas. Current (2003) and future (2020) pumping reduces total streamflow by about 4 and 9 cubic feet per second (ft^3/s), corresponding to about 5 percent and 9 percent, respectively, of total streamflow.

Natural recharge varies with time, over both monthly and multiyear time scales. Monthly changes in recharge cause pond levels to vary between 1 and 2 feet in an average year; annual changes in recharge, which can be much larger than monthly variations, can cause pond levels to vary by more than 10 feet in some areas over a period of years. Streamflow, which also changes in response to changes in recharge, varies by a factor of two over an average year and can vary more over multiyear periods. On average, monthly pumping ranges from 15.8 Mgal/d in March to 45.3 Mgal/d in August. Pumping and the distribution of return flow can seasonally affect the hydrologic system by lowering ground-water and pond levels and by depleting streamflows, particularly in the summer months. Maximum drawdowns in March and August exceed 3 feet and 6 feet, respectively, for current (2003) pumping. Simulated drawdowns from projected (2020) pumping, relative to water levels representing 2003 pumping conditions, exceed 2 feet in March and 5 feet in August. Current (2003) and future (2020) pumping can decrease pond levels in some areas by more than 3 feet; drawdown generally is largest during the month of August of an average year. Over multiyear periods, seasonal pumping can lower pond levels in some areas by more than 4 feet; the effects of seasonal pumping are largest during periods of reduced recharge. Monthly streamflow depletion varies in individual streams but can exceed 2 ft^3/s in some streams.

The combined effects of seasonal pumping and drought can reduce pond levels by more than 10 feet below average levels. Water levels in Mary Dunn Pond, which is in an area of large current and projected pumping, are predicted (2020) to decline during drought conditions by about 10.6 feet: about 6.9 feet from lower recharge, about 2.3 feet from current (2003) pumping, and about 1.4 feet from additional future (2020) pumping. The results indicate that pumping generally does not cause substantial streamflow depletion and that the primary effect of pumping is on water levels in ponds. Natural changes in recharge account for most of the variation in pond levels; however, pumping can cause substantial declines in the levels of ponds near pumping wells. Also, the effects of pumping and recharge can combine to cause drawdowns of more than 10 feet in some areas.

Introduction

The sand and gravel sediments underlying Cape Cod, Massachusetts (fig. 1), compose a shallow, unconfined aquifer that is the sole source of water to local communities. The year-round population of Cape Cod more than doubled between 1970 and 2000 and the population of some areas on Cape Cod has increased by more than 70 percent since 1990. The population of Cape Cod changes seasonally, increasing by nearly 300 percent during the summer months. The Sagamore and Monomoy flow lenses (fig. 1) underlie most of the population of Cape Cod. These flow lenses are the largest of the six flow lenses within the Cape Cod aquifer system; these two flow lenses compose the area of investigation for this study. Regional population increases have increased the demand for potable water and, as a result, pumping from the Cape Cod aquifer system has increased.

Urbanization and development have resulted in changes in land-use patterns on Cape Cod. There are concerns regarding ground-water contamination originating from both nonpoint sources, such as septic-system return flow, and point sources, such as municipal waste-disposal facilities (WDFs) and contaminant sources on the Massachusetts Military Reservation (MMR) and elsewhere (fig. 1). Large increases in the demand for potable water coupled with the effects of human activities on ground-water quality make it important to delineate areas contributing recharge to existing water supplies and to identify potential source areas for future water supplies.

Pumping has local effects on ponds and streams, which are important recreational and ecological resources on Cape Cod. Pumping can have adverse effects on surface-water resources by lowering pond levels, drying vernal pools, and depleting streamflow. Ponds and vernal pools are important ecosystems and minimum streamflows are needed to support fish populations. These effects vary seasonally and are larger in the summer months when demand for water supply is higher and areal recharge to the aquifer system is lower than in winter months.

In 2001, the U.S. Geological Survey (USGS), in cooperation with the Massachusetts Department of Environmental Protection (MDEP), began an investigation into the water resources of the Sagamore and Monomoy flow lenses. Specifically, the objectives of the investigation were to (1) delineate areas contributing recharge to present and possible future production wells, (2) determine the effects of current (2003) and future (2020) pumping on long-term average pond levels and streamflows, 3) determine the effects of natural changes in recharge over monthly and yearly time scales on ponds and streams, and 4) determine the effects of transient pumping stresses on the hydrologic system.

As part of the source-approval process, MDEP currently requires water suppliers to establish source-protection areas for new sources. These analyses often are done independently and can lead to estimated source-protection areas that are not hydrologically consistent from well to well. In addition, local analyses for individual wells often do not account for the effects of pumping in other areas on local hydraulic gradients. The recharge areas determined as part of the USGS investigation were developed by using regional ground-water-flow models and represent the area at the water table that contributes recharged water to a pumping well for a specified pumping and recharge rate. The source-protection areas used by MDEP for source approval (Massachusetts Department of Environmental Protection, 2004) generally are not based on a mass-balance hydrologic analysis and are larger than the recharge areas presented in this report. Although not based on a rigorous hydrologic analysis, the larger MDEP source areas do represent a qualitative margin of uncertainty and are considered by MDEP as the best approach to prudent source-area protection.

Purpose and Scope

This report documents regional ground-water flow models of the Sagamore and Monomoy flow lenses that were used to evaluate water resources of the region. The areas contributing recharge to existing and future production wells are presented for both current (2003) and future (2020) pumping conditions. The long-term-average effects of these pumping conditions on the hydrologic system also are presented. In addition, the report presents analyses of the potential effects of ground-water pumping on surface-water resources under conditions of time-varying recharge and pumping. Analyses of the effects of recharge and pumping changes are presented for two different time scales: (1) average monthly changes and (2) long-term (multiyear) changes in recharge with seasonal changes in pumping.

Methods of Analyses

The evaluation of the water resources of the Sagamore and Monomoy flow lenses included data-collection efforts, the development and calibration of numerical flow models, and the use of those models to address specific questions regarding the ground-water flow in the aquifers and the response of the hydrologic system to changing hydrologic stresses. The results, conclusions, and limitations discussed in this report are based on the results of modeling analyses.

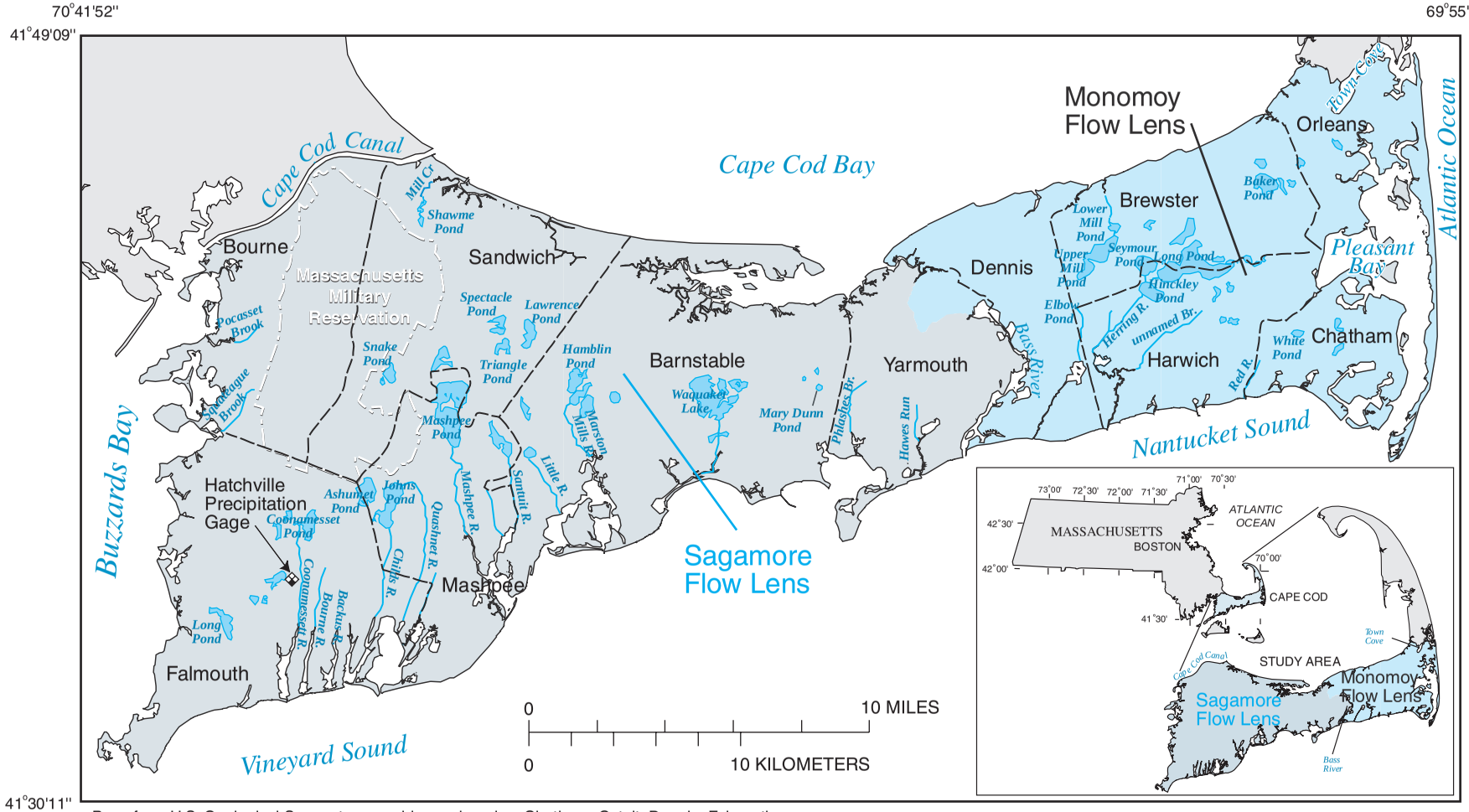

Base from U.S. Geological Survey topographic quadrangles, Chatham, Cotuit, Dennis, Falmouth, Harwich, Hyannis, Onset, Orleans, Pocasset, Sagamore, Sandwich, and Woods Hole, Massachusetts, Universal Transverse Mercator grid, Polyconic projection, zone 19 NAD, 1:25,000

EXPLANATION

- SAGAMORE FLOW LENS
- MONOMOY FLOW LENS
- TOWN BOUNDARY
- PRECIPITATION GAGE

Figure 1. Location of Sagamore and Monomoy flow lenses, Cape Cod, Massachusetts.

Data Collection

Four types of data were collected or compiled as part of this investigation: (1) lithologic data regarding sediment characteristics, (2) hydrologic data consisting of precipitation records, historical water levels in wells and ponds, and streamflows, (3) water-use data from local water suppliers, and (4) spatial land-use data. In addition, information from previous investigations from Cape Cod and from areas with similar hydrogeologic settings was reviewed and compiled. These data were incorporated into numerical ground-water models of the Sagamore and Monomoy flow lenses. Details regarding the compilation and collection of data are presented in the appendix of this report.

Numerical Models

The models were calibrated by using available and newly collected hydrologic data. Models were developed that simulate long-term average conditions in the aquifer system underlying the Sagamore and Monomoy flow lenses (steady-state simulations), under the assumptions of constant recharge and pumping; separate models were developed for each flow lens. Transient models also were developed for each flow lens to simulate hydrologic conditions resulting from changes in recharge and pumping stresses over monthly and multiyear time scales (transient simulations). The models were developed by using the U.S. Geological Survey's modeling software MODFLOW-2000 (Harbaugh and others, 2000). The development and calibration of the numerical models are documented in detail in the appendix of this report.

Limitations of Analyses

The use of numerical models to simulate the hydrologic systems of the Sagamore and Monomoy flow lenses has inherent limitations; however, proper design and calibration of the flow models can minimize these limitations. Differences between simulated and actual hydrologic conditions arise from a number of sources and are collectively known as model error. One component of model error relates to model discretization. Models represent a hydrologic system as a series of discrete spatial units, throughout which intrinsic properties and stresses are uniform. The use of a discretized model to represent a hydrologic system introduces some limitations, especially if model discretization is much larger than the hydrologic features being simulated; these limitations are minimized by designing models with the appropriate discretization for the hydrologic system. Transient models are further discretized into a series of discrete units of time, during which hydrologic stresses are constant. The use of discretized time introduces additional sources of model inaccuracy, which can be minimized by choosing appropriate temporal discretization to address the time scale of interest. Model errors also can arise from the numerical solution; these errors are minimized by ensuring that the model solution reaches a reasonable state of mass balance. An additional component of model error arises from how well model-input values represent the actual hydrologic system. The degree of model error is difficult to quantify; however, the capacity of a model simulation to provide a reasonable representation of the hydrologic system can be evaluated by comparing simulated hydrologic conditions with those observed in the field. Comparisons of simulated and observed hydrologic conditions are included in the appendix of the report.

Hydrogeology of the Sagamore and Monomoy Flow Lenses

The unconsolidated sediments underlying Cape Cod generally are sandy and were deposited by glacial meltwater during the Pleistocene Epoch. The aquifer receives all of its water from precipitation. Ground water leaves the system as discharge into freshwater and saltwater bodies and at wells.

Geologic History

The glacial sediments underlying Cape Cod were deposited by a retreating continental ice sheet during the Pleistocene Epoch, between 15,000 and 16,000 years ago (Oldale and Barlow, 1986). In the area of present-day Cape Cod, the ice sheet consisted of three separate lobes of ice: the Buzzards Bay, the Cape Cod Bay, and the South Channel ice lobes (fig. 2). The maximum extent of ice was to the south of Cape Cod, near present-day Martha's Vineyard and Nantucket (fig. 2). Sediment deposition occurred at or near the edges of these ice lobes through direct deposition from the ice and proglacial deposition from meltwater.

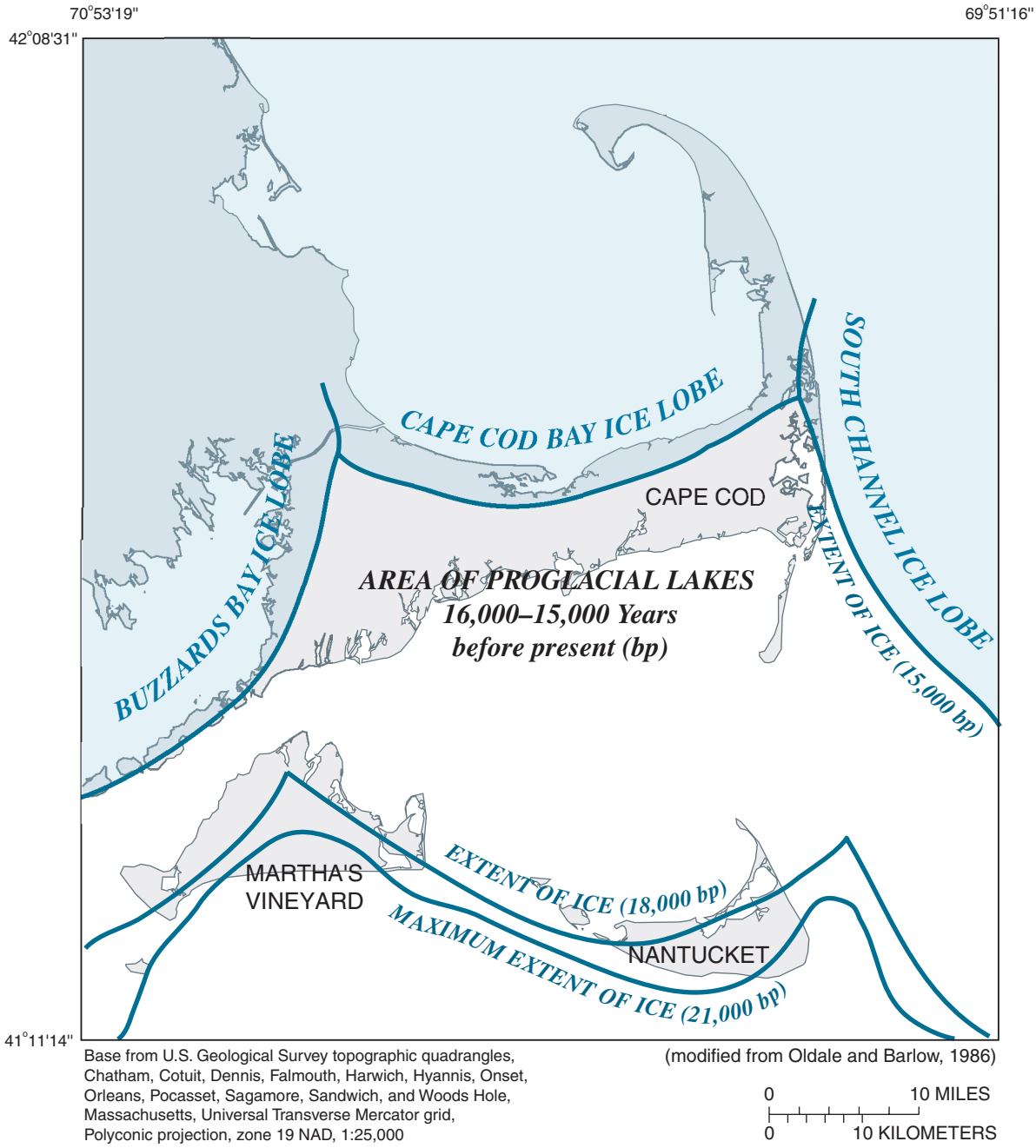

Figure 2. Location of continental ice sheets near present-day Cape Cod during the late Pleistocene, Massachusetts.

The surficial geology of western and central Cape Cod is characterized by broad, gently sloping glacial-outwash plains and hummocky terrain associated with glacial moraines (fig. 3). Different types of glacial deposits are present on Cape Cod. Moraines were deposited at or near the edges of the ice lobes. Moraines are either ablation moraines, such as the Buzzards Bay Moraine, that were deposited in place by melting ice; or tectonic moraines, such as the Sandwich Moraine, that consist of reworked outwash sediments pushed into place by local readvances of the ice lobes (Uchupi and others, 1996; Oldale, 1992; Oldale and O'Hara, 1984). Kames are ice-contact deposits that were deposited in high-energy meltwater environments within holes in the ice sheets. Ice-contact deposits also include sediments that were deposited by meltwater in high-energy fluvial environments near the ice margin. Outwash sediments, which compose most of the unconsolidated sediments underlying Cape Cod, were deposited by meltwater streams in depositional environments associated with pro-glacial lake deltas. The glacial sediments are underlain by basal till in most places; basal till, which can include sand, silt, and, clay, are generally compact, low-permeability sediments produced by mechanical erosion of bedrock during movement of the overlying ice sheet. The unconsolidated glacial sediments are underlain by crystalline bedrock that is much less permeable than the glacial sediments.

As the ice lobes retreated northward, glacial meltwater formed pro-glacial lakes that were dammed to the south by older moraine deposits near present-day Martha's Vineyard and Nantucket (fig. 2). Sediment originally entrained within the ice sheet was deposited in these lakes by meltwater streams, forming lacustrine deltas. Sediment sources generally were in interlobate areas of the ice sheet; these areas received most of the glacial meltwater and associated sediment because of elevation gradients on the surface and within the ice sheet. The different depositional environments within the deltas were analogous to environments observed in present-day deltas (Oldale, 1992; Uchupi and others, 1996). Deltaic sediments can be divided into three general facies: topset, foreset, and bottomset deposits (Masterson and others, 1997a).

Topset deposits are glaciofluvial sediments that were deposited by meltwater streams in high-energy environments above the water level of the lakes. Foreset and bottomset deposits are glaciolacustrine sediments that were deposited in the lakes. Foreset deposits were deposited in nearshore areas of the lakes proximal to a delta front under moderate-energy conditions; bottomset deposits were deposited in deeper, off-shore areas of the lake under low-energy conditions. Lake-bottom sediments underlie bottomset beds and were deposited in low-energy conditions. There is variability within each of set of depositional environments; low-energy depositional environments associated with inter-channel ponded areas likely developed within high-energy glaciofluvial environments, and high-energy depositional environments associated with subaqueous gravity flows likely developed within low-energy lacustrine environments. A number of deltaic systems underlie Cape Cod; each system is the result of proglacial sedimentation during different periods of time and different ice margin positions (Oldale and Barlow, 1986). As the deltaic sediments were deposited, the deltas prograded into their respective lakes. The result is a stratigraphy in which topset sediments overlie foreset sediments that, in turn, overlie bottomset deposits within each deltaic system (fig. 4*A*). Four separate deltaic units were deposited in the area of present-day central and western Cape Cod: the Buzzards Bay, Mashpee, the Barnstable, and the Harwich Plains (fig. 3).

The positions of the ice lobes as they retreated to the north determined the patterns of sedimentation observed in the present-day surficial geology of Cape Cod (B.D. Stone, U.S. Geological Survey, written commun., 2002). The general positions of the ice lobes during important periods of sediment deposition are illustrated in figure 3. The Buzzards Bay ice lobe retreated slowly during the period of regional sedimentation as compared to the Cape Cod Bay and South Channel ice lobes. This sequence of ice retreat created a number of different sediment sources and complex sedimentation patterns. The oldest glacial sediments on Cape Cod are the Nantucket Ice-Contact Deposits. These sediments, which are kame deposits along the southern shore of western Cape Cod (fig. 3), were deposited when the ice margin was near position 1 on figure 3 (B.D. Stone, U.S. Geological Survey, written commun., 2002). The next major period of sediment deposition formed the Falmouth Deposits; these ice-contact deposits were deposited when the ice lobes had retreated to near position 2. The deltaic sediments of the Mashpee Plain were deposited during a period when the ice lobes had retreated to near position 3. The source of the sediments was in an area between the Buzzards Bay and Sandwich Moraines, near the Cape Cod Canal (fig. 3). The Buzzards Bay and Sandwich Moraines were deposited near the ice margin during this same general period. Deltaic sediments of the Barnstable Plain were deposited next, when the ice margin was near position 4. The source for these sediments was located in north-central Cape Cod (fig. 3). Sediments of the Buzzards Bay Plain, part of which is found along the western shore of Cape Cod, likely were deposited after deposition of the sediments of the Barnstable Plain (Oldale and Barlow, 1996). The Harwich Plain likely has a more complex depositional history and may be derived from various different sediment sources (B.D. Stone, U.S. Geological Survey, written commun., 2002). The sediments were deposited when the ice sheets were retreating from near position 4 to near position 7 (fig. 3). The primary source for these sediments was near the intersection of the Cape Cod Bay and South Channel ice lobes in the northeast part of the Harwich Plain (fig. 3). Some older, secondary sediment sources were associated with the Dennis Ice-Contact Deposits, located along the northern boundary of the Harwich Plain (fig. 3). The outwash plains contain many glacial-collapse structures. These structures formed when buried blocks of remnant glacial ice melted and caused overlying sediments to collapse. Collapse structures form topographic depressions that can contain kettle-hole ponds.

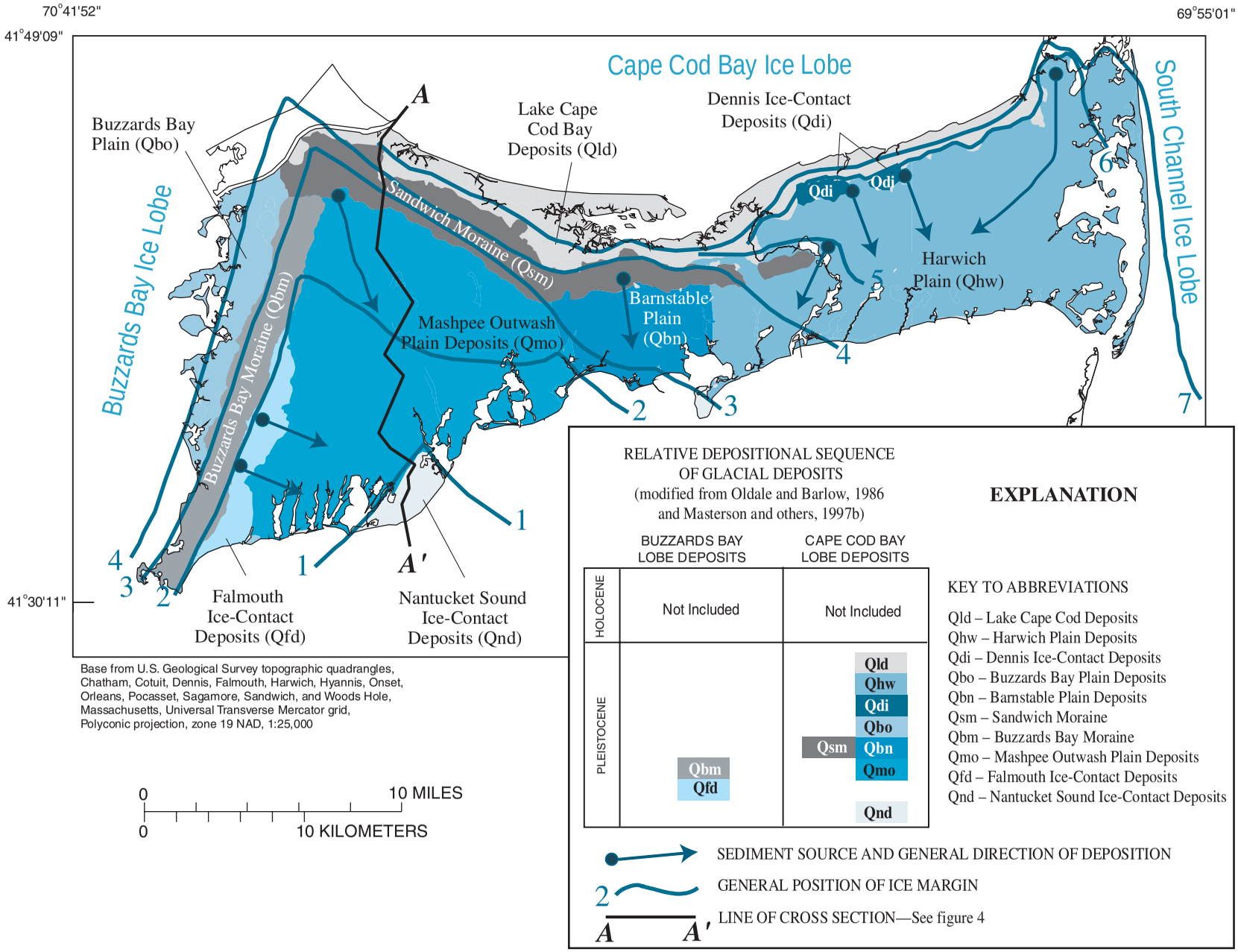

Figure 3. Surficial geology of western and central Cape Cod and location of glacial ice margins during the late Pleistocene, Massachusetts.

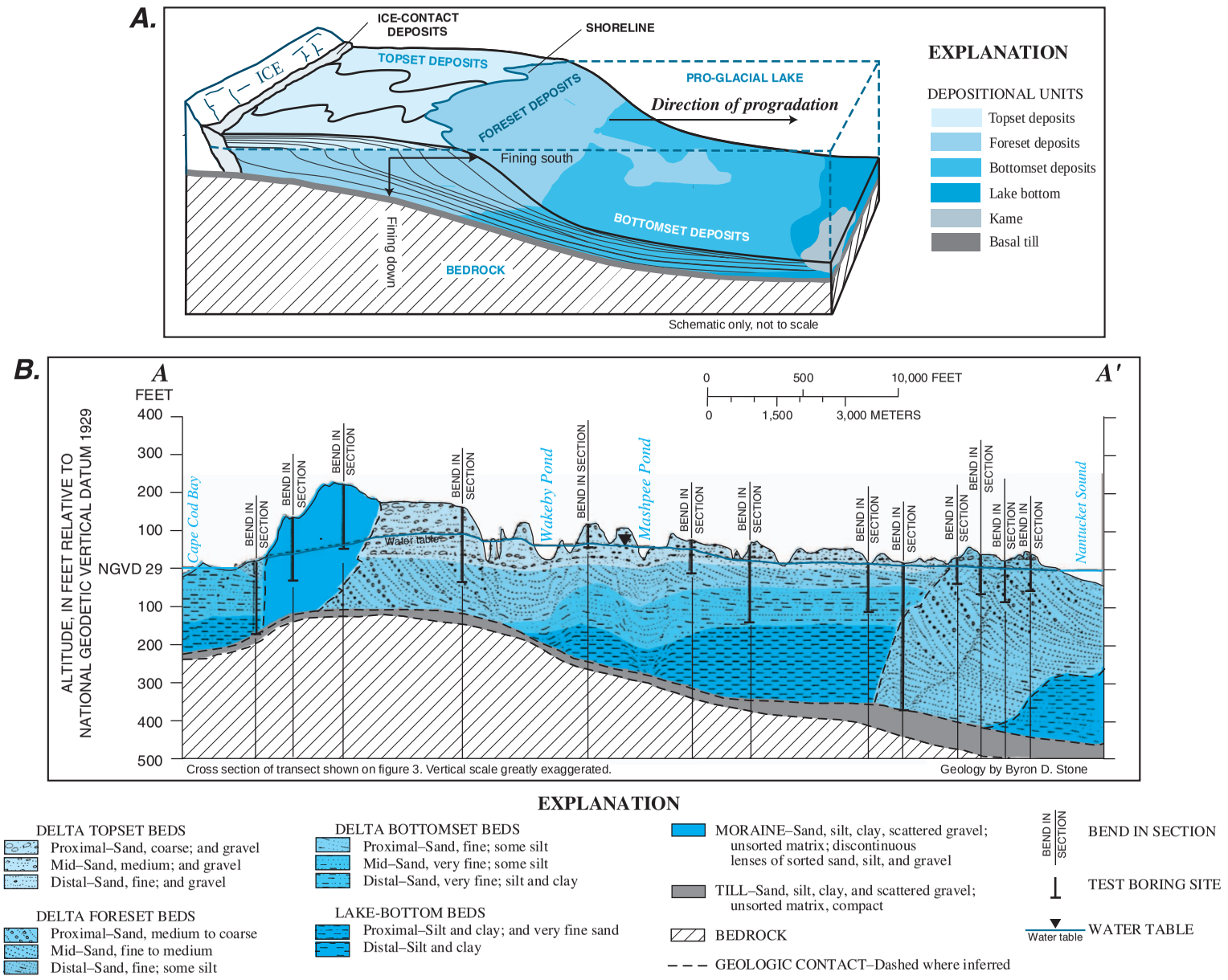

Figure 4. *A*, Depositional model for western Cape Cod; and *B*, geologic section along A–A′ (fig. 3) on western Cape Cod, Massachusetts. Modified from Masterson and others, 1997a and b.

The youngest sediments on Cape Cod are found along the shore of Cape Cod Bay (fig. 3). These sediments, which are characterized by sand, silt and clay, were deposited within Lake Cape Cod. This lake formed during a period when the ice sheet had retreated to an area north of Cape Cod (outside the area shown in figure 3). The sediments are part of distal foreset and proximal bottomset deposits that were deposited in low-energy, offshore areas of the lake.

Hydrogeologic Framework

The sediments underlying Cape Cod consist of gravel, sand, silt, and clay deposited in aqueous environments associated with Pleistocene continental glaciers. The lithology of the aquifer sediments varies according to the environment in which the sediments were deposited. The water-transmitting properties, which are related to the grain size and degree of sorting of the sediments, also vary within the aquifer.

The elevation of the bedrock surface on Cape Cod ranges from about 50 ft below NGVD 29 near the Cape Cod Canal to more than 900 ft below NGVD 29 beneath the outer part of Cape Cod; the bedrock surface beneath central and western Cape Cod is as deep as 500 ft below NGVD 29 along the shore of Nantucket Sound. The sequence of glacial deposits on central and western Cape Cod ranges in thickness from 70 ft near the Cape Cod Canal to more than 500 ft along Nantucket Sound. The lithology of the glacial sediments, which include moraines, kames and other ice-contact deposits, and stratified outwash, differs according to the environment in which the sediments were deposited.

The location of sediment sources and general directions of sediment transport for the outwash plains on central and western Cape Cod are shown in figure 3. Deltaic outwash sediments generally are characterized by two grain-size trends: (1) a downward fining trend in which grain sizes decrease and silt and clay content increases with depth and (2) a trend in which sediments become finer-grained, and coarse-grained sand and gravel deposits become thinner with increasing distance from the sediment sources. Topset deposits, which are the shallowest deltaic sediments underlying Cape Cod, generally are coarse-grained and consist primarily of cross-bedded medium to coarse sand and gravel. Foreset deposits underlie topset deposits and consist generally of fine to medium sand with little or no bedding. Bottomset deposits, which are the deepest deltaic sediments, generally are fine-grained and consist of fine sand, silt, and clay. The relative positions of deltaic facies within a proglacial lake delta are shown in figure 4*A*. The generalized relation of grain size within topset, foreset, and bottomset deposits along a north-south trending section of the Mashpee Plain is shown in figure 4*B*. Coarse-grained fluvial sediments generally extend deeper in the section in areas close to the sediment source and within collapse structures (fig. 4*B*). The lithology within topset, foreset, and bottomset deposits depends upon transport distance from the sediment source; proximal sediments deposited closer to the sediment sources generally are coarser grained than distal sediments deposited at greater distances from the sediment source. The contacts between depositional units typically are gradational because of the continuous nature of deposition within the deltas; as an example, the lithology of distal foreset deposits would be similar to the lithology of proximal bottomset deposits. Distal bottomset beds are underlain by lake-bottom deposits that consist of silt and clay (fig. 4). There is local variability within the general deltaic facies as well. Interbeds of fine sand and silt are observed within shallow, coarse-grained sediments, and lenses of sand and gravel occur within deep, fine-grained sediments; these sediments represent deposition in ponded areas within glaciofluvial environments and within subaqueous gravity flows within offshore lacustrine environments, respectively.

Moraine sediments were deposited in low-energy depositional environments and consist of gravel, sand, silt, and clay. Whereas outwash sediments generally are well sorted and show some stratigraphic continuity, moraine deposits have a more variable lithology and, generally, on a regional scale are finer-grained than outwash deposits. Ice-contact deposits and kame deposits are coarse-grained sediments that were deposited in high-energy meltwater environments. These deposits generally consist of well-sorted medium to coarse sand and gravel that is similar in lithologic character to coarse-grained outwash deposits. Moraines, kames, and ice-contact deposits also show grain-size trends similar to those seen in outwash sediments: fining with increasing depth and distance from the sediment source. Basal till is fine-grained, generally homogenous, and consists primarily of clay. The basal till is underlain by less permeable crystalline bedrock.

Grain size and degree of sorting determine the water-transmitting properties of aquifer sediments. The trends in hydraulic conductivity of outwash sediments are parallel to the trends in grain size; the hydraulic conductivity of sediments generally decreases with depth and with increasing distance from sediment sources, or generally southward (Masterson and others, 1997a). Previous investigations have identified general relations between sediment grain size and hydraulic conductivity, as determined from aquifer tests (Masterson and others, 1997a; Masterson and Barlow, 1997). Medium to coarse sand and gravel deposits, typical of fluvial topset deposits, have hydraulic conductivities that range from 200 to 350 ft/d. Fine to medium sand typical of foreset deposits has hydraulic conductivities typically ranging from 70 to 200 ft/d. The hydraulic conductivities of fine sand and silt, typical of distal foreset and proximal bottomset deposits, typically range from 30 to 70 ft/d; silt and clay typical of lake-bottom deposits have hydraulic conductivities ranging from 10 to 30 ft/d.

Ice-contact and kame deposits generally consist of medium to coarse sand and gravel and have hydraulic conductivities similar to those of coarse-grained outwash deposits. Moraine deposits have a variable lithology—ranging from gravel and sand to silt and clay—and generally have lower average hydraulic conductivities than outwash deposits. Most areas, including moraines, have trends of decreasing hydraulic conductivity with depth. In some areas, however, such along Cape Cod Bay, fine-grained sediments overlie coarser-grained sediments; in this area, the fine-grained, younger bottomset sediments were deposited in Lake Cape Cod and overlie older sandy sediments associated with the Mashpee Plain or Sandwich Moraine (fig. 3).

Hydrologic System

The unconsolidated glacial sediments underlying Cape Cod compose an unconfined aquifer system that is surrounded by salt water: Cape Cod Bay to the northeast, Cape Cod Canal to the northwest, Buzzards Bay to the west, and Vineyard Sound to the south (fig. 1). The Sagamore and Monomoy flow lenses (fig. 1) underlying central and western Cape Cod are the largest and southernmost of six separate ground-water-flow lenses that underlie Cape Cod (LeBlanc and others, 1986); the two flow lenses are hydraulically separated by the Bass River (fig. 1). The Sagamore flow lens is hydraulically separated at its western extent from mainland Massachusetts by the Cape Cod Canal. The Monomoy flow lens is hydraulically separated from an adjacent flow lens by Town Cove at its northeastern extent.

Ground Water

The saturated sediments underlying each flow lens represent a distinct aquifer system that is hydraulically separate from the saturated sediments of adjacent flow lenses. The aquifer system is bounded below by relatively impermeable bedrock (when compared to the aquifer system) and at the top by the water table across which recharge enters (fig. 5). Recharge from precipitation is the sole source of water to the aquifer system. About 45 in. of precipitation falls during an average year on Cape Cod. More than half of the precipitation recharges the aquifer at the water table (LeBlanc and others, 1986). The remainder is lost to evapotranspiration; surface runoff is negligible owing to the sandy soils of the area. If the average recharge rate to the aquifer system is assumed to be 27 in/yr, about 328 and 137 Mgal/d of water enters the Sagamore and Monomoy flow lenses, respectively.

Ground water flows outward from regional ground-water divides toward natural discharge locations at streams, coastal estuaries, and the ocean (fig. 5*A*). Most of the water flows through shallow sediments and discharges to streams and estuaries; ground water recharging the aquifer near the central ground-water divides flows deeper in the aquifer and discharges into the open saltwater bodies (fig. 5*B*). Most ground-water (about two-thirds) discharges into saltwater bodies. About 25 percent of ground water discharges at freshwater streams and wetlands, and a small amount (less than 10 percent) is removed from the aquifer system for water supply (Masterson and others 1997b). Maximum water-table altitudes of the Sagamore and Monomoy flow lenses are over 65 and 30 ft above NGVD 29, respectively (fig. 5*A*).

Precipitation, and therefore recharge, fluctuate both seasonally and over multiyear time periods (fig. 6). Over a 55-year period (1941–95), annual precipitation at Hatchville, MA (fig. 1), on Cape Cod averaged about 45 in/yr and ranged from 25 in. in 1965 to 73 in. in 1972 (fig. 6*A*). In an average year, precipitation is lowest in July and highest in November (fig. 6*B*). Recharge is lowest in the summer season (May–September) owing to lower precipitation rates and higher evapotranspiration rates than in winter. Annual and monthly fluctuations in precipitation and recharge affect the hydrologic system, including streamflows, pond stages, and ground-water levels (figs. 6*A*–*B*). Measured water levels in some ponds can fluctuate by more than 2 ft seasonally and by more than 6 ft between periods of drought and above-average rainfall. Base flows in streams also change seasonally in response to changing recharge conditions; some streams can vary by 50 percent over an average year and by more than a factor of two between wet and dry years.

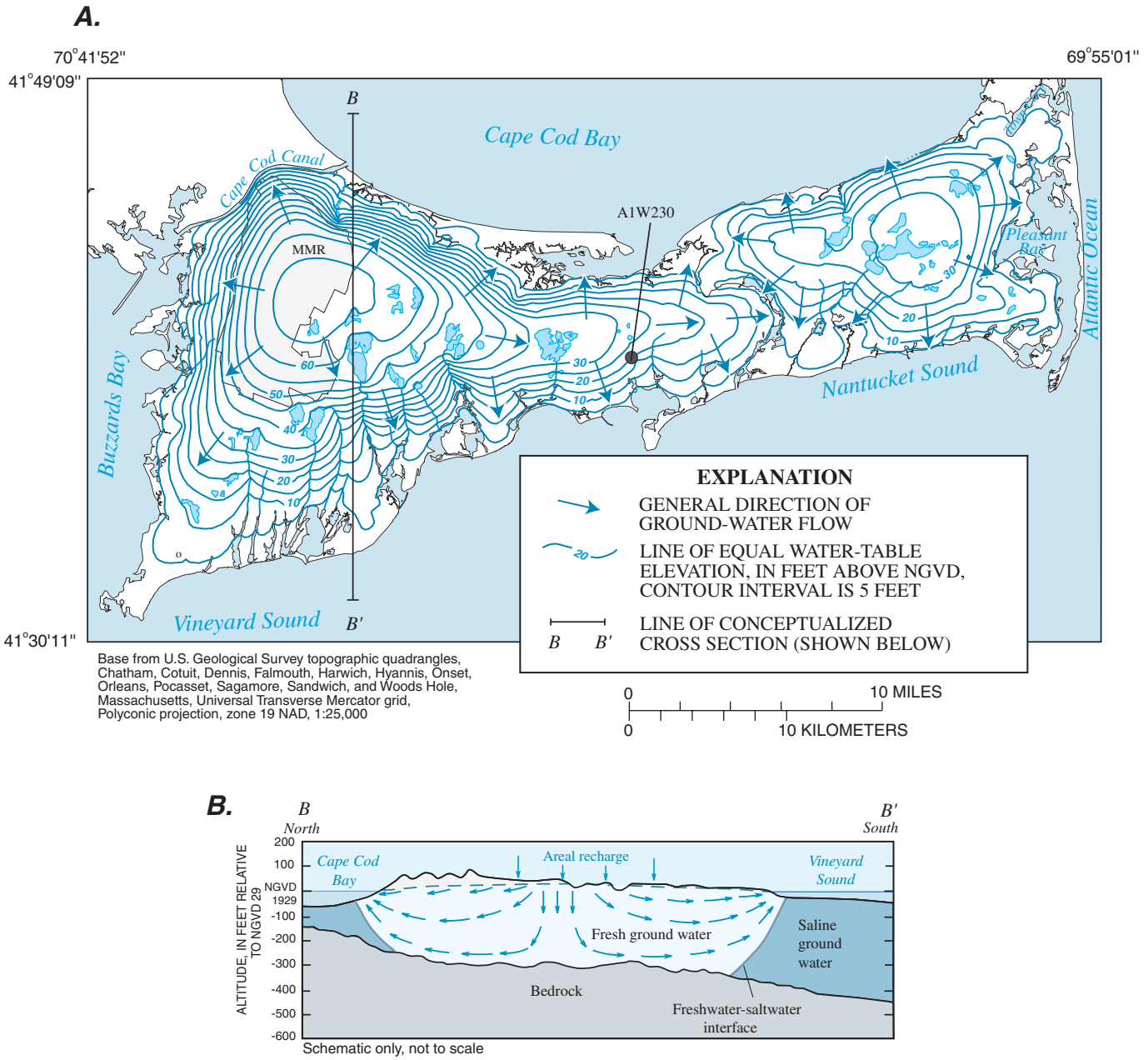

Figure 5. *A*, Regional water table for central and western Cape Cod; and *B*, generalized vertical ground-water flow, western Cape Cod, Massachusetts.

Surface Water

Water-table contours and ground-water-flow patterns on Cape Cod are strongly affected locally by numerous kettle-hole ponds because the ponds offer no effective resistance to flow. The ponds are flow-through ponds; ground-water-flow paths converge in areas upgradient of the ponds, where ground water discharges into the ponds, and diverge in downgradient areas, where pond water recharges the aquifer. Some ponds have surface-water outlets where ponds drain into freshwater streams. Streams generally are areas of ground-water discharge (gaining streams) and receive water from the aquifer over most of their length. Streamflow entering the channel as ground-water discharge (base flow) generally is the primary component of streamflow; however, streamflow may be augmented by surface-water runoff during heavy precipitation events. Some stream reaches may lose water to the aquifer (losing streams), particularly in areas downgradient of pond outflows. Surface runoff is negligible owing to the sandy soils and gentle topography, except during extremely wet periods.

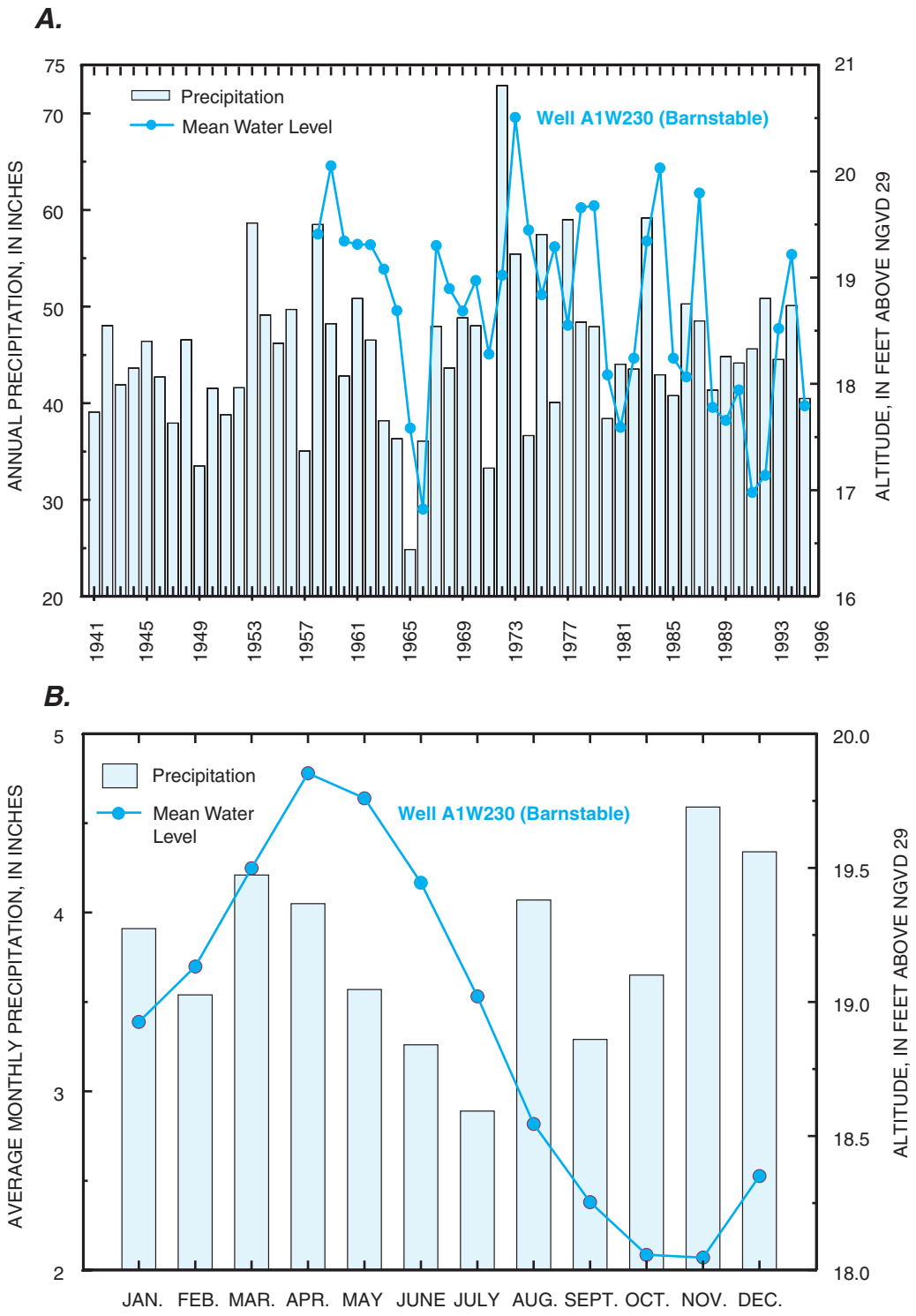

Figure 6. Variability of precipitation at Hatchville, and water levels at well A1W230, Barnstable, Massachusetts: *A*, annual averages; and *B*, monthly averages for precipitation for the period 1941–95, and for water levels for the period 1963–95.

Water Use

Five to 10 percent of the water recharging the Cape Cod aquifer system is removed for water supply (Masterson and others, 1997b). Most of this water is returned to the hydrologic system as disposed wastewater, either as dispersed septic-system discharge or as point discharges to the aquifer at waste-disposal facilities. Although most of the pumped water is returned to the aquifer—creating a near regional mass balance—the wastewater usually is disposed of in areas some distance from where it was withdrawn, particularly in areas served by public-water supply. Large-capacity pumped wells decrease ground-water levels and can affect natural resources by drying vernal pools, drawing down ponds, and decreasing streamflows by changing hydraulic gradients and either intercepting water that would have discharged to a surface-water body or by inducing infiltration of water from the surface-water body to the well. In the vicinity of large waste-disposal facilities, ground-water mounding can occur.

The effect of pumping (withdrawals) on the hydrologic system changes seasonally. Owing to large seasonal changes in regional population, about two-thirds of the total volume of ground-water withdrawals occurs between May and September. This period of largest pumping occurs when recharge rates are lowest. Thus, the effects of pumping are largest during the summer months.

The recharge area to a well represents the area at the water table that contributes water to the wells for specific recharge and pumping rates; this area represents an equilibrium condition in which recharge and pumping are in a state of mass balance. As a result, increases in recharge or decreases in the pumping rate of the well will proportionally decrease the size of the contributing area. Natural hydrologic features, such as ponds, streams, and coastal water bodies, are discharge areas; therefore, they also have recharge areas similar in concept to the areas contributing recharge to wells. However, unlike wells, which have a specified, constant flux under steady-state conditions, surface-water bodies are passive receptors. As a result, the general size and shape of the areas contributing recharge to these features are similar for different recharge rates, whereas fluxes of water into the receptors do change in response to changing recharge rates.

On Cape Cod, the areas contributing recharge to production wells can be made more complex by the presence of nearby surface-water bodies, such as flow-through ponds. In some cases, wells capture water from direct recharge across the water table and from an upgradient pond. In these cases, the total recharge area to the well includes areas contributing recharge to both the well and the pond.

Simulated Water Sources to Wells and Surface Waters

All water recharging the aquifer eventually discharges into surface-water bodies or is removed as water supply. The areas at the water table that contribute water to natural receptors and wells are a function of long-term hydrologic gradients in the aquifer. Therefore, modeling tools that simulate constant recharge and pumping conditions are suitable for estimating areas at the water table that contribute water to natural hydrologic features, such as ponds, streams, and coastal water bodies, and to anthropogenic features, such as production wells.

The hydrologic systems of the Sagamore and Monomoy flow lenses were simulated by using steady-state numerical models developed from field data and the conceptual models of the hydrogeology of the region. The models simulate long-term average hydrologic conditions in the aquifers, including hydrologic budgets, ground-water-flow patterns, and the sources of water to wells and natural receptors. A detailed documentation of the models, including model development and calibration, is presented in the appendix of this report.

Hydrologic Budgets and Source Areas to Ponds, Streams, and Coastal Boundaries

Recharge from areal precipitation is the sole source of water to the hydrologic systems of the Sagamore and Monomoy flow lenses. Ground water flows away from regional water-table divides towards natural discharge boundaries at streams and coastal water bodies; some water flows through kettle-hole ponds prior to discharging and some water is removed from the system for water supply. The simulated hydrologic budgets for the Sagamore and Monomoy flow lenses are reported in table 1. Under current (2003) pumping conditions, the flow lenses receive a total of about 252 and 103 Mgal/d of recharge, respectively. Most water discharges to the coastal boundaries (coast and estuaries) in both flow lenses, about 66 percent In the Sagamore flow lens and 77 percent in the Monomoy flow lens (table 1). Ground-water discharge to freshwater streams on the Sagamore and Monomoy flow lenses accounts for about 28 and 16 percent of total discharge, respectively. Pumping for water supply accounts for about 7 percent of total pumping in both flow lenses (table 1). Although simulated ponds account for only about 4 percent of the total surface area of the Sagamore flow lens, about 25 percent of total ground-water flow, or 62.0 Mgal/d, flows through ponds before discharging at streams or coastal boundaries. Simulated ponds account for about

Table 1. Simulated hydrologic budgets for the Sagamore and Monomoy flow lenses, for nonpumping, current (2003), and future (2020) pumping conditions, Cape Cod, Massachusetts.

[Mgal/d; million gallons per day]

Component	Nonpumping		Current (2003)		Future (2020)	
	Flow	Percent	Flow	Percent	Flow	Percent
Sagamore flow lens						
Inflow (Mgal/d)						
Recharge	252.1	99	252.1	94	252.1	91
Wastewater	.0	0	14.8	5	21.8	8
Streams	2.3	1	2.3	1	2.4	1
Total	254.3		269.2		276.7	
Outflow (Mgal/d)						
Estuaries	105.8	42	105.4	39	106.1	38
Coast	71.6	28	72.3	27	72.6	26
Streams	77.0	30	74.2	28	70.9	26
Wells	.0	0	17.3	7	26.7	10
Total	254.4		269.2		276.3	
Monomoy flow lens						
Inflow (Mgal/d)						
Recharge	103.2	99	103.2	93	103.2	91
Wastewater	.0	0	6.5	6	9.3	8
Streams	.9	1	.9	1	1.0	1
Total	104.1		110.6		113.5	
Outflow (Mgal/d)						
Estuaries	46.0	44	46.4	42	46.2	41
Coast	39.0	37	39.0	35	38.7	34
Streams	19.1	18	17.6	16	16.8	15
Wells	.0	0	7.6	7	11.8	10
Total	104.1		110.6		113.5	

6 percent of the total surface area of the Monomoy flow lens; a total of 22.9 Mgal/d, or about 20 percent of total ground water, flows through ponds prior to discharging at hydrologic boundaries.

The simulated water table and the sources of water to pumped wells and natural receptors, including streams, estuaries, and coastal boundaries, for current (2003) hydrologic conditions are shown in figure 7. The maximum water-table elevation is about 69 ft above NGVD 29 in the Sagamore flow lens in central Sandwich and about 34 ft above NGVD 29 in the Monomoy flow lens in central Brewster (fig. 7). The areas contributing water to wells and natural receptors reflect the hydrologic budgets shown in table 1.

Areas Contributing Recharge to Wells

A well may capture water directly from the water table or from one or more ponds located upgradient of the well; the ponds, in turn, capture water from an area of the water table farther upgradient. The total recharge area consists of both the areas contributing water directly to the well and, in some cases, areas that contribute recharge to ponds prior to capture by the well. The size of the recharge area is a function of recharge and pumping rates; the shape of the recharge areas generally is a function of location within the flow system. Recharge areas in regions with steep hydraulic gradients are elongated, whereas recharge areas in regions with gentle hydraulic gradients, such as the vicinity of ground-water divides, are broader and can theoretically be circular in shape.

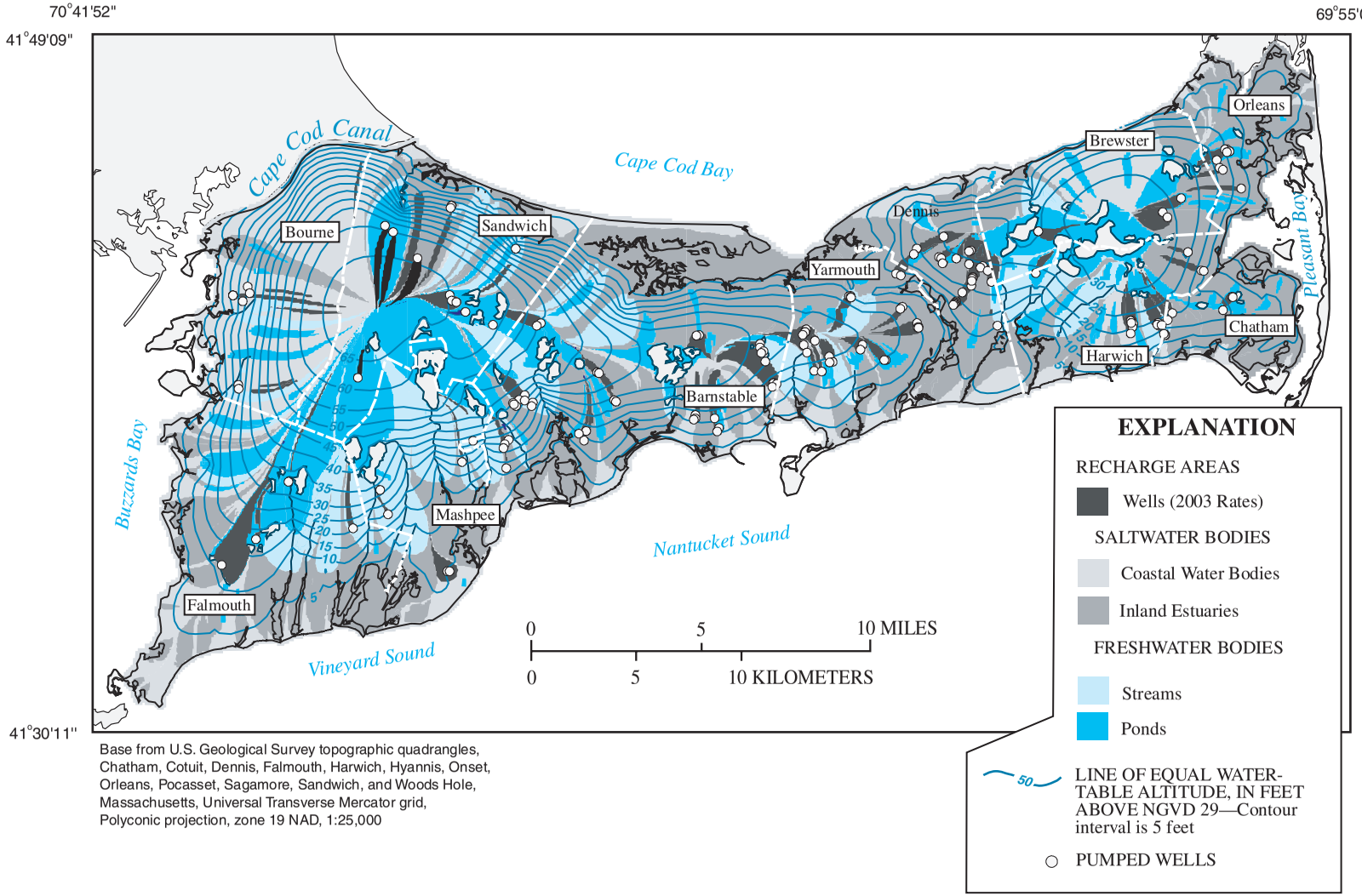

Figure 7. Simulated heads and sources of water to wells and natural receptors—ponds, streams, and coastal estuaries—the Sagamore and Monomoy flow lenses, Cape Cod, Massachusetts.

Current (2003) Conditions

The areas at the water table that contribute recharged water to existing wells for current (2003) pumping conditions are shown in figure 8; these recharge areas are based on pumping rates summarized in table 1-2 in the appendix. About 89 percent of the water withdrawn by production wells in the Sagamore flow lens is captured directly from the water table; the remaining 11 percent flows through ponds prior to removal at the well. The areas at the water table that contribute water directly to a production well (fig. 8) total about 11.7 mi^2, or about 6.2 percent of the total land area; this percentage is similar to the percentage of outflow to wells shown in the hydrologic budget in table 1. On the Monomoy flow lens, about 89 percent of withdrawn ground water is captured directly from the water table. These areas total about 5.7 mi^2 and represent about 6 percent of the total area receiving recharge; this percentage also is similar to the percentage of outflow to wells shown in the hydrologic budget in table 1.

Future (2020) Conditions

Areas contributing recharge to production wells for future (2020) conditions are larger than for current (2003) conditions owing to higher pumping rates (fig. 9). About 87 percent of water withdrawn from both the Sagamore and Monomoy flow lenses is captured directly from the water table. The remaining 13 percent is captured from areas contributing water to ponds (fig. 9). A total of about 16.5 mi^2 on the Sagamore flow lens and 6.9 mi^2 on the Monomoy flow lens contribute water directly from the water table to production wells. These areas are about 47 percent and 40 percent larger than the areas calculated for current (2003) conditions, an increase similar to the increases in pumping for the two flow lenses between 2003 and 2020 (Appendix 1).

Limitations of Analyses

Inaccurate results can be produced if a regional model is used to estimate areas contributing recharge to wells that withdraw a volume of water that is small relative to the total flux of water through the model cell representing the well. These wells are known as weak sinks in the model. The size of the recharge area to a well multiplied by the recharge rate is equal to the pumping rate of the well. In a model, however, the product of the simulated recharge area and the simulated recharge rate is equal to the total flux of water through the model cell representing the well. As a result, the simulated areas contributing recharge to wells that are weak sinks in the model will be larger than the actual recharge area to the well. The actual size of the recharge area to a weak-sink well is proportional to the fraction of total flow in the model cell that is attributed to the well. As an example, if a well represents 80 percent of total flow in the model cell, then the actual recharge area is 80 percent of the model-calculated recharge area to the well (or the model-calculated recharge area overestimates the actual recharge area by about 25 percent).

Simulated wells generally are strong sinks within models of both the Sagamore and Monomoy flow lenses (fig. 10). Wells that represent greater than and less than 75 percent of total flows in the model cells for current (2003) and future (2020) conditions are shown on figures 8 and 9. On average, currently operating wells represent about 91 percent of total flow through the cells representing the wells; for future pumping, the wells represent 95 percent of the total flow through the model cells. Of the 154 wells currently operating, 131 wells represent more than 75 percent of total flow in the cells that represent them. A total of 9 of the 154 wells represent less than 50 percent of total flow in model cells. A total of 174 wells are projected to be in operation in 2020; 6 of these wells represent less than 50 percent and 165 wells represent more than 75 percent of total flow in the model cells representing the wells (fig. 10).

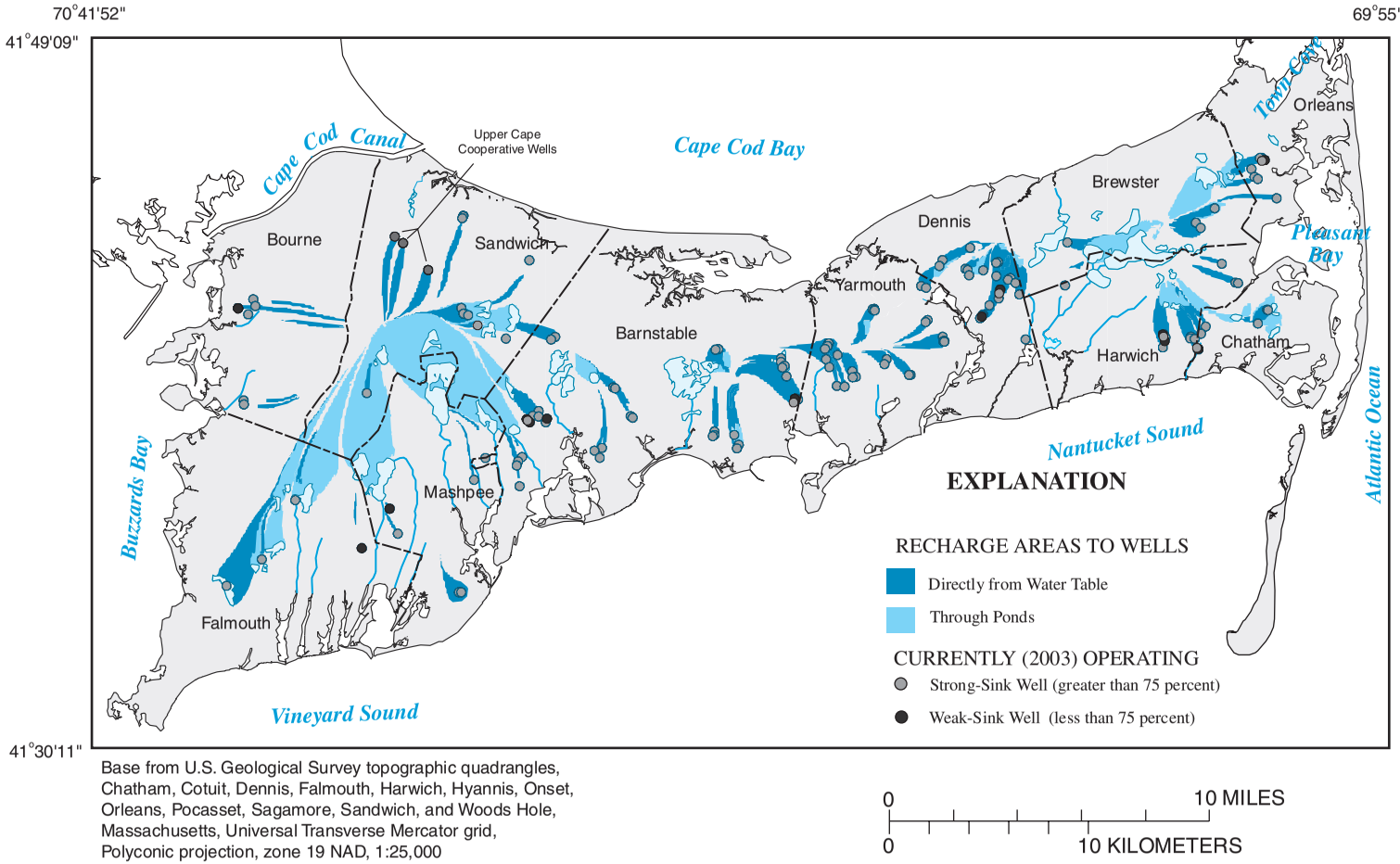

Figure 8. Areas contributing recharge to pumped wells and associated ponds for current (2003) pumping conditions in the Sagamore and Monomoy flow lenses, Cape Cod, Massachusetts.

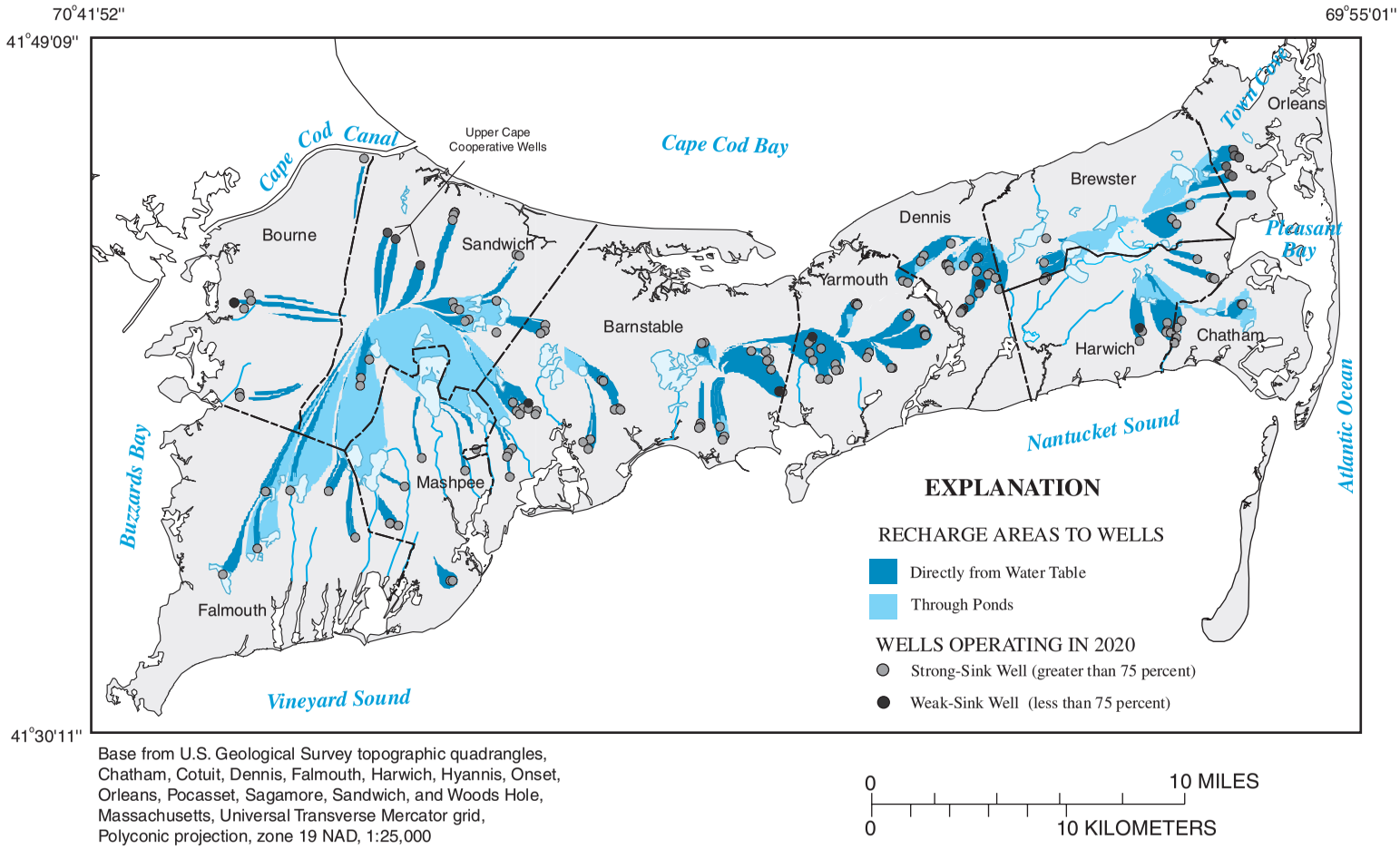

Figure 9. Areas contributing recharge to pumped wells and associated ponds for future (2020) pumping conditions in the Sagamore and Monomoy flow lenses, Cape Cod, Massachusetts.

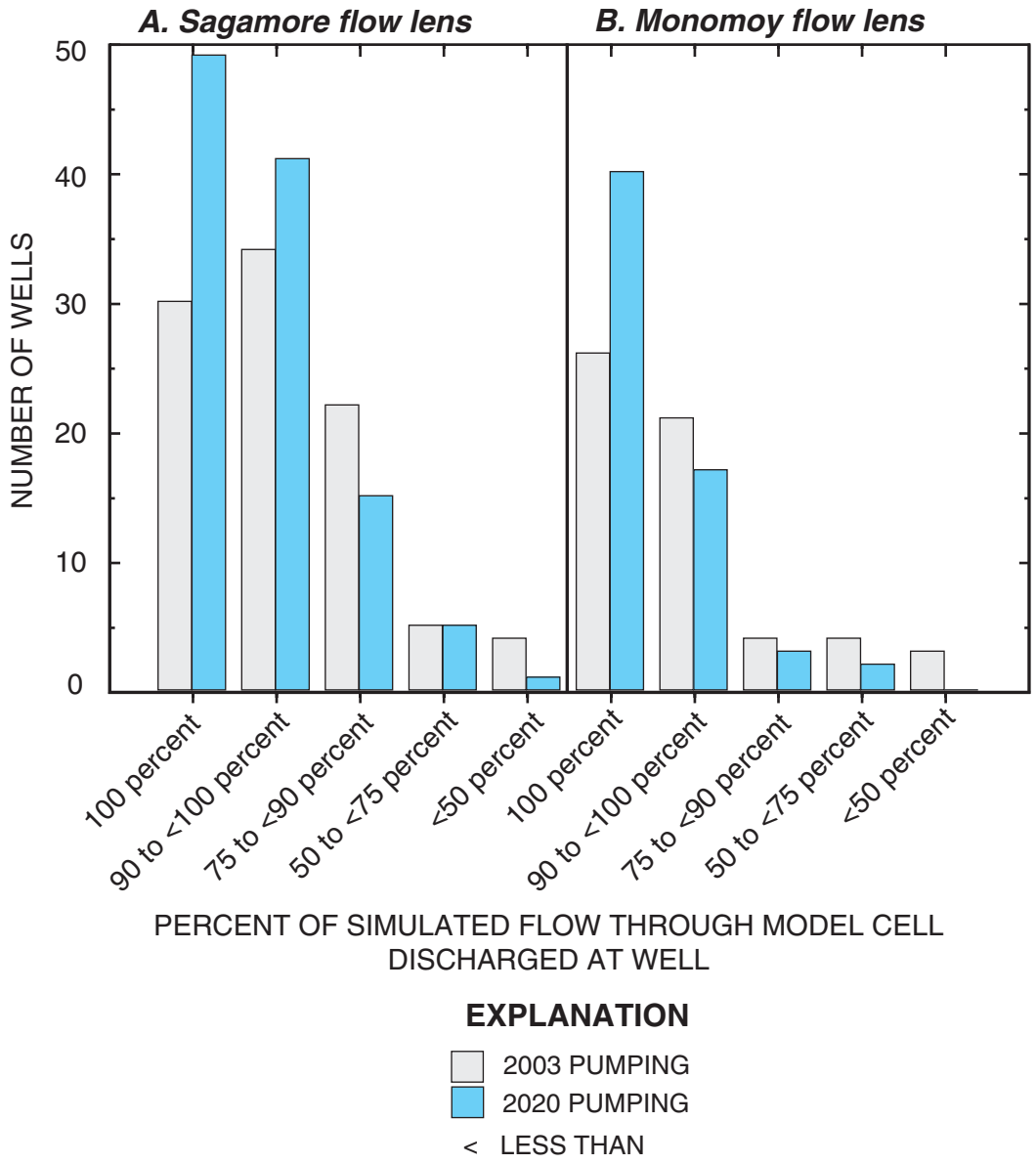

Figure 10. The extent to which wells are weak sinks in the regional models of the Sagamore and Monomoy flow lenses, Cape Cod, Massachusetts.

Simulated Effects of Pumping on the Hydrologic System

Withdrawals of ground water from the aquifer change water levels, flow directions, and the rate of ground-water discharge into streams and coastal boundaries. Although most pumped water (about 85 percent) is returned to the aquifer at the water table, the effects of pumping and redistribution of water on the hydrologic system are greatest near pumping wells where there is a local net loss of water. The transient nature of natural recharge and pumping rates on Cape Cod causes the effects of pumping to be largest during the summer months. Effects of pumping include water-table-elevation decreases, which can dry vernal pools; pond-level declines, which can affect pond-shore ecosystems; and streamflow depletions, which can affect fish habitats.

Long-Term Average Conditions

Steady-state models can be used to evaluate long-term-average effects of pumping on water levels and streamflows. These effects, such as long-term drawdowns and streamflow depletions, represent changes in baseline hydrologic conditions upon which variations in water levels and streamflows would be superimposed in response to seasonal and annual changes in recharge.

Water Levels

Simulated current (2003) pumping is predicted to decrease the elevation of, or drawdown, the water table, relative to nonpumping water levels. Drawdowns exceeding 0.5 ft occur in various areas in the Sagamore and Monomoy flow lenses (fig. 11*A*). Areas of large drawdowns occur in Sandwich, Falmouth, Barnstable, and Yarmouth on the Sagamore flow lens, where ground-water withdrawals are largest (fig. 1-6, Appendix 1); the simulated decline in the water table exceeds 4 ft in some areas. Current pumping causes drawdown in two general areas on the Monomoy flow lens: in Dennis, along the western boundary of the flow lens, and in parts of Orleans, Brewster, and Harwich near the eastern boundary of the flow lens. The largest drawdowns on the Monomoy flow lens are in Dennis, where drawdowns locally exceed 3 ft.

Simulated future (2020) pumping is predicted to cause additional drawdown of the water table, relative to water levels simulated with 2003 pumping, in some areas (fig. 11*B*). Drawdowns in Sandwich, Falmouth, and Mashpee, on western Cape Cod, are predicted to increase by an additional 1 to 2 ft around proposed pumping wells. The largest additional drawdowns are predicted in Barnstable and the western part of Yarmouth, the towns with the largest projected increases in ground-water demand (Appendix 1); additional drawdowns in some areas will exceed 3 ft (fig. 11*B*). The largest drawdowns in the Monomoy flow lens are in Dennis and the area near the boundary between Orleans and Brewster, where an additional water-table decline of 2 ft is predicted (fig. 11*B*). The area of large drawdown in Orleans results because of a proposed interlens transfer of water from Orleans to the neighboring town of Eastham; because the water is transferred to another flow lens, the pumped ground water is not returned to the aquifer as return flow and represents a loss of water from the aquifer system. Other areas where additional drawdowns are projected to exceed 1 ft are in the southern part of Brewster.

Negative drawdowns indicate that increases in water-table elevations, or mounding, are predicted in the vicinity of centralized waste-disposal facilities, such as those in Falmouth, Barnstable and Bourne. The largest increase in water-table elevations is nearly 5 ft in Barnstable (fig. 11*A*). For future (2020) pumping conditions, water-table elevations are predicted to increase by an additional 1 ft around the Barnstable wastewater disposal facility in response to additional wastewater disposal and by more than 2 additional ft near Long Pond in Falmouth because of a projected decrease in future water withdrawals from the pond (fig. 11*B*).

Streamflow

Current (2003) pumping affects streamflow in the region by intercepting ground water that would have discharged to the streams or by inducing infiltration from the streams. Comparisons of streamflow in selected large (greater than 1 ft^3/s) streams for current, future (2020), and a no-pumping condition are shown in figure 12. Current pumping on the Sagamore flow lens is predicted to cause streamflow depletions of more than 1 ft^3/s at the outlet of Shawme Pond to Mill Creek (identifier 10 on fig. 11*A*) and in Marston Mills River (identifier 5 on fig. 11*A*; fig. 12); these depletions correspond to percent decreases from prepumping discharge of 17 and 11 percent, respectively. Both of these streams are in areas with large drawdowns in Sandwich and the eastern part of Barnstable (fig. 11*A*). Streamflow increases in some areas of Falmouth and Mashpee, such as the Backus, Bourne, and Childs Rivers, in response to current pumping stresses (fig. 12). This increase likely results because of the distribution of pumping and return flow in the area. Most of the water (about 70 percent) pumped from the Upper Cape Cooperative wells in Sandwich goes to areas south of the MMR (fig. 1) and enters the aquifer as septic return flow; this results in a net increase in water in these areas, which increases water levels and streamflows.

In the Monomoy flow lens, depletions exceed 1 ft^3/s at three locations (fig. 12): Herring River, the outlet from Lower Mill Pond, and the Red River. The Herring River and the outlet from Lower Mill Pond are in an area with large regional drawdowns in Dennis; the Red River is near an area with large drawdowns in the eastern part of Harwich (fig. 11*A*). Streamflow depletions in the Herring River, the outlet from Lower Mill Pond, and the Red River, because of current (2003) pumping, represent decreases of 14 percent, 19 percent, and 51 percent, respectively, from prepumping streamflows.

Additional streamflow depletion from future (2020) pumping, relative to current (2003) conditions, is predicted to exceed 1 ft^3/s at the Coonamessett, Childs, and Quashnet Rivers in Falmouth and Mashpee (fig. 12). These streams are in an area of drawdowns associated with proposed pumping in those areas (fig. 11*B*). These streamflow depletions represent between 6 and 7 percent of the current low in the Quashnet and Coonamessett Rivers and about 18 percent in the Childs River. In the Monomoy flow lens, additional streamflow depletion is predicted to exceed 1 ft^3/s in the Herring River, or an additional decrease of about 23 percent. This decrease in streamflow is a result of projected increases in ground-water pumping in the southern part of Brewster.

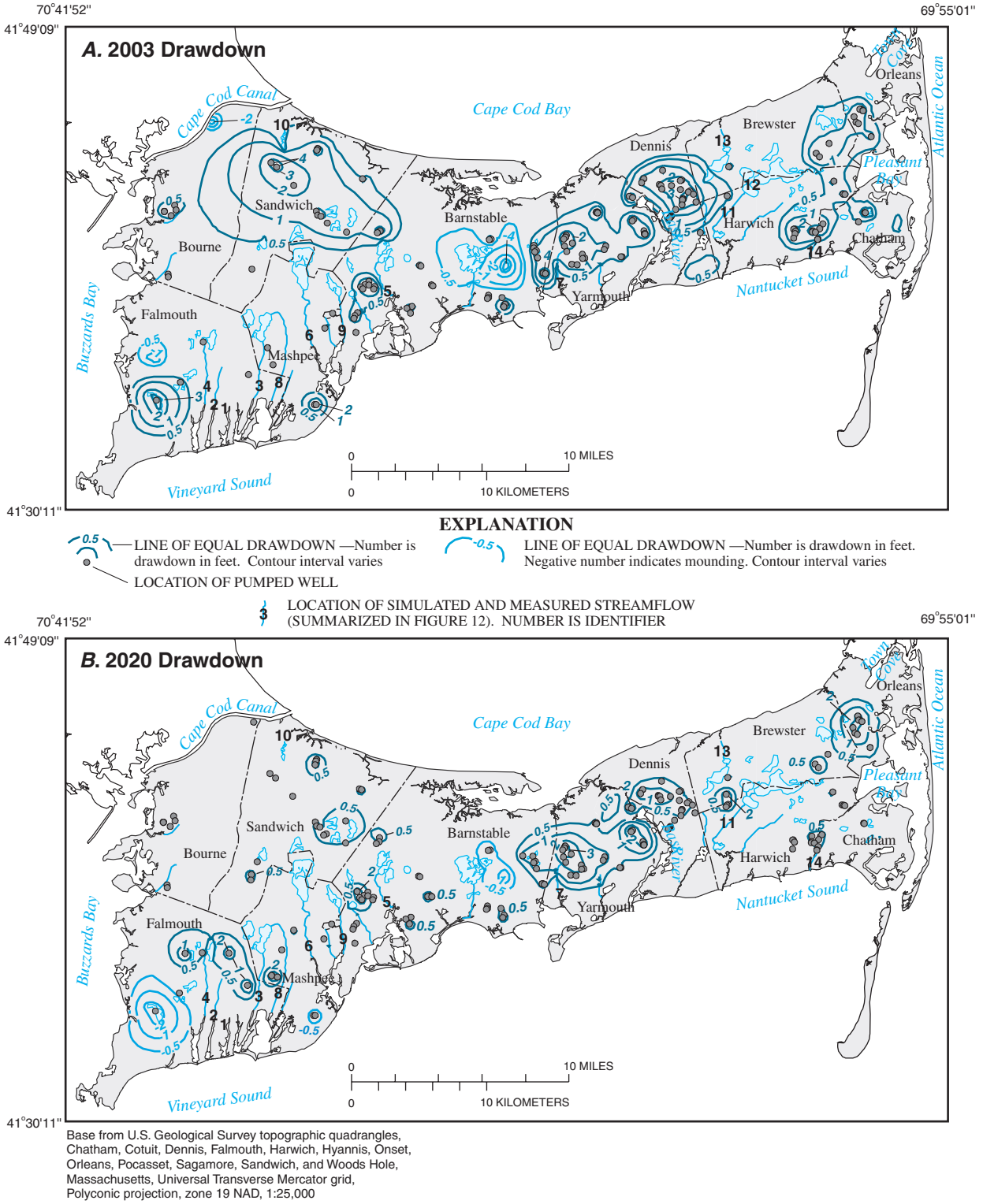

Base from U.S. Geological Survey topographic quadrangles, Chatham, Cotuit, Dennis, Falmouth, Harwich, Hyannis, Onset, Orleans, Pocasset, Sagamore, Sandwich, and Woods Hole, Massachusetts, Universal Transverse Mercator grid, Polyconic projection, zone 19 NAD, 1:25,000

Figure 11. Steady-state drawdowns associated with *A*, current (2003) ground-water withdrawals; and *B*, future (2020) ground-water withdrawals, Sagamore and Monomoy flow lenses, Cape Cod, Massachusetts.

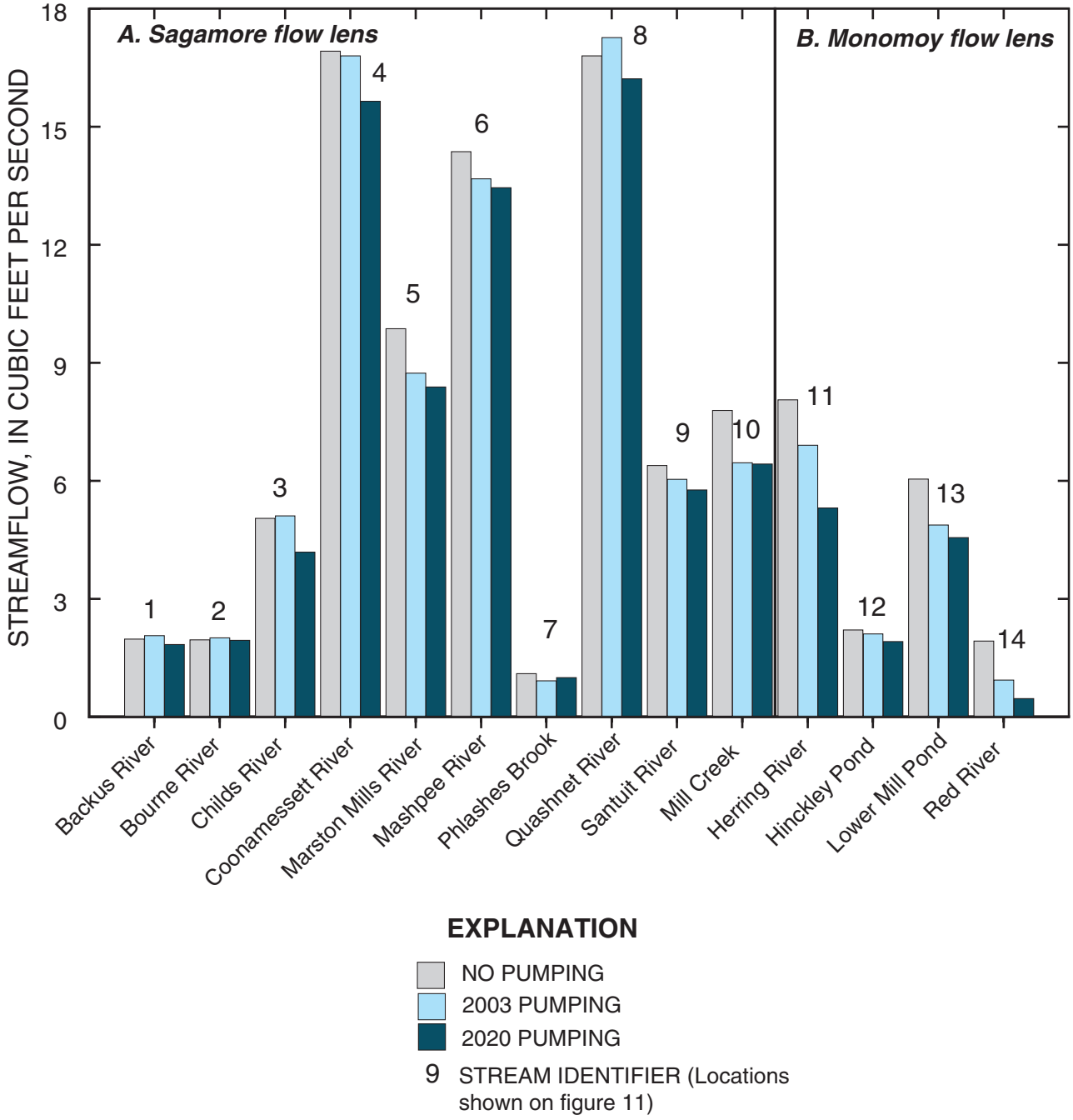

Figure 12. Simulated streamflows for current (2003) and future (2020) pumping conditions at select sites in the Sagamore and Monomoy flow lenses, Cape Cod, Massachusetts.

Effects of the Upper Cape Cooperative Wells

The relation of pumping and the redistribution of return flow to regional water levels and flows is illustrated by the operation of the Upper Cape Cooperative (UCC) on western Cape Cod. These wells were installed in 2002 to offset the loss of potable water, because of ground-water contamination, in communities surrounding the MMR (fig. 1). The wells are in the northern part of the MMR, in Sandwich (figs. 8 and 9). Currently (2003), the wells withdraw about 1.7 Mgal/d, primarily in the summer months, but are approved for a combined withdrawal of 3 Mgal/d. The wells supply water to the communities of Falmouth, Bourne, Mashpee, Sandwich and the MMR. Most (about 65 percent) of the water goes to Falmouth, which is on the opposite side of the regional ground-water divide from the UCC wells (fig. 13); only about 6 percent of the water stays in Sandwich near the UCC wells. The withdrawal of ground water from the UCC wells is offset by decreases in pumping in towns receiving water from the wells so that there is no net change in regional pumping. The effects of the UCC wells, relative to a condition in which the UCC wells are not in operation and other production wells are pumped at their original rates, include declines in the water table and decreases in streamflow.

For a current (2003) withdrawal rate of 1.7 Mgal/d (about 2.6 ft^3/s), operation of the UCC wells causes about 3 ft of additional drawdown, relative to water levels under current pumping with no operation of the UCC wells, in Sandwich and decreases flow by about 0.6 ft^3/s at the outlet of nearby Shawme Pond to Mill Creek (fig. 13*A*). Conversely, water levels increase in Falmouth and flows increase in local streams, including the Bourne, Backus, Coonamessett, and Childs Rivers (fig. 13*A*), because of declines in pumping in the town. Streamflows decrease in streams in Mashpee and the eastern part of Barnstable, such as the Santuit, Mashpee and Marston Mills Rivers (fig. 13*A*), although the rivers are on the other side of the regional ground-water mound from the UCC wells. Operation of the UCC wells reduces flow into Mashpee Pond, the outflow of which feeds Mashpee River. Outflow from Mashpee Pond decreases by about 0.4 ft^3/s and total flows in the Mashpee River, at its southernmost reach, decrease by about 0.5 ft^3/s (fig. 13*A*). Similar effects reduce streamflow in the Santuit and Marston Mills Rivers by about 0.1 ft^3/s.

If the UCC wells operate at the MDEP-approved rate of 3 Mgal/d (4.6 ft^3/s), drawdowns near the wells increase to more than 6 ft and flow out of Shawme Pond to Mill Creek outlet decreases by about 1 ft^3/s (fig. 13*B*). The larger decrease in pumping from other areas causes larger increases in water levels in Falmouth and larger increases in streamflows in the nearby Coonamessett River (fig. 13*B*). Conversely, the outflows from Mashpee and Marston Mills Ponds decrease by about 0.7 and 0.4 ft^3/s, respectively, and total flow in the Mashpee River at its southernmost reach decreases by about 0.7 ft^3/s. The results indicate that the operation of wells in the northern part of the flow lens, as well as adjustments in the pumping rates of other wells to maintain the same total pumping in the region, can, nonetheless, affect regional water levels and streamflows throughout the region. These effects can be transmitted to areas on the other side of the regional ground-water mound through a complex relation between surface and ground waters.

Effects of Time-Varying Hydrologic Stresses

Changing recharge and pumping stresses over time causes monthly and annual variations in water levels and streamflows. These variations can cause declines in pond levels, drying of vernal pools, and decreases in streamflows. Various factors, including the size and location of the surface-water body within the flow system and the proximity of the surface-water body to a pumping well, can affect the magnitudes of the variations. The effects of recharge and pumping on the hydrologic system are additive and the total changes in water levels and streamflows represent the combined effects of both stresses. Transient numerical models that incorporate time-varying stresses were used to evaluate the effects of changes in recharge and pumping on the hydrologic system; the development and calibration of these models are documented in the appendix of this report. Recharge and pumping stresses were simulated for two time scales: (1) monthly stresses during an average year and (2) in-season and off-season stresses over a 40-year period. Average monthly recharge is based on average monthly precipitation (fig. 6*A*) and, therefore, the stresses represent recharge in an average year. In-season and off-season recharge rates are based on the apportionment of annual averages for the period 1955–95 (fig. 6*B*); in-season is defined as the months of May through September and off-season is defined as the months October through April. Average monthly pumping is based on MDEP pumping records; average seasonal pumping is based on an apportionment of average monthly pumping for the in-season and off-season periods. A detailed discussion of average monthly recharge and pumping estimates as wells as estimates of seasonal stresses over a 40-year period are included in the appendix. The simulated annual recharge rates incorporate variability resulting from periods of high recharge and droughts; for purposes of prediction, it is assumed that variability in recharge over the next 40 years will be similar to historical variability over the 40-year period 1955–95.

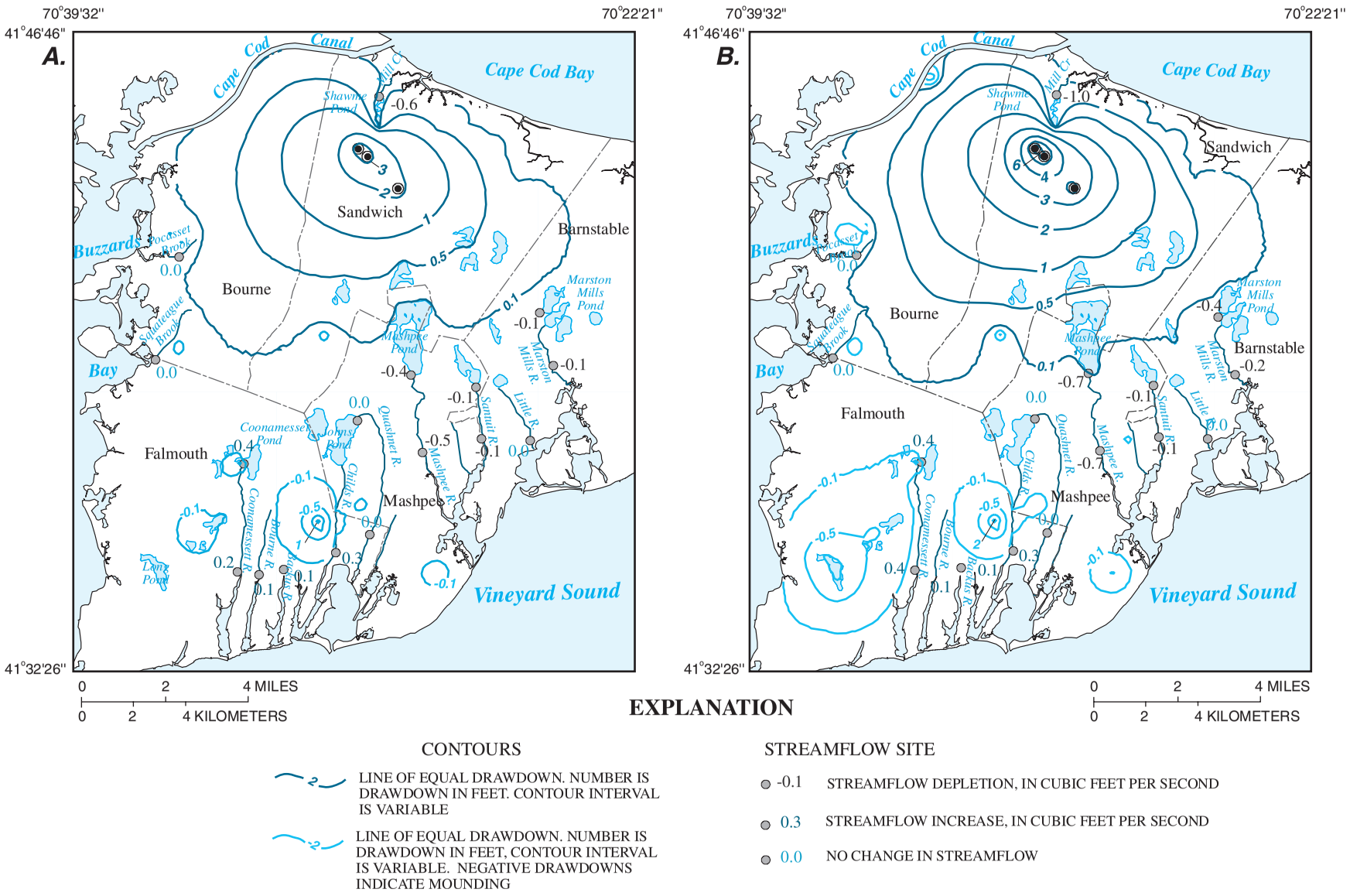

Figure 13. The effects of operation of the Upper Cape Cooperative wells on regional heads and streamflows for *A*, current (2003) pumping rates; and *B*, Massachusetts Department of Environmental Protection-approved pumping rates, Massachusetts.

The hydrologic systems of the flow lenses change in response to changes in recharge to the systems. Simulated hydrologic budgets for the modeled area for the months of March and August in an average year (table 2) and for in-season and off-season conditions in wet and dry years (table 3) illustrate the temporal variability of recharge, storage, and boundary discharges in different recharge regimes. In August of an average year, more than half of the water discharging from the system comes from storage in the aquifer; in March of an average year, about a third of recharge entering the system goes into storage within the aquifer (table 2). Total hydrologic budgets, including seasonal recharge and changes in storage, also vary from year to year according to changes in annual recharge (table 3).

As recharge to the hydrologic system decreases, such as during the summer months, water levels decline and discharge at hydrologic boundaries—streams and coastal water bodies—decreases; these decreases are accompanied by a release of water from storage within the aquifer. In a steady-state system, outflows at boundaries are in a state of equilibrium with recharge; at a given point in time in a transient system, however, the total discharge to boundaries and specified withdrawals at wells are in a state of mass balance with the net sum of recharge and storage (fig. 14). Decreases in recharge and the associated release of water from storage are manifested as decreases in water levels in the aquifer.

Time-Varying Recharge

Recharge, which is the sole source of water to the hydrologic system (tables 1–3), is the most important hydrologic stress to the aquifer and changes in recharge substantially affect water levels in the aquifer. Recharge from precipitation varies monthly over an average year with the lowest recharge entering the hydrologic system in the summer, when precipitation in lowest (fig. 6*A*). Ground-water altitudes can vary by more than 2 ft in response to monthly changes in recharge; water levels typically are highest in April–May and lowest in October–November (fig. 6*A*). Water-table altitudes vary the most (by 2 ft or more) near ground-water divides and in areas with high hydraulic gradients; the areas with the lowest variability in water levels are near streams, ponds, and the coast (figs. 5*A* and 15*A*). Ponds generally have less variability in water levels than wells owing, in part, to both their higher storage and to their position as potentiometric lows in the flow system. Flow-through ponds, such as Lawrence Pond in Sandwich, vary by about 1 ft in response to monthly changes in recharge over an average year (fig. 16*A*). Water levels are less variable (less than 0.5 ft) in ponds that are drained by streams, such as Johns Pond in Mashpee (fig. 16*B*). In these cases, water discharging from the pond into a nearby stream acts as a control on the water level of the pond; when the water level increases, discharge from the pond into the stream increases and the pond level is stabilized.

Table 2. Simulated combined hydrologic budgets [current (2003) conditions] for the Sagamore and Monomoy flow lenses: average budget (steady-state), budget for mid-March, and budget for mid-August, Cape Cod, Massachusetts.

[Mgal/d; million gallons per day; --, not applicable]

Component	Steady-State		March		August	
	Flow	Percent	Flow	Percent	Flow	Percent
			Inflow (Mgal/d)			
Storage	--	--	0.0	0	199.6	53
Recharge	355.2	94	701.9	100	165.8	46
Wastewater	21.3	5	13.4	0	38.5	0
Streams	3.2	1	2.4	0	5.6	1
Total	379.7		717.7		410.5	
			Outflow (Mgal/d)			
Storage	--	--	264.2	37	.0	0
Recharge	.0	--	.0	0	27.7	7
Estuaries	151.8	39	183.2	25	149.2	36
Coast	111.3	27	133.8	19	109.9	27
Streams	91.8	28	123.3	17	80.3	19
Wells	24.9	7	15.8	2	45.3	11
Total	379.8		720.3		412.4	

Table 3. Simulated combined hydrologic budgets [current (2003) conditions] for the Sagamore and Monomoy flow lenses, Cape Cod, Massachusetts: steady-state budget, budget for a typical dry year (1967), and budget for a typical wet year (1973).

[Mgal/d; Million gallons per day; --, not applicable]

Component	Steady-state		1967 (dry year)				1973 (wet year)			
			Off-season		In-season		Off-season		In-season	
	Flow	Percent	Flow	Percent	Flow	Percent	Flow	Percent	Flow	Percent
Inflow (Mgal/d)										
Storage	--	--	1.4	0	95.7	28	0.1	0	138.7	28
Recharge	355.2	94	501.8	96	211.0	61	742.0	97	328.2	65
Wastewater	21.3	5	14.6	3	33.9	10	14.6	3	33.9	6
Streams	3.2	1	2.9	1	3.1	1	1.7	0	3.1	1
Total	379.7		520.8		343.7		767.4		503.9	
Outflow (Mgal/d)										
Storage	--	--	143.6	28	.2	0	97.0	13	.2	3
Recharge	.0	.0	.0	0	65.9	19	.0	0	16.5	0
Estuaries	151.8	39	172.6	33	108.5	31	287.1	38	192.4	38
Coast	111.3	27	122.9	24	79.0	23	205.5	27	139.1	27
Streams	91.8	28	60.0	12	55.9	16	157.6	21	118.7	23
Wells	24.9	7	17.2	3	39.9	11	17.2	2	39.9	8
Total	379.8		516.3		349.4		764.4		506.8	

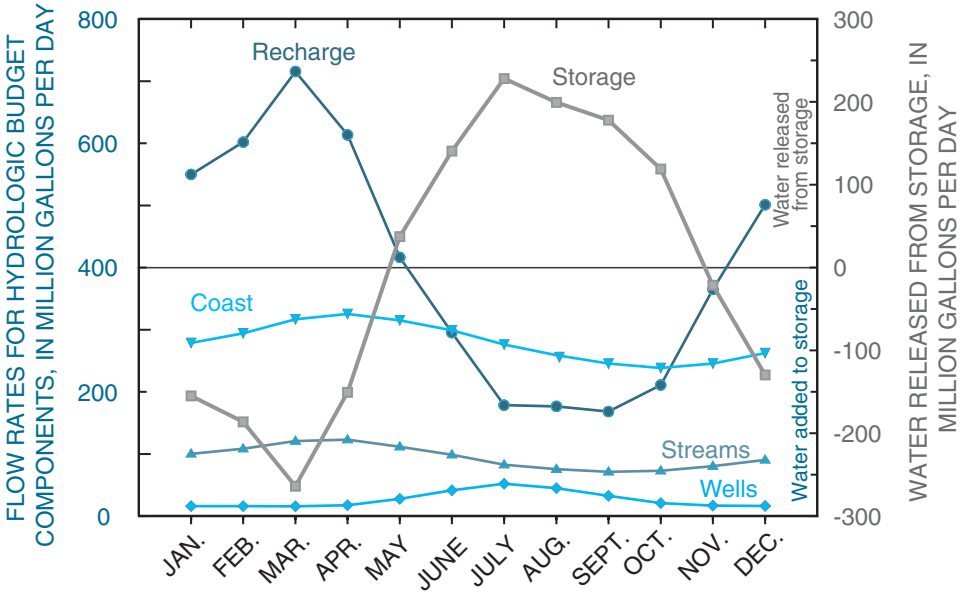

Figure 14. Midmonthly hydrologic budgets for an average year for current (2003) pumping conditions in the Sagamore and Monomoy flow lenses, Cape Cod, Massachusetts.

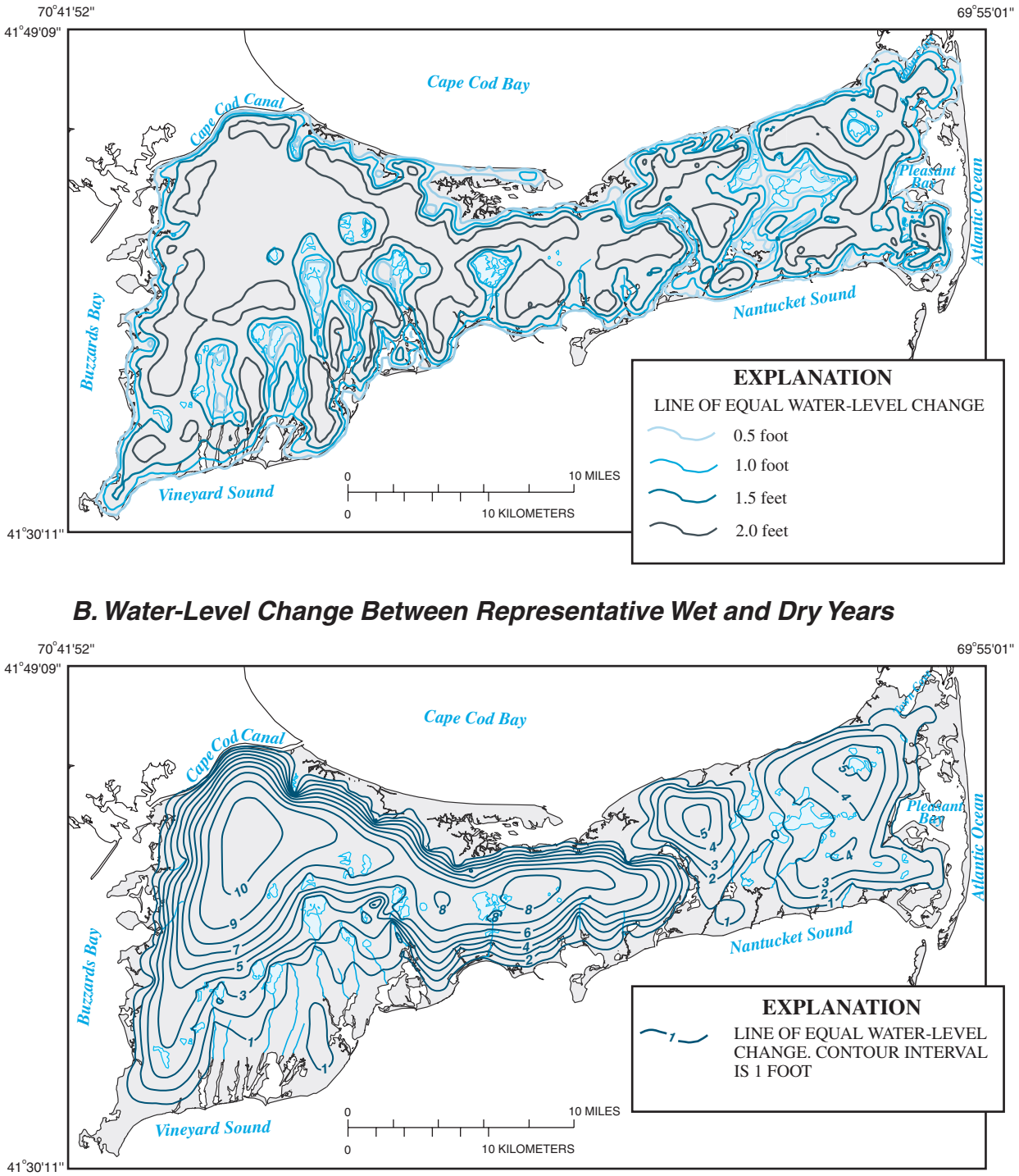

Figure 15. Changes in water-table altitudes arising from changes in natural recharge for *A*, from May to November of an average year; and *B*, between representative wet (1967) and dry (1973) years in the Sagamore and Monomoy flow lenses, Cape Cod, Massachusetts.

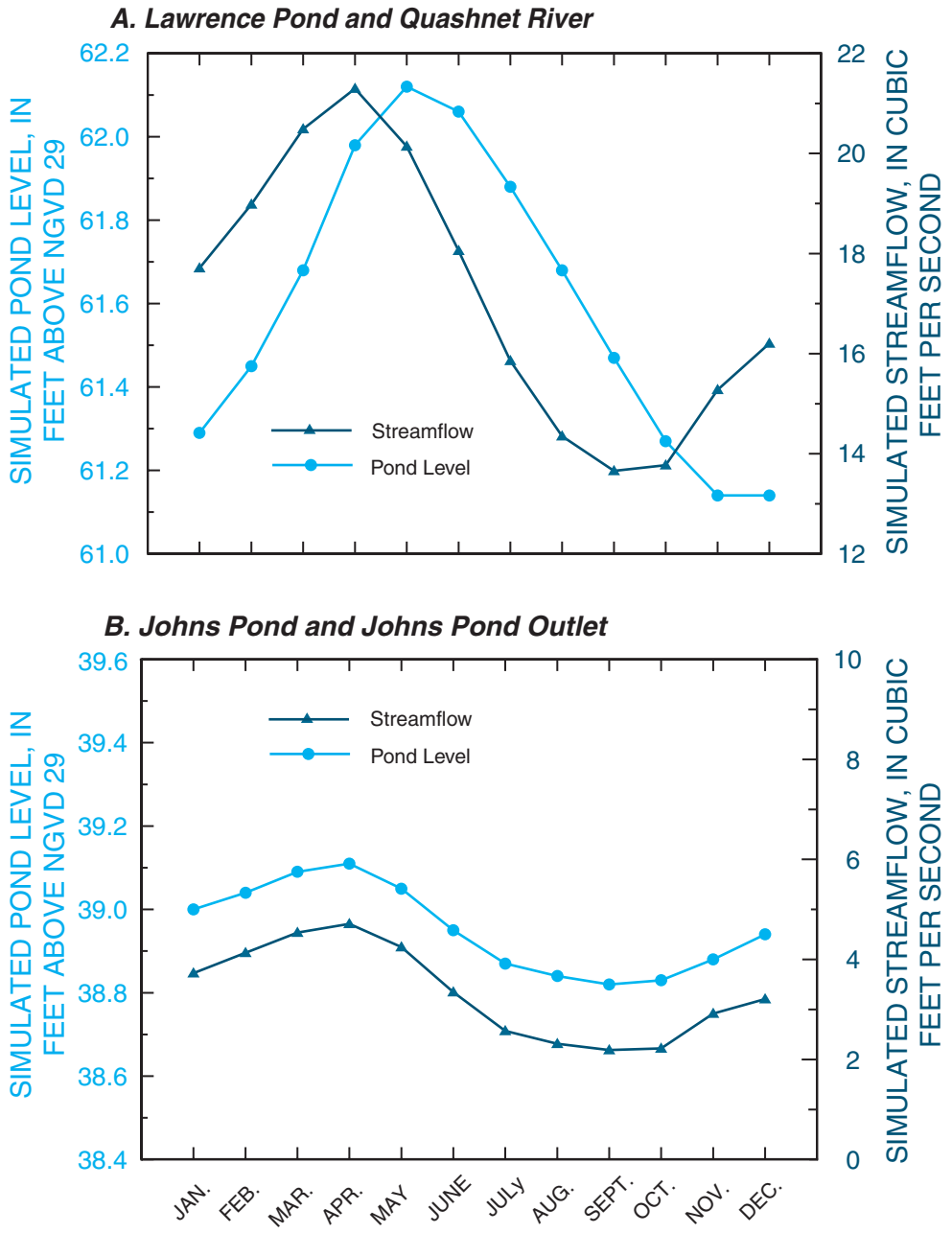

Figure 16. Changes in pond levels and streamflow because of monthly changes in recharge for an average year, Cape Cod, Massachusetts: *A*, Lawrence Pond and Quashnet River; and *B*, Johns Pond and Johns Pond Outlet.

Annual changes in recharge generally are larger than average monthly variations in an average year and ground-water levels can vary by 3–5 ft (fig. 6*B*). Total water-level fluctuations can exceed 10 ft in some areas near ground-water divides from wet to dry years (fig 15*B*). Flow-through ponds, such as Lawrence Pond in Sandwich, also can vary by about 10 ft over a multiyear time scale (fig. 17*A*); ponds near ground-water divides, such as Lawrence Pond, would be expected to have larger water-level fluctuations than ponds nearer the coast. Also, pond-level fluctuations are much less (about 2 ft) in ponds that are drained by streams, such as Johns Pond in Mashpee (fig. 17*B*), because of the control of the pond levels by stream outflow. The lowest simulated water levels occur during a period of drought that is similar in scale to an historic drought that occurred in the mid-1960s (fig. 6*B*).

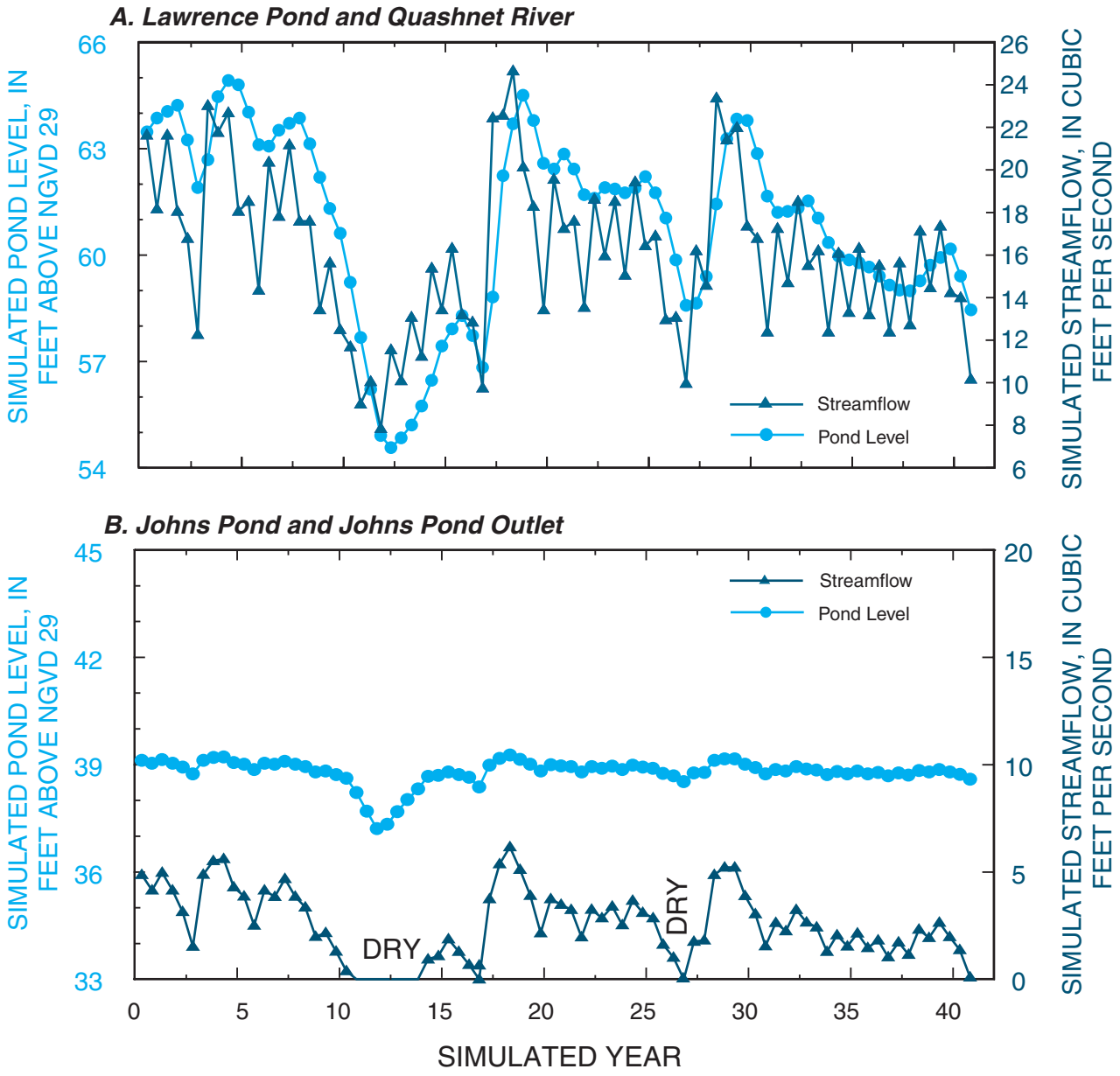

Figure 17. Changes in pond levels and streamflow because of annual changes in recharge over a representative 40-year period, Cape Cod, Massachusetts: *A*, Lawrence Pond and Quashnet River; and *B*, Johns Pond and Johns Pond Outlet.

Changes in recharge also affect streamflows over both monthly and multiyear time scales. In response to monthly changes in recharge, base flow in streams can vary considerably. Simulated streamflow at the mouth of the Quashnet River (fig. 1) varied by more than 7 ft^3/s between April and September–October of an average year (fig. 16*A*). Flow from ponds to outlet streams generally varies by less owing to the effect of the large storage in the ponds on the pond levels and resultant streamflow; flow at the outlet from Johns Pond, near the headwaters of the Quashnet River (fig. 1), in Mashpee varied between 2 and 3 ft^3/s over an average year (fig. 16*B*).

Streamflows also change in response to multiyear changes in recharge; variations in streamflow are larger on a multiyear time scale owing to the larger variations in recharge over multiple years as compared to average monthly variations (fig. 6). Simulated streamflow in the Quashnet River varied by more than 17 ft^3/s (fig. 17*A*), or about 50 percent of average flow. Flow at the outlet to Johns Pond varied by about 6 ft^3/s and went dry during simulated periods of drought (fig. 17*B*). This variation corresponds to a doubling of flow relative to mean flow during high-flow conditions.

Time-Varying Pumping

An average of about 24.9 Mgal/d of water is withdrawn from the aquifer at production wells; this volume represents about 7 percent of total ground-water flow through the aquifer (table 1). Pumping varies seasonally and ranges from about 15.8 Mgal/d in March to 45.3 Mgal/d in August, representing 2 and 11 percent, respectively, of total ground-water flow in the aquifer (tables 2 and 3). About 85 percent of pumped ground water is returned to the system as increased recharge in residential areas. Overall, less than 1 percent of recharge is lost from the hydrologic system. Although pumping represents a small hydraulic stress in the aquifer, pumping and the redistribution of water to other areas can cause local declines in the water table, affect water levels in nearby ponds, and decrease flows in local streams.

Average Monthly Conditions

The effects of pumping on the hydrologic system vary with changes in pumping over an average year. Drawdowns at the water table are smaller in winter months when pumping rates are lowest and greater in the summer when pumping rates are highest and recharge rates are low. Drawdowns in March and August in an average year relative to March and August water levels with no simulated pumping are shown on figure 18. For current (2003) pumping, drawdown is at a minimum in March; the largest drawdowns in March are more than 3 ft in Barnstable and Dennis (fig. 18*A*). Drawdowns in August, when drawdowns are at a maximum, exceed 6 ft in these same areas (fig. 18*B*). Comparisons of March, August, and long-term average (steady-state) drawdowns (figs. 11 and 18) indicate that the size and shape of areas affected by pumping, as defined by drawdowns greater than 0.5 ft, are similar for March and August and for long-term average conditions and that the areas with the largest variations in drawdown are closest to the wells. Additional drawdown resulting from future (2020) pumping, relative to water levels representing 2003 pumping conditions, ranges from a maximum of about 3 ft in March to a maximum of more than 5 ft in August (figs. 19*A* and *B*).

Seasonal changes in pumping affect water levels in nearby ponds; these effects vary with time through an average year. Ponds typically vary from 0.5 to 1.5 ft over an average year due to natural changes in recharge (fig. 16*A*); seasonal pumping near a pond also would be expected to affect seasonal changes in water levels. Mary Dunn Pond is near a number of production wells in Barnstable (fig. 18) and has been observed to be affected seasonally by local pumping (Richard McHorney, The Nature Conservancy, oral commun., 2002). Simulated average monthly pond levels in Mary Dunn Pond vary by about 1.6 ft under current (2003) pumping conditions (fig. 20); these fluctuations are a function of variations arising from both time-varying natural recharge and pumping. Natural recharge, in the absence of pumping, results in about 1.7 ft of water-level fluctuations over an average year. The operation of the nearby production wells at current pumping rates (under the condition of constant, average recharge) results in about 1 ft of water-level changes over an average year (fig. 20). Because the effects of stresses generally are additive, the sum of the separate fluctuations from natural recharge and pumping stresses generally equals water-level fluctuations simulated with both monthly recharge and 2003 pumping stresses (fig. 20).

Seasonal pumping causes decreases in pond levels over the entire year (figs. 21*A*-*B*). Water-level fluctuations (relative to the year-round average) are similar for predevelopment, current (2003), and projected (2020) pumping; however, water levels are lower throughout the year with pumping. At Mary Dunn Pond, pond levels decrease, relative to a nonpumping condition, by about 1 ft in the winter and by a maximum of more than 2 ft in August because of 2003 pumping (fig. 21*C*). At Lawrence Pond, which is in Sandwich, current drawdowns are generally about 1 ft over nonpumping conditions and were fairly uniform throughout the year. Projected pumping near Mary Dunn Pond could cause increased drawdowns in the winter months of about 2 ft, and in the summer months of about 3.5 ft (fig. 21*C*). At Lawrence Pond, which is in an area where additional water supplies are proposed, future water pumping could cause drawdowns in the winter of about 1.5 ft and in the summer months of nearly 2.5 ft (fig. 21*D*).

Seasonal pumping also affects streamflows by intercepting potential ground-water discharge or by inducing infiltration from streams. During an average year, total streamflow depletion resulting from current (2003) pumping generally is similar throughout the year. Streamflow depletion in the Sagamore flow lens ranges from 4.2 to 5.5 ft^3/s. Streamflow depletion in the Monomoy flow lens ranges from 2.3 to 3.1 ft^3/s (fig. 22). These depletions correspond to 4 and 9 percent of total streamflow in the Monomoy and Sagamore flow lenses, respectively. Future (2020) pumping in the Sagamore flow lens results in a total streamflow depletion of about 8 ft^3/s in September and about 11 ft^3/s in March; these depletions represent about 8 percent of total streamflow in both months. In the Monomoy flow lens, future pumping causes between 4.0 and 4.5 ft^3/s of streamflow depletion throughout the year. The effects of pumping near individual streams depend on the proximity of wells to the streams and seasonal pumping rates. Relative to a nonpumping condition, streamflow in Mill Creek at the outlet to Shawme Pond decreases by 1.2 to 1.4 ft^3/s, or about 18 percent of total flow, over an average year due to both current and future pumping (fig. 23). In the Herring River, streamflow depletion from current pumping is about 0.5 ft^3/s throughout the year. Future pumping decreases streamflow by a maximum of about 1 ft^3/s in October (fig. 23).

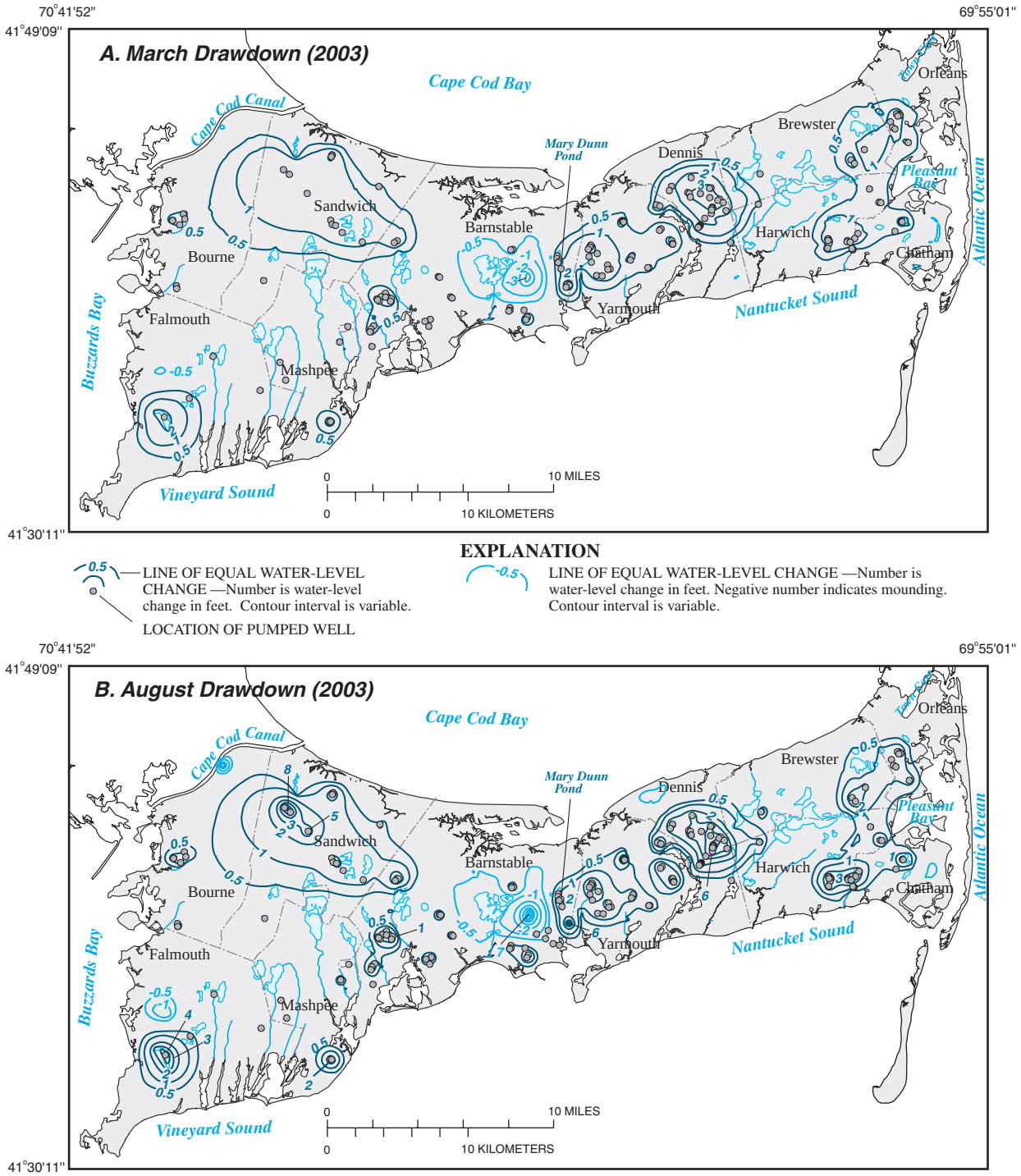

Base from U.S. Geological Survey topographic quadrangles, Chatham, Cotuit, Dennis, Falmouth, Harwich, Hyannis, Onset, Orleans, Pocasset, Sagamore, Sandwich, and Woods Hole, Massachusetts, Universal Transverse Mercator grid, Polyconic projection, zone 19 NAD, 1:25,000

Figure 18. Drawdowns associated with current (2003) pumping in *A*, March of an average year; and *B*, August of an average year in the Sagamore and Monomoy flow lenses, Cape Cod, Massachusetts.

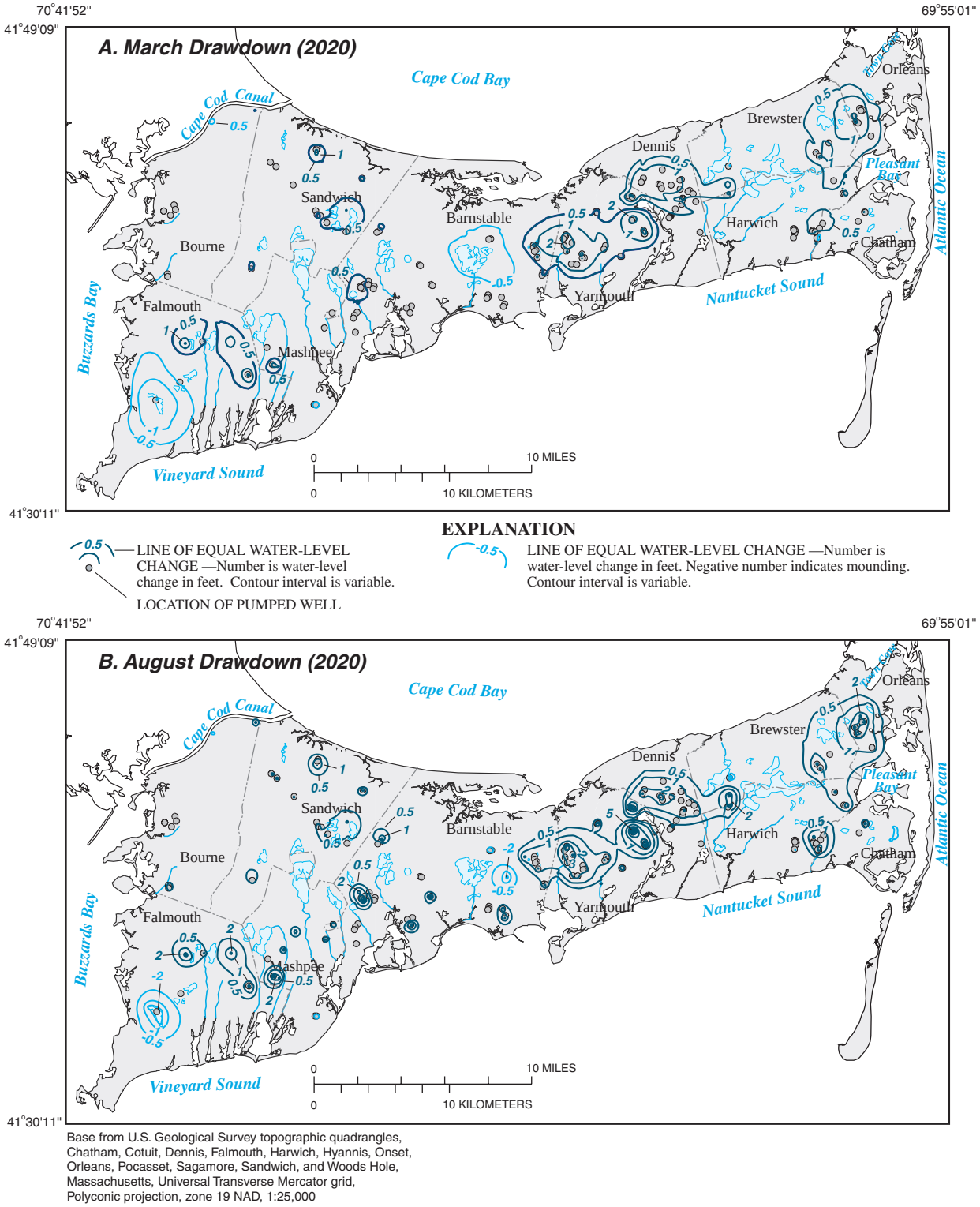

Base from U.S. Geological Survey topographic quadrangles, Chatham, Cotuit, Dennis, Falmouth, Harwich, Hyannis, Onset, Orleans, Pocasset, Sagamore, Sandwich, and Woods Hole, Massachusetts, Universal Transverse Mercator grid, Polyconic projection, zone 19 NAD, 1:25,000

Figure 19. Drawdowns associated with future (2020) pumping in *A*, March of an average year; and *B*, August of an average year in the Sagamore and Monomoy flow lenses, Cape Cod, Massachusetts.

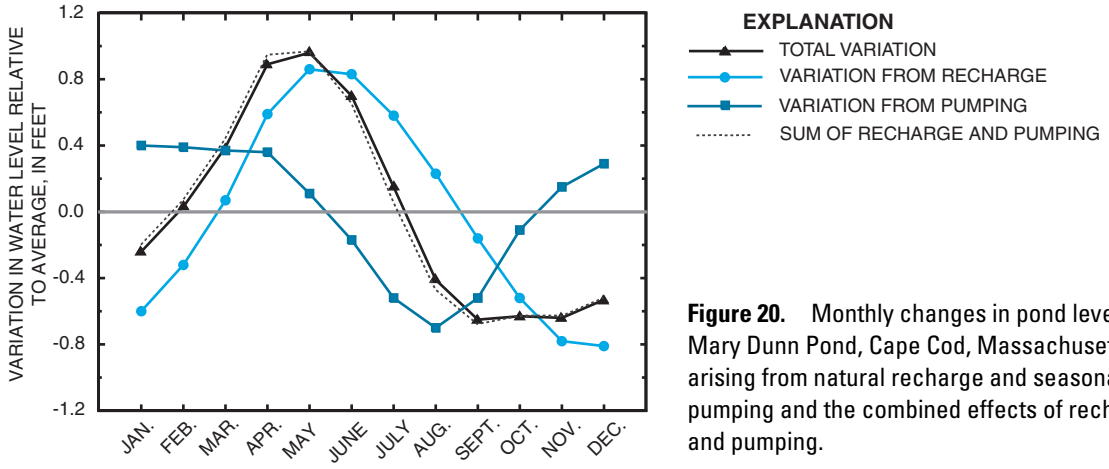

Figure 20. Monthly changes in pond levels at Mary Dunn Pond, Cape Cod, Massachusetts, arising from natural recharge and seasonal pumping and the combined effects of recharge and pumping.

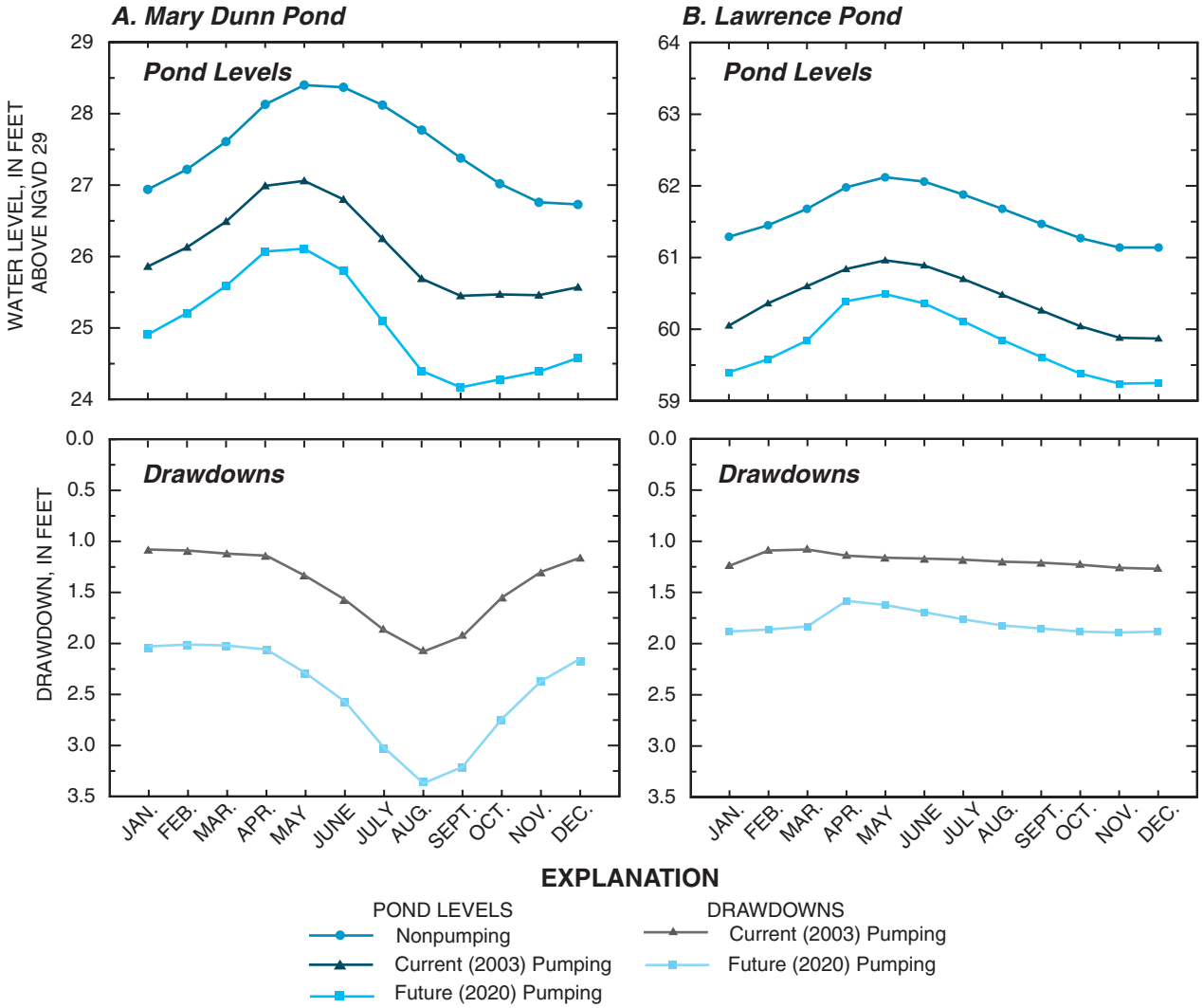

Figure 21. Monthly changes in pond levels and drawdowns at *A*, Mary Dunn; and *B*, Lawrence Ponds, Cape Cod, Massachusetts, arising from natural recharge and current (2003) and future (2020) monthly seasonal pumping.

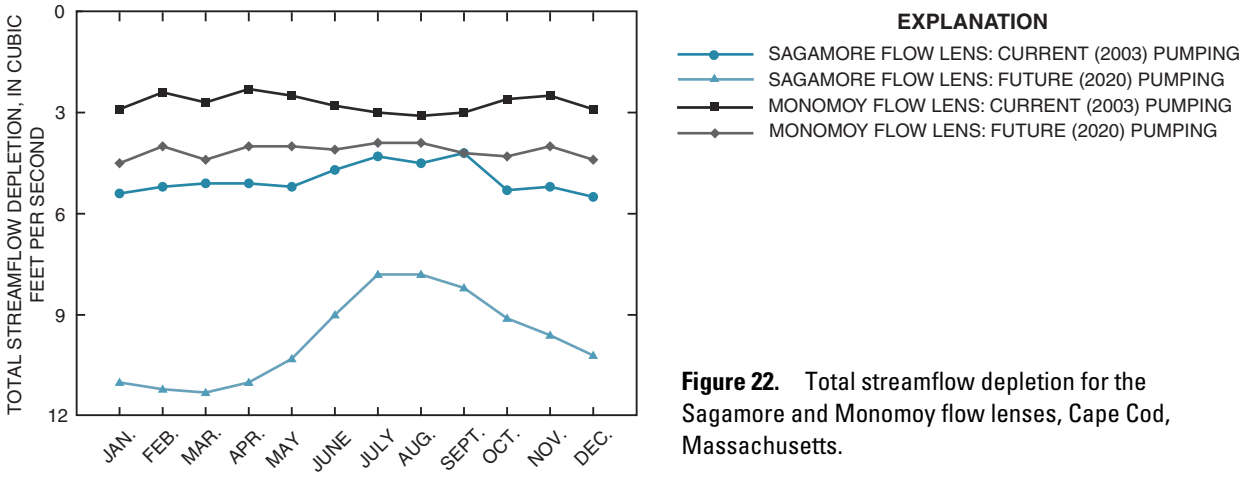

Figure 22. Total streamflow depletion for the Sagamore and Monomoy flow lenses, Cape Cod, Massachusetts.

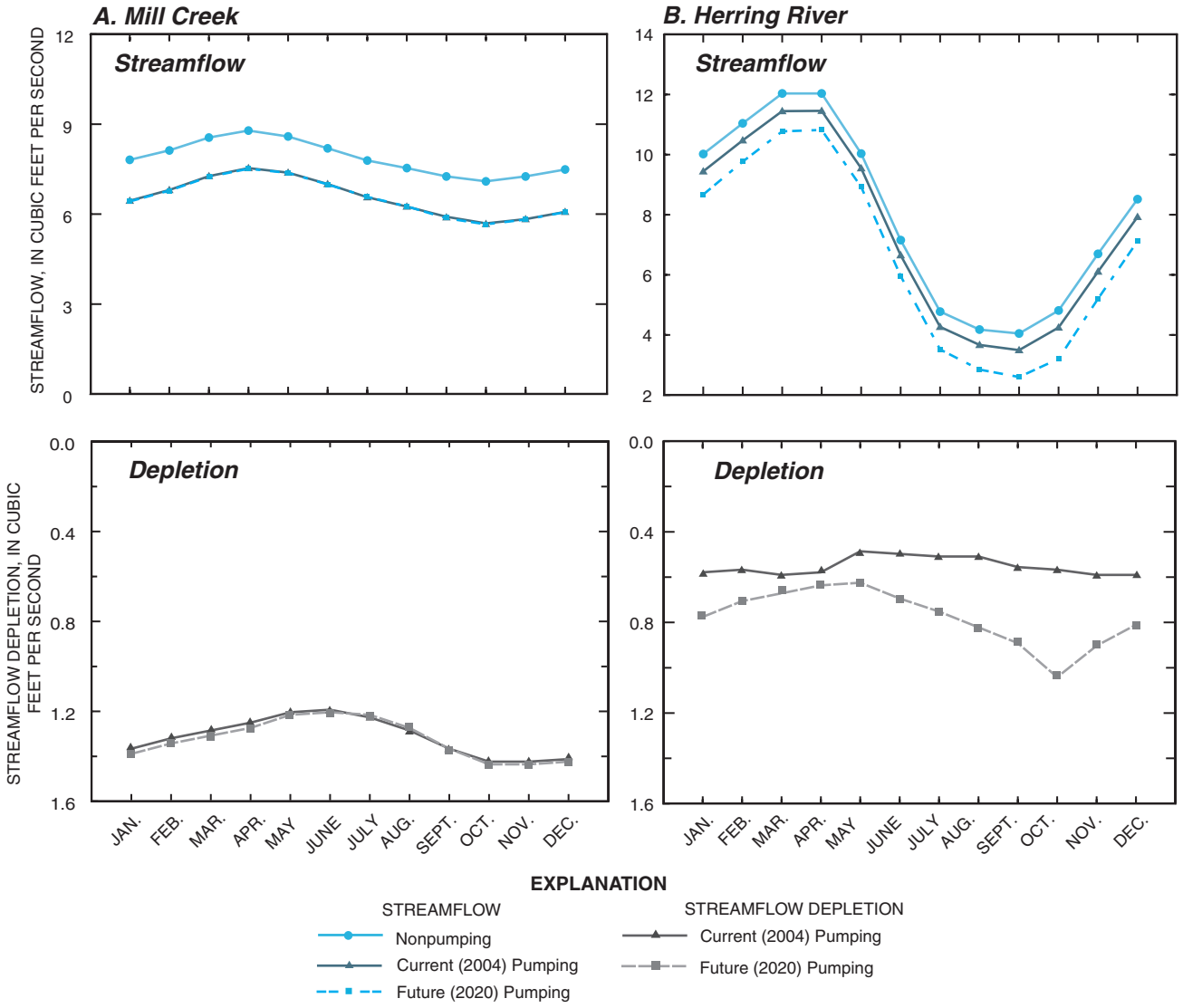

Figure 23. Monthly changes in streamflow and streamflow depletion for nonpumping, current (2003), and future (2020) pumping conditions at *A*, Mill Creek (Shawme Pond Outlet) and *B*, the Herring River, Cape Cod, Massachusetts.

Annual and Seasonal Conditions

Seasonal variations in natural recharge over multiyear time scales cause large fluctuations in water levels in the aquifers underlying the flow lenses, more than 10 ft in some areas between periods of drought and periods of high recharge. In addition to natural fluctuations, the seasonal effects of pumping also affect water levels over time. An average of about 17.2 Mgal/d of water is withdrawn during the seven off-season months (October–April) and about 39.9 Mgal/d is withdrawn during the five in-season months (May–September). In-season and off-season pumping stresses decrease water levels in the aquifer; however, water-level fluctuations during an extended period of time are controlled primarily by changes in recharge, and therefore are similar for nonpumping, current (2003) pumping, and future (2020) pumping conditions (fig. 24*A*). At Mary Dunn Pond, drawdowns arising from current in-season and off-season pumping, relative to nonpumping conditions, differ by about 0.6 ft; those seasonal differences generally are similar through time (fig. 24*B*). Although in-season and off-season pumping rates are the same in all years, current drawdown relative to a nonpumping condition changes over time (fig. 24*B*). In-season drawdowns range from about 1.5 to 2.2 ft; the largest drawdowns occur during year 12, the period when water levels are lowest (fig. 6*B*). For future pumping, differences in drawdowns associated with in-season and off-season pumping range from 0.4 to 1.1 ft (fig. 24*B*). Drawdowns associated with in-season pumping range from 2.2 to 3.5 ft; the largest drawdown occurs during a simulated drought when water levels are lowest for nonpumping and current and future pumping conditions (year 12 in simulation), which is similar in scale to the drought of the mid-1960s (figs. 6*B* and 24*B*).

The results indicate that the effects of seasonal pumping are largest, relative to nonpumping conditions, during periods of drought. The largest effects of pumping would, therefore, be expected when water levels already are lower because of natural changes in recharge. Drawdowns associated with current (2003) in-season pumping during a drought are shown in figure 25*A*; the period represented, which corresponds to September of a dry year within a number of successive dry years, is analogous in scale and duration to the drought of the mid-1960s (fig. 6) and represents the period of lowest simulated water levels. The largest seasonal drawdowns, relative to nonpumping conditions, because of current pumping, exceed 6 ft in Sandwich, 5 ft in Dennis and near the border of Harwich and Chatham, and 3 ft in Yarmouth (fig. 25*A*). The largest additional drawdowns, relative to current water levels, resulting from future (2020) pumping, exceed 3 ft in Yarmouth and Orleans, where large increases in pumping are projected, and 2 ft in Dennis and Harwich (fig. 25*B*). These drawdowns represent additional lowering of the water table beyond the water-level decreases, relative to average conditions, resulting from successive dry years. As an example, the combined effect of simulated drought conditions and seasonal pumping at Mary Dunn Pond results in a total decrease of 10.6 ft from average pond levels—about 6.9 ft resulting from lower areal recharge, about 2.3 ft from current pumping, and about 1.4 ft from additional pumping in the future.

Annual and seasonal variations in recharge also cause large changes in streamflows; total streamflow in the Sagamore and Monomoy flow lenses can be nearly three times larger in wet years than in dry years (table 3). Seasonal pumping also affects streamflow; however, changes in natural recharge are the primary control on stream fluctuations (fig. 26*A*). Changes in flow in Mill Creek (at the outlet from Shawme Pond) are similar over time for nonpumping conditions and both current (2003) and future (2020) pumping conditions (fig. 26*A*). Current pumping decreases streamflow by about 1.2 ft^3/s (fig. 26*B*); differences in streamflow depletion are only about 0.1 ft^3/s between in-season and off-season conditions. This small difference indicates that seasonal pumping does not cause substantial seasonal differences in streamflow depletion (fig. 26*B*). Future pumping has a similar effect on streamflow because large increases in pumping are not projected for the area near Mill Creek (fig. 26*B*).

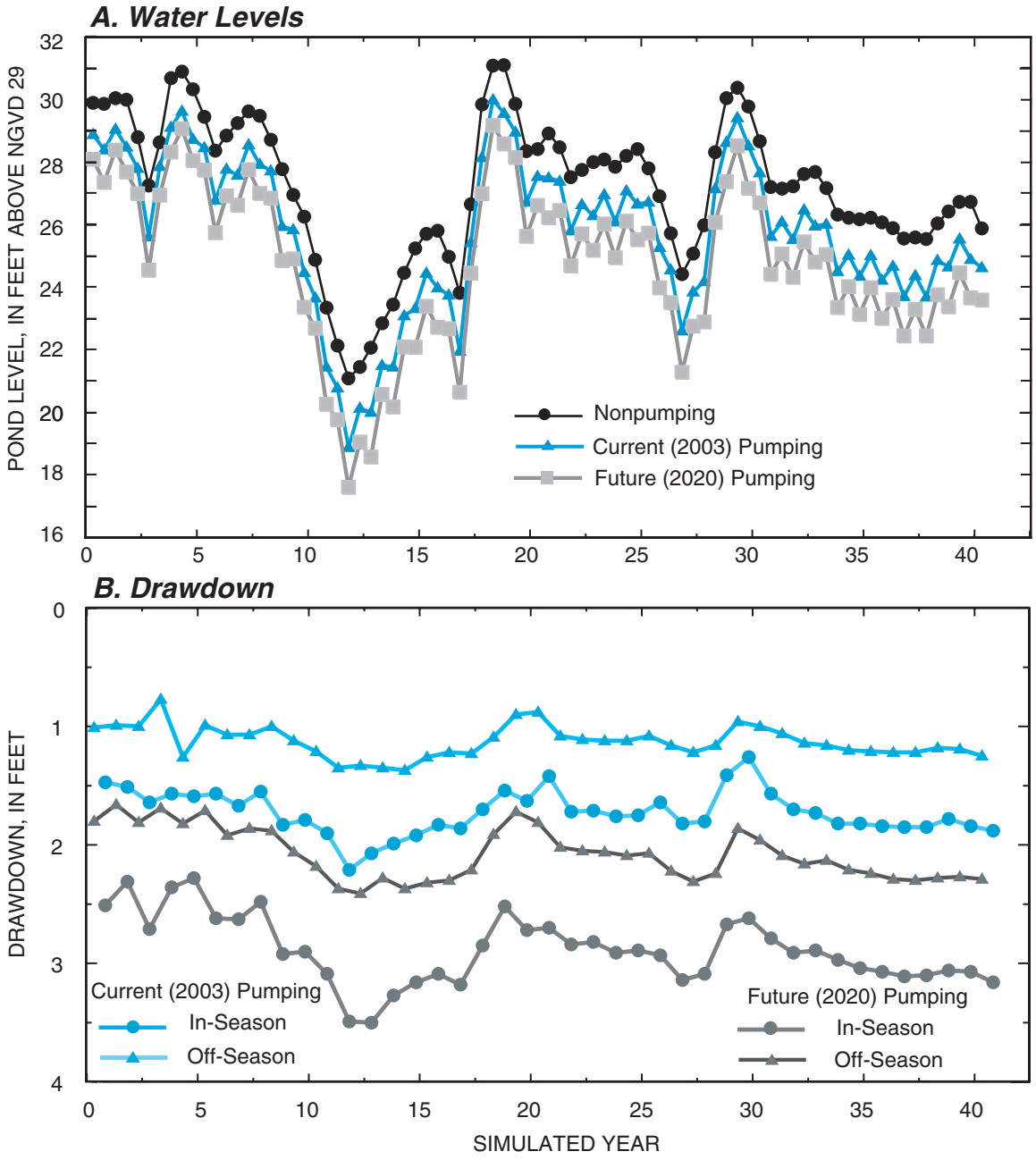

Figure 24. Seasonal changes in pond levels and drawdowns over a 40-year period for nonpumping, current (2003), and future (2020) pumping conditions at Mary Dunn Pond, Cape Cod, Massachusetts.

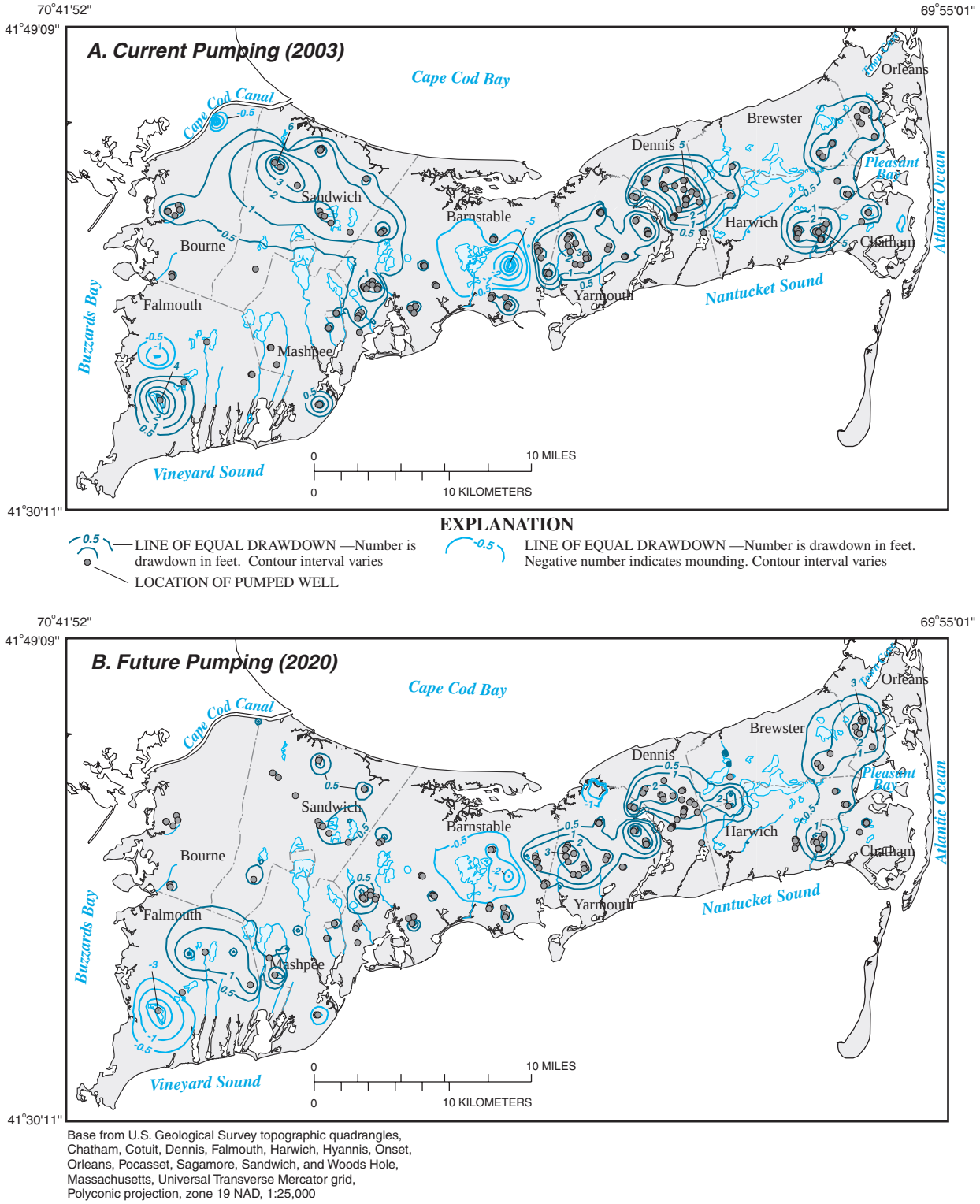

Base from U.S. Geological Survey topographic quadrangles, Chatham, Cotuit, Dennis, Falmouth, Harwich, Hyannis, Onset, Orleans, Pocasset, Sagamore, Sandwich, and Woods Hole, Massachusetts, Universal Transverse Mercator grid, Polyconic projection, zone 19 NAD, 1:25,000

Figure 25. Drawdowns associated with seasonal pumping under drought conditions for *A*, current (2003) pumping; and *B*, future (2020) pumping in the Sagamore and Monomoy flow lenses, Cape Cod, Massachusetts.

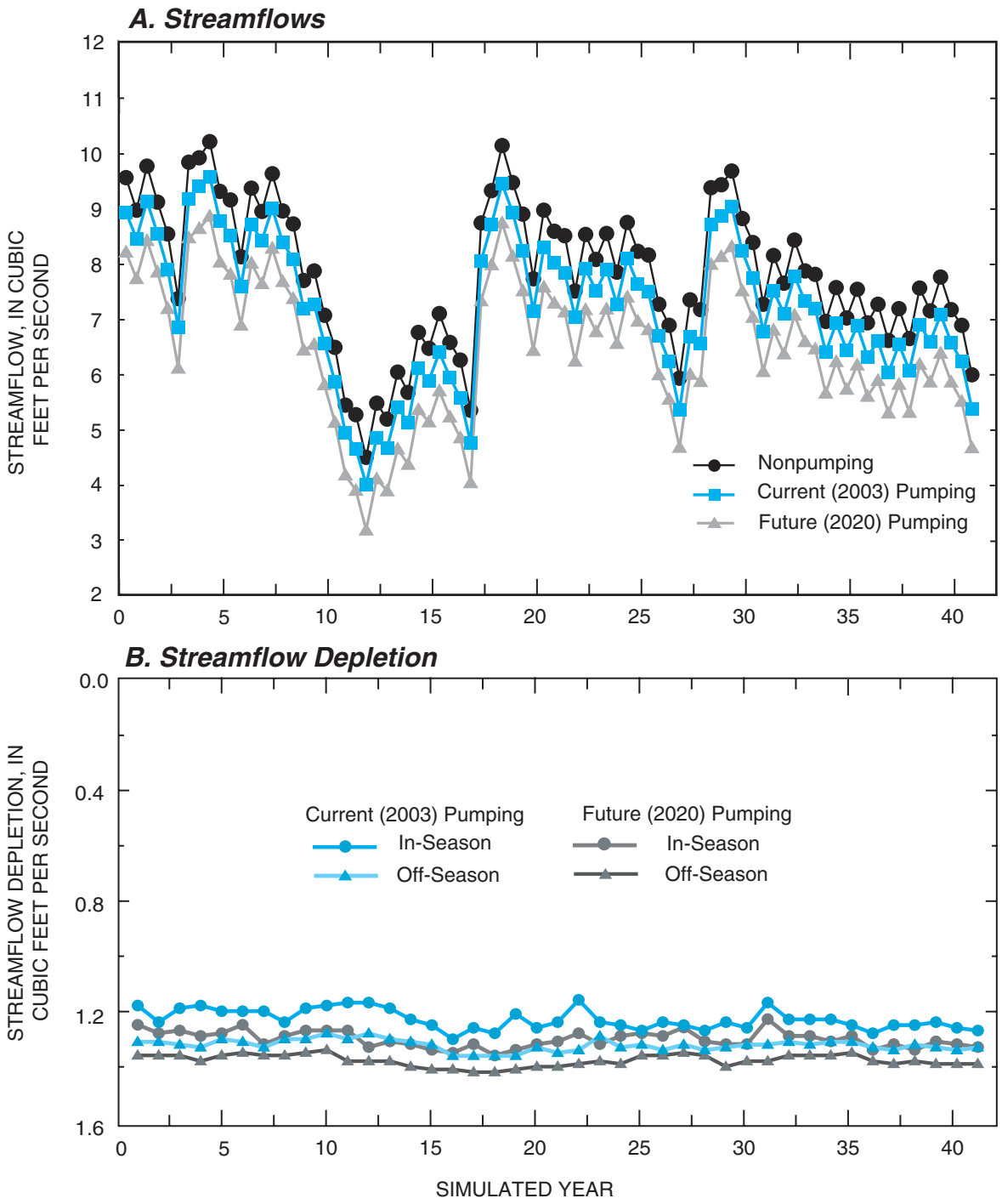

Figure 26. Seasonal changes in streamflow levels and streamflow depletion for Mill Creek (outlet to Shawme Pond) during a 40-year period for nonpumping, current (2003), and future (2020) pumping conditions, Cape Cod, Massachusetts.

Summary

The unconsolidated sediments underlying Cape Cod, Massachusetts, compose an aquifer system that is the sole source of water to local communities. The population of the region has more than doubled since 1970 and is much larger in the summer months than in the winter. These population increases have resulted in substantial changes in land-use patterns and large increases in the demand for potable drinking water. The effects of urbanization on the water supply include adverse effects of land use on water quality in the aquifer and increases in pumping that can adversely affect surface-water resources. These environmental effects are particularly important in the Sagamore and Monomoy flow lenses, which are the largest and most populous of the six flow lenses that compose the aquifer system underlying Cape Cod.

The U.S. Geological Survey, in cooperation with the Massachusetts Department of Environmental Protection, has conducted a study of the water resources of the Sagamore and Monomoy flow lenses. Specifically, the objectives of the investigation were to (1) determine areas contributing recharge to production wells in the region, (2) evaluate the long-term average effects of pumping on the hydrologic system, and (3) assess the combined effects of time-varying recharge and pumping stresses on the hydrologic system, particularly on pond levels and streamflows. Various types of data were compiled for the investigation including (1) lithologic data from boreholes, (2) hydrologic data regarding precipitation, ground-water levels, pond stages, and streamflows, and (3) data regarding water use for local communities. This information was incorporated into numerical ground-water-flow models of the Sagamore and Monomoy flow lenses. Two sets of pumping scenarios were analyzed, pumping conditions that reflect current (2003) water demands and pumping conditions that reflect projected water demands in the year 2020. Models were developed that simulated steady-state conditions as well as transient conditions with time-varying recharge and pumping stresses. Hydrologic changes over two sets of time scales were evaluated: (1) a monthly time scale incorporating monthly changes in pumping and recharge during an average year and (2) a multiyear time scale incorporating annual and seasonal changes in recharge and seasonal changes in pumping.

Recharge is the sole source of water to the aquifer system. On average, about 355 Mgal/d of water recharges the regional aquifer system, about 252 Mgal/d in the Sagamore flow lens and about 103 Mgal/d in the Monomoy flow lens. Ground water flows through the aquifer and discharges at the coast (about 66 percent) and into streams (28 percent); about 25 percent of ground water flows through kettle-hole ponds prior to discharging. Currently (2003), about 24.9 Mgal/d, or about 7 percent of total recharge, is withdrawn for water supply; most (about 85 percent) of the water is returned to the aquifer as wastewater return flow. The net loss of water from the hydrologic system is about 1 percent. A total of about 17 mi^2 of the water-table surface contributes water directly to production wells; this area corresponds to about 6 percent of total area that receives recharge in the region. Of the total volume of water withdrawn from the pumped wells, about 90 percent comes from direct recharge from the water table; the remaining 10 percent flows through kettle-hole ponds prior to reaching the wells. Pumping is projected to increase to 38.5 Mgal/d in 2020; the area at the water table contributing recharge to production wells is projected to increase to about 24 mi^2 in 2020.

Pumping affects the hydrologic system by drying vernal pools, lowering pond stages, and depleting streamflows. Under steady-state, or long-term-average, conditions, current (2003) pumping results in a maximum drawdown of about 4 ft in areas with large amounts of pumping. Projected future (2020) increases in pumping may result in maximum additional drawdowns of about 2 ft in the same areas. For current (2003) and future (2020) pumping, total streamflows in the region are projected to decrease by about 6 ft^3/s and 12 ft^3/s (about 4 and 8 percent of total streamflow), respectively.

Recharge varies both monthly and over multiyear time scales. In an average year, recharge is highest in March and lowest in August and September. Historically, estimated recharge rates vary by more than a factor of 2 between wet and dry years. These natural changes in recharge affect ground-water levels, pond stages and streamflows. Ground-water levels can change by more than 2 ft and pond levels can vary by 1 to 2 ft in response to natural changes in recharge over an average year. Over longer (multiyear) time scales, water levels can vary by more than 10 ft between wet and dry years in some areas, such as near ground-water divides. During an average year, flows in streams also vary in response to changes in recharge. As an example, flow in the Quashnet River, the largest stream in the region, varies by more than 7 ft^3/s, which represents about 25 percent of average streamflow, in response to monthly changes in recharge; streamflows in the Quashnet River can vary by more than 17 ft^3/s between periods of successive wet and dry years.

Seasonal variations in pumping also contribute to seasonal changes in water levels and streamflow. Pumping is larger in the summer months, when seasonal populations are highest, than in winter; average pumping ranges from about 51.2 Mgal/d in July to about 14.8 Mgal/d in March. The largest ground-water withdrawals are when recharge to the aquifer is lowest; thus, the effects of pumping on the hydrologic system vary seasonally. In an average year, maximum drawdowns of nearly 7 ft occur in August; drawdowns in March for these same areas are less, about 3 ft. Future (2020) pumping is predicted to cause additional drawdowns exceeding 2 and 5 ft in March and August, respectively. The seasonal pumping effects add to the effects caused by natural changes in recharge. Declines in pond levels associated with pumping are largest in the late summer when most pumping occurs; the effects depend on various factors, including the size of the pond, the location of the pond in the flow system, and the proximity of the pond to pumping wells. Large ponds in areas with little pumping likely would not be affected by seasonal pumping, whereas small ponds near pumping wells would be affected. As an example, drawdowns because of pumping near Mary Dunn Pond, which is a small pond near various production wells in an area with large regional drawdowns, ranges between 1 and 2 ft over an average year with the largest drawdowns in August; future projected (2020) increases in pumping are estimated to cause between 2 and 3.5 ft of total pumping-induced drawdown at the pond. The effects of pumping on streamflows do not vary substantially over an average year and generally do not exceed 1–2 ft^3/s for streams in the region.

Drawdowns from seasonal pumping are largest during periods of drought caused by lower than average natural recharge in successive years. At Mary Dunn Pond, maximum drawdowns associated with seasonal pumping vary from less than 2.5 ft during wet periods to more than 3.5 ft during dry periods. These drawdowns add to the changes in water levels caused by changes in natural recharge, which can be on the order of 5–10 ft. As an example, under conditions of in-season 2020 pumping, water levels in Mary Dunn Pond are predicted to decline by about 10.6 ft relative to conditions of no pumping and average recharge; of this total decline, about 6.9 ft are predicted to result from lower than average (drought) recharge, about 2.3 ft from current (2003) pumping, and about 1.4 ft from future (2020) increases in pumping. The effect of seasonal pumping on streamflows does not vary substantially between wet and dry periods and typically is less than 2 ft^3/s for streams in the region.

Changes in pond levels and streamflows arising from seasonal effects of pumping typically are substantially less than the variability caused by changes in natural recharge. The results indicate that the primary effect of pumping on the hydrologic system is the decrease in pond levels in some areas. The effect of pumping is substantially less than the effects of changes in natural recharge over average monthly and multi-year time scales, although seasonal pumping can exacerbate the adverse effects of droughts on ponds in some areas, particularly near areas with concentrated pumping far from hydrologic boundaries.

Acknowledgments

The authors wish to thank Byron Stone, a glacial geologist with the U.S. Geological Survey, for his invaluable assistance in interpreting the geologic history of Cape Cod and developing the depositional model used to develop the ground-water-flow models used in this investigation. A number of groups, both public and private, have provided data necessary for the completion of this investigation. Specifically, the authors would like to acknowledge the assistance of Joseph Cerutti of the MDEP Drinking Water Program, staff at the MDEP Southeast Region, local water suppliers, and personnel at the Cape Cod Commission. The authors also thank staff at the Camp Edwards Impact Area Ground Water Study (IAGWS), the Air Force Center for Environmental Excellence (AFCEE), Jacobs Engineering Group, AMEC, Inc., and EarthTech Inc. for their assistance in the acquisition of data.

References Cited

LeBlanc, D.R., Guswa, J.H., Frimpter, M.H., and Londguist, C.J., 1986, Ground-water resources of Cape Cod, Massachusetts: U.S. Geological Survey Hydrologic Atlas 692, 4 pls.

Massachusetts Department of Environmental Protection, 2004, Groundwater and wellhead protection, accessed September 23, 2004, at URL http://www.mass.gov/dep/brp/dws/protect.htm

Masterson, J.P., Stone, B.D., Walter, D.A., and Savoie, Jennifer, 1997a, Hydrogeologic framework of western Cape Cod, Massachusetts: U.S. Geological Survey Hydrologic Atlas HA-741.

Masterson, J.P., Walter, D.A., and Savoie, Jennifer, 1997b, Use of particle tracking to improve numerical model calibration and to analyze ground-water flow and contaminant migration, Massachusetts Military Reservation, western Cape Cod, Massachusetts: U.S. Geological Survey Water-Supply Paper 2482, 50 p.

Oldale, R.N., 1992, Cape Cod and the islands—The geologic story: East Orleans, MA, Parnassus Imprints, 205 p.

Oldale, R.N., and Barlow, R.A., 1986, Geologic map of Cape Cod and the Islands, Massachusetts: U.S. Geological Survey Miscellaneous Investigations Series Map I-1763, scale 1:100,000.

Oldale, R.N., and O'Hara, C.J., 1984, Glaciotectonic origin of the Massachusetts coastal end moraines and a fluctuating late Wisconsinan ice margin: Geological Society of America Bulletin, v. 95, p. 61–74.

Uchupi, Elazar, Giese, G.S., and Aubrey, D.G., 1996, The late Quaternary construction of Cape Cod, Massachusetts—A reconsideration of the W.M. Davis Model: Geological Society of America Special Paper 309, 69 p.

APPENDIX 1

Contents

Figures

Tables

Model Development

Numerical ground-water-flow models were developed for the Sagamore and Monomoy flow lenses on Cape Cod, Massachusetts. The finite-difference ground-water modeling software MODFLOW-2000 (Harbaugh and others, 2000; McDonald and Harbaugh, 1988) was used to simulate the hydrologic systems of each of the two flow lenses. Two sets of models were developed for each flow lens: steady-state models that represent long-term average hydrologic conditions and transient models that simulate dynamic changes in hydrologic conditions in response to time-varying recharge and pumping stresses. Two time scales were simulated: (1) a monthly time-scale that represents monthly changes in recharge and pumping during an average year and (2) a semiannual time scale that incorporates both seasonal changes in recharge over a multiyear (1941–95) time scale and seasonal changes in pumping. The particle-tracking algorithm MODPATH4 (Pollock, 1994) was used to simulate advective transport in the aquifer under steady-state conditions; particle tracking was used to estimate sources of water to wells and natural receptors. Graphic display of spatial model results was done by using a version of the software suite MODTOOLS that was modified to work with MODFLOW-2000 (Orzol, 1997).

Steady-state model development was done in three stages: (1) the formulation of model grids, boundaries, and hydrologic stresses; (2) sensitivity analyses, based on simplified aquifer properties, to determine the relative importance of intrinsic aquifer and boundary properties on simulated water levels; (3) incorporation of lithologic zonations, representing depositional models of the region, and initial estimates of aquifer properties, into the models; and (4) trial-and-error changes in aquifer and boundary properties to provide the best fit of simulated long-term-average water levels and streamflows to the corresponding measured values (model calibration). Transient models were developed from the steady-state models by incorporating time-varying recharge and pumping stresses; adjustments were made to initial storage parameters to provide the best fit between simulated and measured changes in water levels and streamflows. Intrinsic aquifer and boundary properties were not altered from those in the steady-state models during calibration of the transient models.

Steady-State Models

Steady-state models operate on the assumption of constant recharge and pumping stresses over time and represent long-term-average hydrologic conditions in the aquifer. Although water levels and flows in the aquifer system change over time in response to changes in recharge, advective transport through the aquifer system occurs over a time scale that can be on the order of decades. Therefore, advective flow patterns are strong indicators of long-term average hydrologic conditions in the aquifer (Masterson and others, 1997b; Walter and Masterson, 2003). As a result, steady-state models can be used to simulate advective transport and to estimate areas contributing recharge to wells and natural receptors.

Grid and Boundaries

The finite-difference model grids consist of a series of orthogonal model cells used to simulate aquifer sediments. A detailed discussion of the use of finite-difference equations to simulate ground-water flow is presented in McDonald and Harbaugh (1988). Model inputs include intrinsic characteristics in each model cell, such as hydraulic conductivity. Boundary conditions are applied at some model cells to simulate hydrologic features, including streams and coastal estuaries.

Model Discretization

The total active modeled area for the study area is about 361 mi^2: 246 mi^2 in the Sagamore flow lens and 106 mi^2 in the Monomoy flow lens (fig. 1-1*A*). The finite-difference model grid representing the Sagamore flow lens consists of 246 rows, 365 columns, and 20 layers; the model grid representing the Monomoy flow lens consists of 164 rows, 220 columns, and 20 layers. A total of 847,590 cells—or about 47 percent of the total—are active in the Sagamore model and a total of 366,901 cells—or about 51 percent of the total—are active in the Monomoy model. Both grids have a uniform horizontal discretization of 400 by 400 ft and are coincident where the models overlap.

Both models have the same vertical discretization (fig. 1-1*B*, table 1-1). The upper 17 layers extend to a uniform altitude of 100 ft below NGVD 29 and have uniform thicknesses of 10 ft. The top model layer (layer 1) has a uniform bottom altitude of 60 ft above NGVD 29; each subsequent layer has a bottom altitude 10 ft lower than the bottom of the overlying layer. Layer 18 is 40 ft thick and extends from 100 to 140 ft below NGVD 29; layer 19 is 100 ft thick and extends to 240 ft below NGVD 29. The lowest layer (layer 20) varies in thickness and extends to a no-flow boundary at the bedrock surface: as deep as 519 ft below NGVD 29 in the Sagamore model and 525 ft below NGVD 29 in the Monomoy model (table 1-1). Layer thicknesses for layers 12 through 20 are constant except where truncated by bedrock (fig. 1-1*B*). The top seven layers are above NGVD 29. The top of the model layer is the model-calculated water table in those areas where the water table is within the model layer; model cells are dry in areas where the model-calculated water table is below the bottom of the layer. The rewetting capability of MODFLOW-2000, which allows for model cells to dry and rewet during a simulation, was used to simulate the unconfined water table.

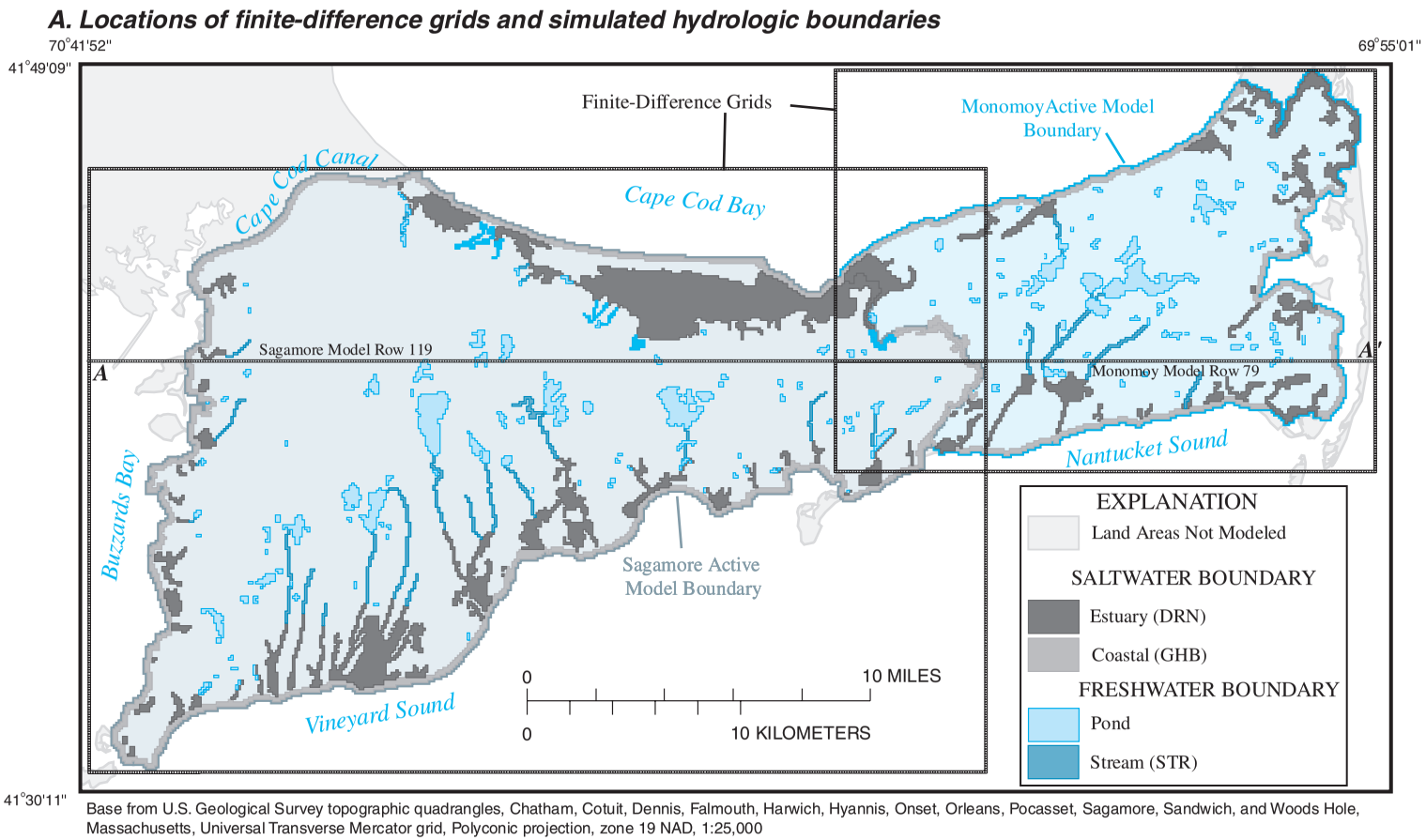

Figure 1-1. *A*, Locations of finite-difference grids and simulated hydrologic boundaries; and *B*, vertical discretization for Sagamore and Monomoy flow lenses and bedrock altitude along model row 119, central and western Cape Cod, Massachusetts.

Table 1-1. Vertical layering and ranges of horizontal hydraulic conductivity for the Sagamore and Monomoy flow models, central and western Cape Cod, Massachusetts.

[Ponds are represented with horizontal hydraulic conductivities of 100,000 ft/d; ft, foot, ft/d, foot per day]

Model layer	Sagamore flow model		Monomoy flow model	
	Maximum depth of model layer relative to NGVD 29 (ft)	Range of horizontal hydraulic conductivity (ft/d)	Maximum depth of model layer relative to NGVD 29 (ft)	Range of horizontal hydraulic conductivity (ft/d)
1	60	350–130	Dry	300–130
2	50	350–130	Dry	300–130
3	40	350–120	Dry	300–120
4	30	330–100	30	250–100
5	20	320–100	20	250–100
6	10	300–100	10	230–100
7	0	300–100	0	300–70
8	-10	300–100	-10	200–40
9	-20	290–70	-20	200–30
10	-30	270–50	-30	150–30
11	-40	270–50	-40	150–20
12	-50	220–30	-50	130–20
13	-60	220–30	-60	130–20
14	-70	210–30	-70	100–20
15	-80	210–30	-80	210–10
16	-90	190–20	-90	190–10
17	-100	190–20	-100	70–10
18	-140	170–10	-140	70–10
19	-240	150–10	-240	60–10
20	-519	30–10	-525	30–10

The interface between fresh and saltwater is simulated as a no-flow boundary in the layers below NGVD 29 and as a specified-head boundary at the seabed along the coast. Ground water flows upward along the interface and discharges through the seabed near the coast. This flow pattern is consistent with the conceptual model of the flow system (fig. 5*B*) and observations of coastal discharge within Red Brook Harbor, which is along the western shore of the Sagamore flow lens (McCobb and others, 2002). The interface position is fixed in the models and does not change in response to pumping or recharge stresses. This assumption is based on previous modeling of the salt/freshwater interface indicating that pumping was not sufficient to cause saltwater intrusion into the aquifers beneath the Sagamore and Monomoy flow lenses (Masterson and Barlow, 1997). The interface is truncated from below by bedrock and is represented laterally as a vertical no-flow boundary (fig. 1-1*B*). To test the assumption of a vertical interface, a version of the Monomoy flow model was produced that had an interface position based on a Ghyben-Herzberg relation (Reilly and Goodman, 1985) between simulated heads and the interface position. Comparisons showed negligible differences between simulated heads for the two interface positions and, therefore, the simpler, vertical interface position was used. There is an implicit no-flow boundary between the Sagamore and Monomoy flow models beneath the Bass River, although freshwater extends to bedrock in that area and there is a hydraulic connection between the two aquifer systems. The assumptions are that (1) no water is transmitted across the regional ground-water divide formed by upward flow into the Bass River and (2) withdrawals of ground water near this boundary do not reverse hydraulic gradients and induce flow across the boundary. A test of these assumptions is discussed in the following section.

Hydrologic Boundaries

The hydrologic boundaries of the flow system, through which all natural discharge occurs, are simulated as head-dependent flux boundaries. Heads are specified at the boundaries and discharge fluxes are calculated by the model on the basis of the hydraulic gradient between the calculated head in the adjacent model cell and the specified-boundary head and the conductance at the boundary face. Specified-head boundaries are used to simulate coastal boundaries, inland estuaries, and streams (fig. 1-1*A*). Coastal saltwater boundaries were simulated by the General Head Boundary Package (GHB) (McDonald and Harbaugh, 1988; fig. 1-1*A*); general-head boundaries can both receive water from and contribute water to the aquifer. Estuaries, which are saltwater boundaries that extend inland from the coast, were simulated by the Drain Package (DRN) (McDonald and Harbaugh, 1988); drain boundaries are specified-head boundaries that can only receive water from the aquifer (fig. 1-1*A*). Coastal boundaries and estuaries are discharge boundaries that, in the case of these specific models, should only receive ground water from the simulated aquifer. In these simulations, DRN and GHB boundaries function identically. The GHB boundary was used in some areas to confirm that no simulated induced infiltration from saltwater boundaries was occurring near pumping wells. In all simulations, no water entered the aquifer from head-dependent flux boundaries, which supports the assumptions used in simulating a no-flow boundary beneath the Bass River. If pumping was sufficient to reverse hydraulic gradients between the well and hydrologic boundary, the aquifer system would receive water from the boundary.

Streams were simulated using the Stream Routing Package (STR) (Prudic, 1989; fig. 1-1*A*); this head-dependent boundary condition allows ground-water discharge (gaining stream reaches) as well as infiltration into the aquifer (losing stream reaches). Representing streams using the STR Package allows for the simulation of losing conditions downgradient of pond outlets or near pumping wells. The ground-water models simulate base-flow conditions in the streams; surface-water runoff is negligible on Cape Cod owing to the sandy permeable soils, and base-flow conditions predominate. Most streams on

Cape Cod are gaining; however, losing conditions can develop downstream from pond outlets and near pumping wells. The STR package also accounts for water that is routed through stream networks. This routing capability is used in the models to route water from pond outlets into receiving streams.

The simulated discharge at head-dependent, saltwater boundaries is a function of the conductance or vertical leakance, which represents resistance to flow across the seabed from fine-grained marine sediments. A leakance value of 0.02 ft/d/ft and a seabed thickness of 10 ft were used to determine conductances of coastal seabed boundaries. Leakances of 0.01 ft/d/ft were used for seabed conductances in estuaries, where it was assumed that low-permeability tidal mud was more prevalent than in open coastal waters. These vertical leakance values are consistent with the range of seabed leakance values of 0.0001 to 0.1 ft/d/ft reported for the near-shore sediments in the Kirkwood–Cohansey aquifer system, New Jersey (Nicholson and Watt, 1997) and values of 0.01 to 1.0 ft/d/ft reported for sandy sediments over most of the Atlantic Coast Plain (Leahy and Martin, 1993). Leakances of 1.0 ft/d/ft were used for streambed sediments; it was assumed that streambed sediments are sandier and have higher conductances than marine sediments.

The hydraulic heads used for coastal boundaries are based on tidal-cycle measurements from various coastal water bodies in the region (John Ramsey, Applied Coastal Systems, Inc., written commun., 2002) and from measurements made by the National Oceanic Atmospheric Administration (NOAA). The hydraulic heads of major coastal water bodies (simulated using the GHB Package) ranged from 1.11 ft above NGVD 29 in Nantucket Sound to 0.25 ft above NGVD 29 in the Cape Cod Canal. The departure of water levels from the NGVD 29 datum is attributed to sea-level rise since 1929 and to normal variations in tidal dynamics in different areas. The elevations used in inland estuaries (simulated using the DRN Package) ranged from 1.05 ft above NGVD 29 in Mill Pond in the town of Chatham, to 2.5 ft above NGVD 29 in Frost Fish Creek, also in Chatham. Estuaries can have larger mean tidal water levels because of constrictions in flow between estuaries and coastal water bodies and higher sea-bed elevations in upland estuaries. Versions of the models were developed that had a uniform boundary elevation of 0.0 ft above NGVD 29 to determine the effect of boundary elevation on the simulated ground-water system; comparisons showed that changes in the boundary elevations within the ranges used in the models had small, local effects on hydraulic gradients at the coastal boundaries but did not affect simulated water levels and flow directions in the aquifer. Streambed altitudes were determined from 10-ft topographic contours from USGS orthoquads; altitudes between contours were determined by using linear interpolation.

Ponds on Cape Cod generally are in direct hydraulic connection to the aquifer and are regions of the aquifer with no effective resistance to flow. As a result, ground-water flow lines converge towards ponds in upgradient areas, where water discharges to ponds, and diverge in downgradient areas, where ponds recharge the aquifer. In the models, ponds are simulated as areas of high hydraulic conductivity, 100,000 ft/d, which is about 3 orders of magnitude higher than hydraulic conductivities in the surrounding aquifer. This difference in hydraulic conductivity causes prefer-ential flow through the pond and simulates the observed effects that ponds have on ground-water flow in the aquifer system. Simulated pond geometries were based on bathymetries published by the Massachusetts Department of Fisheries and Wildlife (MDFW) (Massachusetts Department of Fisheries and Wildlife, 1993). Given the model discretization of 400 ft, ponds with areas of less than about 6 acres (about 2.6×10^5 ft^2) were not included in the models. The Horizontal Flow Barrier Package (Hsieh and Freckelton, 1992) was used to simulate resistance to flow across the pond bottoms implicitly; ponds generally are in good hydraulic connection to the aquifer and pond-bottom hydraulic conductivities of 300 ft/d were assumed. Some ponds also drain into nearby streams. In these cases, the pond outlet is simulated as a stream boundary with a large streambed conductance resulting in no effective resistance to flow; the water entering this stream reach is routed by the STR Package into a receiving stream. In the Monomoy flow lens, various ponds near the top of the water table are connected by artificial canals (fig. 5); these canals also are simulated by the STR Package to route water through the network of canals (figs. 1 and 1-1).

The top of the model is a model-calculated water table represented as a free surface. The bottom of the model is a no-flow boundary representing the contact between unconsolidated glacial sediments and impermeable bedrock. The altitude of the bedrock surface ranges from less than 100 to more than 500 ft below NGVD 29 (fig. 1-2).

Aquifer Characteristics

The water-transmitting properties of the aquifer sediments, as represented by hydraulic conductivity (K) and vertical anisotropy, are functions of lithology and differ according to grain size and the degree of sorting of the sediments. The relation between lithology and aquifer characteristics (hydraulic conductivity and vertical anisotropy) is based on reviews of aquifer-test information from the region conducted as part of this and previous investigations (Masterson and others, 1997b; Masterson and Barlow, 1997; Barlow, 1994; Barlow and Hess, 1993; Barlow and Dickerman, 2000, Moench, 1994). Hydraulic conductivities in the Cape Cod aquifer range from 10 to 350 ft/d. Hydraulic conductivity generally increases with increasing grain size: coarse sands and gravels typically have K values ranging from 300 to 350 ft/d, K values for medium to coarse sands generally range from 150 to 250 ft/d, fine sands typically have K values of 70 ranging from 130 ft/d, and very fine sands, silts and clays have K values ranging from 10 to 70 ft/d.

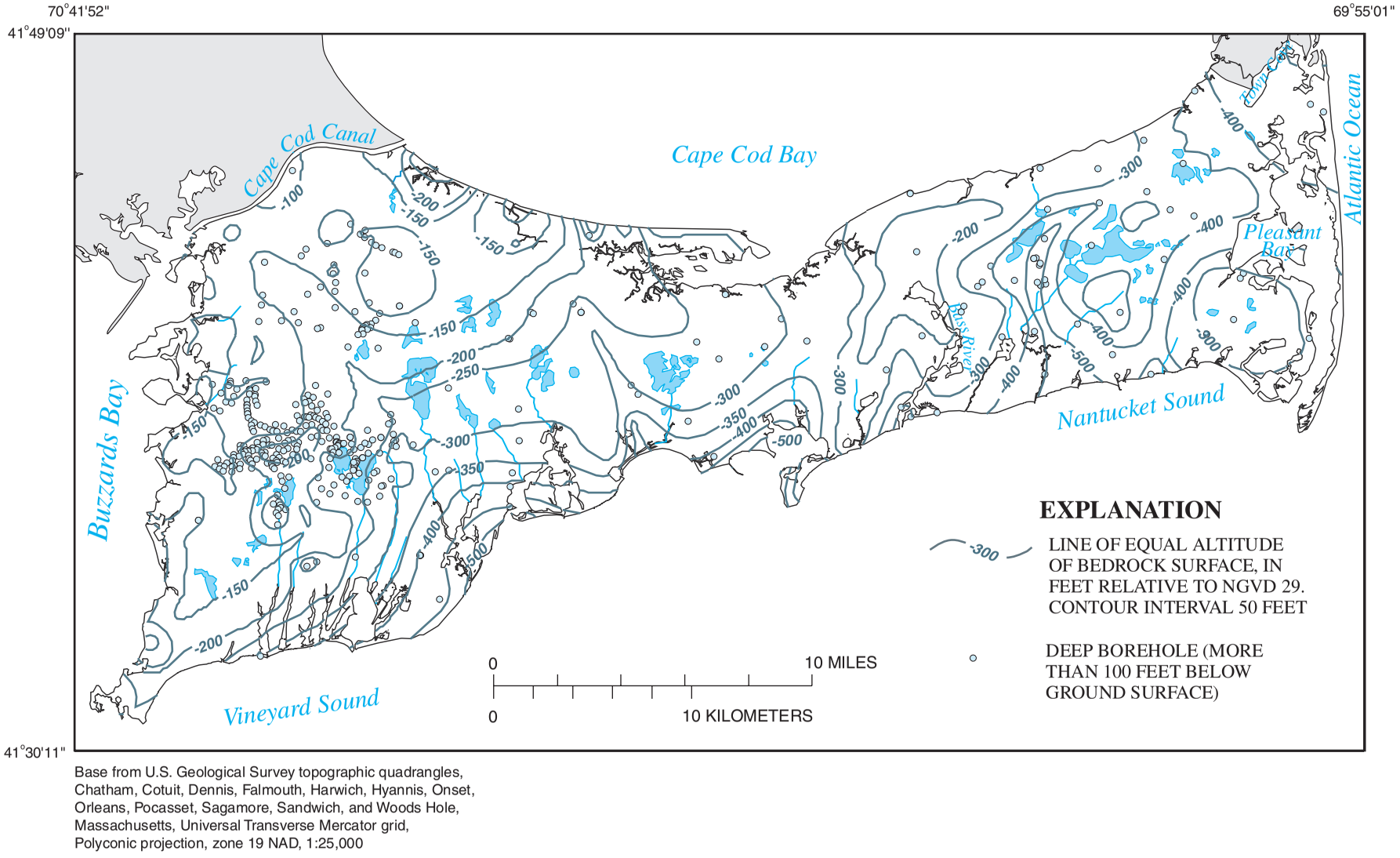

Base from U.S. Geological Survey topographic quadrangles, Chatham, Cotuit, Dennis, Falmouth, Harwich, Hyannis, Onset, Orleans, Pocasset, Sagamore, Sandwich, and Woods Hole, Massachusetts, Universal Transverse Mercator grid, Polyconic projection, zone 19 NAD, 1:25,000

Figure 1-2. Altitude of bedrock surface and locations of deep wells, central and western Cape Cod, Massachusetts.

The lithologies of aquifer sediments were estimated from well borings and the depositional model of the area. Drilling logs were assembled from a variety of sources including local water suppliers and consulting firms in the area in and around the MMR on western Cape Cod (fig. 1); geologic logs were compiled from the Installation and Restoration Program and the Camp Edwards Impact Area Ground Water Study. Drilling logs from deep [more than 100 ft below ground surface (bgs)] well borings were assembled into WELLARC, a geographic information system (GIS) database used to construct well logs and geologic sections (Leonard Orzol, U.S. Geological Survey, written commun., 2003). A total of 187 deep logs were assembled, 140 in the Sagamore flow lens and 47 in the Monomoy flow lens (fig. 1-2). A large number of deep drilling logs, many drilled to bedrock, were available for the area around the MMR from a series of large-scale drilling operations conducted as part of remedial investigations of the area since 1985. Well borings drilled to bedrock were used to refine the configuration of the bedrock surface beneath the aquifer (fig. 1-2); additional information used to map the bedrock surface included previous geophysical measurements conducted by the USGS (Byron Stone, U.S. Geological Survey, written commun., 1993).

The distribution of K in the models, which was adjusted during model calibration, reflects the depositional model developed for the region on the basis of the surficial geology, subsurface lithology, and the glacial history of the region. A summary of K values by model layer for the Sagamore and Monomoy models is given in table 1-1. The values of hydraulic conductivity in table 1 and figure 1-3 represent final values derived from trial-and-error calibration to best fit estimates of long-term-average water levels and streamflows estimated from measured values; calibration of the models is discussed in the section "Calibration to Measured Water Levels and Streamflows." Hydraulic conductivities generally decrease with depth and with increasing distances from the original source of the sediments (fig. 3), which is consistent with the fining down and fining southward sequences observed in the aquifer sediments (Masterson and others, 1997a). In the Sagamore model, K values decrease to the south and with depth within the Mashpee Plain sediments (figs. 1-3*A*–*C*). High-conductivity sediments along the south shore and to the east of the Buzzards Bay Moraine represent ice-contact deposits (figs. 1-3*A*–*B*; fig. 3). Also, K values in the Buzzards Bay Moraine are higher to the south (fig. 1-3*A*–*C*); this K distribution is supported by numerous lithologic logs that show coarser-grained sediments in those areas than in moraine sediments to the north. In the Monomoy model, hydraulic conductivities decrease to the southwest and with depth within the Harwich Plain sediments (figs. 1-3*A*–*C*). Coarser-grained sediments were simulated near kettle-hole ponds and collapse structures. Sediments assumed to represent fine-grained lake-bottom beds in the lowest layer of each model were assigned a K value of 10 ft/d, except near collapse structures (fig. 1-3*D*). Aquifer characteristics are summarized in table 1-2.

Vertical anisotropy (VA), which is the ratio of horizontal to vertical hydraulic conductivity, generally increases with decreasing hydraulic conductivity; general anisotropy values for glacial sediments range from 3:1 for coarse sands and gravels to 100:1 for clay (Masterson and others, 1997a; Masterson and Barlow, 1997). In the Sagamore and Monomoy models, sediments with K values between 250 and 350 ft/d have VA ratios of 3:1 to 4:1. Sediments with K values of between 200 and 250 ft/d have VA ratios of 4:1 to 6:1. VA ratios of 6:1 to 8:1 were assigned to sediments with K values between 150 and 200 ft/d and a VA ratio of 10:1 was assigned to sediments with K values less than 150 ft/d. Observations made during trial-and-error model calibrations done as part of this and previous investigations indicate that VA ratios generally do not have a substantial effect on regional water levels, flows, and advective transport patterns in the aquifer. A more quantitative analysis of model sensitivity to different model parameters, including VA ratios, is discussed in "Steady-State Model Calibration."

A uniform porosity of 0.35 was used in particle-tracking analyses. Porosity affects simulated traveltimes along advective transport paths in the Cape Cod aquifer but does not affect simulated water levels, flows, or advective transport patterns. The value of 0.35 is based on previous field and modeling investigations on Cape Cod (Garabedian and others, 1991; Walter and Masterson, 2003) and is consistent with published values for glacial sediments (Freeze and Cherry, 1979).

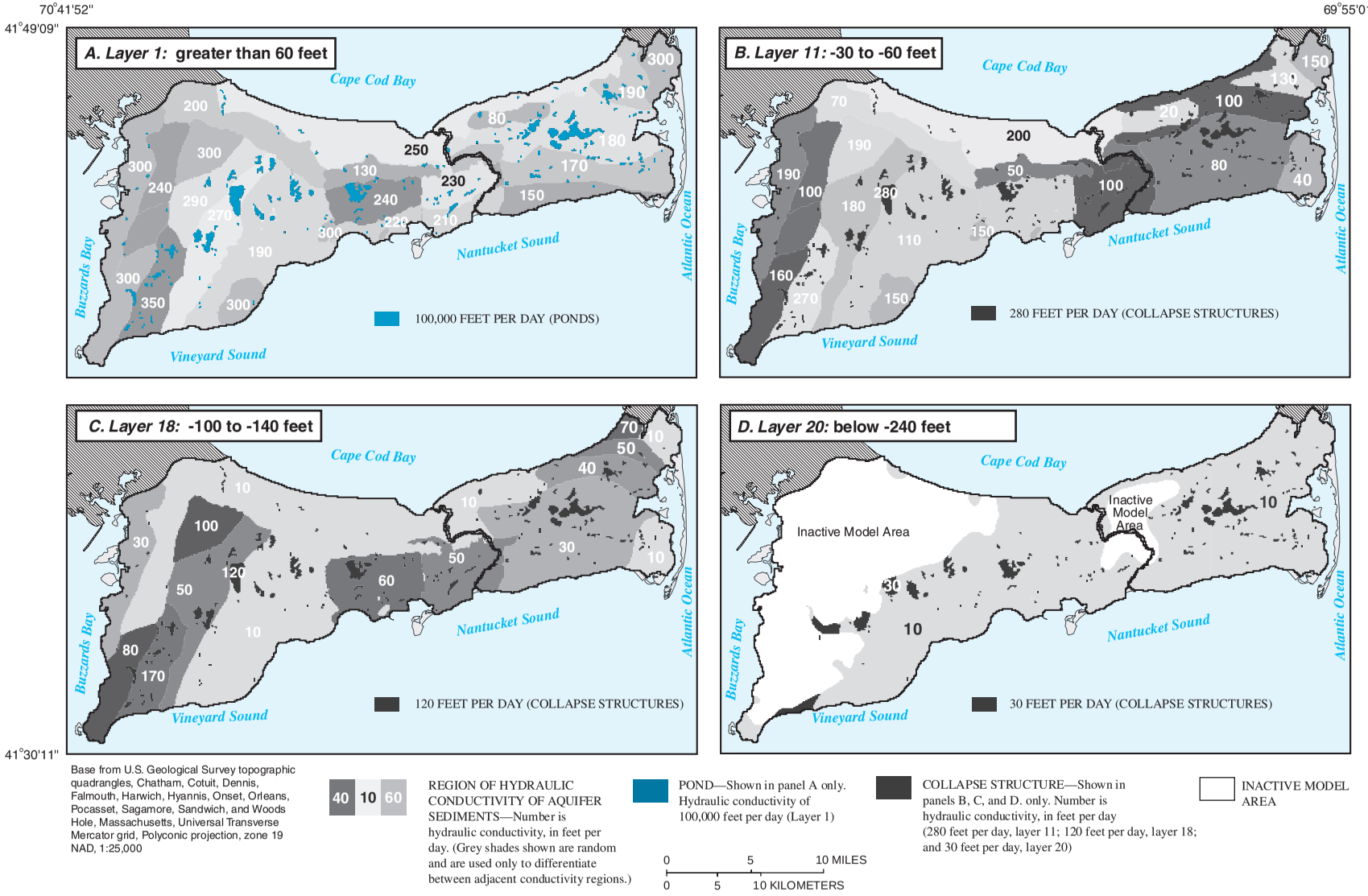

Figure 1-3. Distribution of hydraulic conductivities at selected altitudes within Sagamore and Monomoy flow models, Cape Cod, Massachusetts: *A*, greater than 60 feet; *B*, -30 to -60 feet; *C*, -100 to -140 feet; and *D*, below -240 feet. Layer altitudes are relative to NGVD 29. Layers are shown in the cross section of Appendix figure 1-1, part B.

Table 1-2. Summary of horizontal hydraulic conductivity and vertical anisotropy for general sediment lithologies, Sagamore and Monomoy flow lenses, Cape Cod, Massachusetts.

[ft/d, foot per day]

General lithology	Range of horizontal hydraulic conductivity (K_h,in ft/d)	Range of vertical anisotropy ratio
Medium coarse sand and gravel	350–250	3-4:1
Medium sand	200–250	4–6:1
Fine medium sand	150–200	6–8:1
Fine sand	100–150	8–10:1
Fine sand and silt	30–100	10:1
Silt and clay	10–30	10:1

Stresses

In addition to intrinsic sediment properties and aquifer geometries, model inputs include simulated hydraulic stresses, such as recharge and pumping. Recharge from precipitation is the sole source of water to the aquifer. Pumping for municipal water supply is the only specified withdrawal of water from the aquifer.

Recharge

The sole source of water to the aquifer is recharge derived from areal precipitation. Precipitation at Hatchville, MA, on western Cape Cod (fig. 1) has averaged 44.8 in/yr since 1941. Some precipitation is lost to evapotranspiration; the remainder recharges the aquifer at the water table. Previous estimates of recharge for Cape Cod and eastern Massachusetts have ranged from 18.6 in/yr to 32.0 in/yr (Guswa and LeBlanc, 1985; Gordon Bennett, Papadopoulos and Associates, Inc., written commun., 1998; Masterson and others, 1997b; Masterson and Barlow, 1997; Masterson and Walter, 2000; Desimone and others, 2002; Barlow and Dickerman, 2000; Barlow, 1994; Mike Goydas, Jacobs Engineering, written commun., 2001). In general, simulated recharge estimates used in numerical models of the region have increased over time (Walter and Masterson, 2003). This trend is due, in part, to observations that glacial sediments on Cape Cod are coarser grained and the extents of contaminant plumes in and around the MMR indicate faster traveltimes and higher recharge rates than originally estimated.

Recharge into the model is specified by the RCH Package (McDonald and Harbaugh, 1988). Recharge was applied to three different areas of the model: aquifer, ponds, and wetlands (fig. 1-4). An average recharge rate of 27.25 in/yr is used in the steady-state models to represent recharge into aquifer sediment; this value corresponds to about 60 percent of total precipitation on Cape Cod. Because there are no discernible spatial patterns in precipitation within the modeled region (LeBlanc and others, 1986), the Sagamore and Monomoy flow models were assigned the same average recharge rate. This recharge rate, which is within the range of values discussed above, was varied as part of the trial-and-error model calibration process and yielded the best agreement with measured water levels and streamflows. Evapotranspiration (ET) was not explicitly simulated in the models, but was implicitly simulated by incorporating ET into estimates of net recharge.

Simulated ponds, which are areas of net recharge to the aquifer, were assigned an average recharge of 16 in/yr (fig. 1-4). This value represents the difference between the average annual precipitation and an estimated annual evaporation rate of about 29 in/yr (Farnsworth and others, 1982). Wetlands are assumed to be areas with no net recharge over an annual recharge cycle and received a steady-state recharge rate of zero. Previous modeling efforts on Cape Cod and southeastern New England assigned different nonzero steady-state recharge rates to wetland areas. Wetlands previously have been simulated as areas of net recharge to the aquifer, similar to open surface-water bodies (Masterson, 2004), or as areas of net water loss to the aquifer (DeSimone and others, 2002; Hansen and Lapham, 1990). To test the effect of wetland recharge on the steady-state flow system, steady-state models with wetland recharge rates of 16 in/yr (similar to ponds) and -8 in/yr were developed. There were no appreciable differences in simulated water levels or flows, partly because simulated freshwater wetlands account for only about 1.5 and 2.6 percent of the total area receiving recharge in the Sagamore and Monomoy flow lenses, respectively (fig. 1-4). Saltwater wetlands are areas that receive no recharge (fig. 1-4).

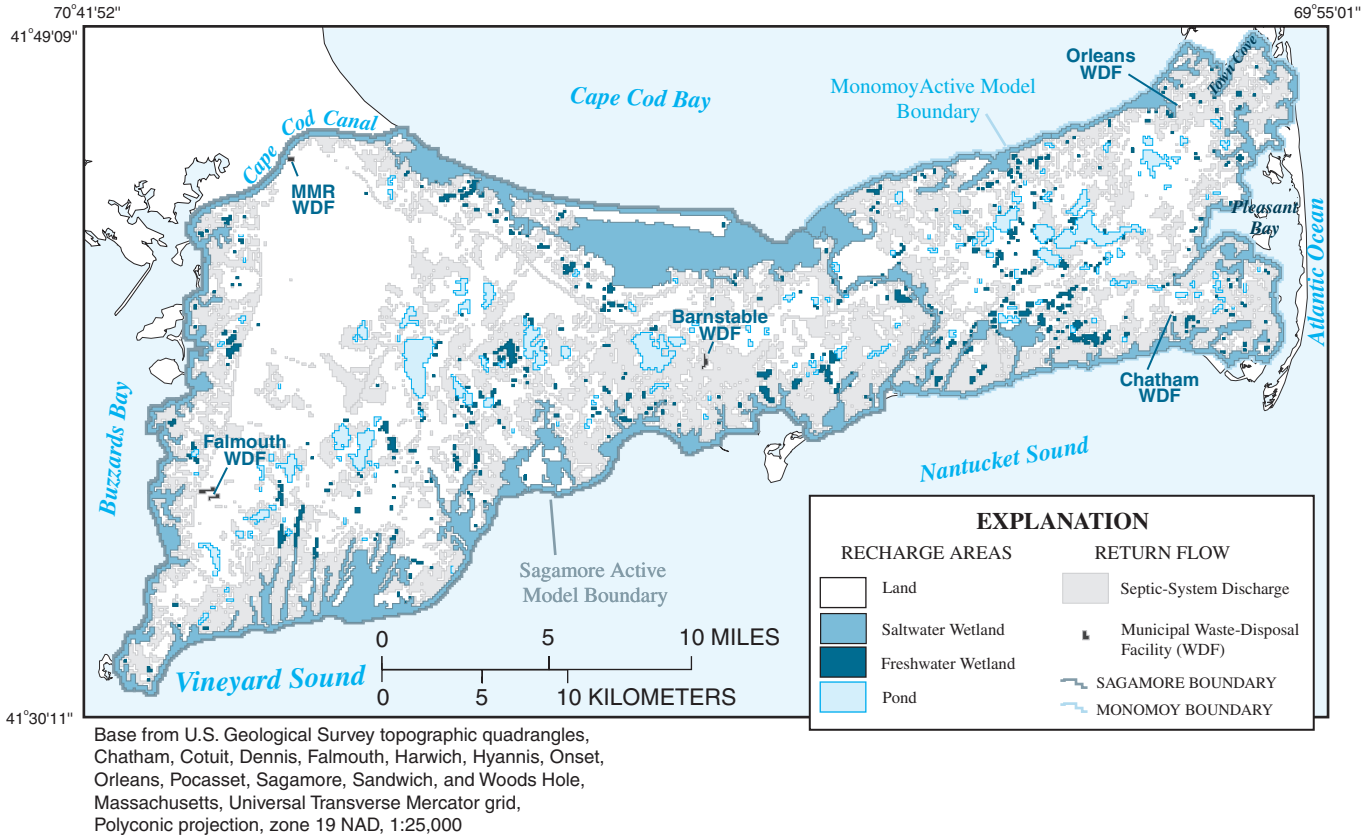

Base from U.S. Geological Survey topographic quadrangles, Chatham, Cotuit, Dennis, Falmouth, Harwich, Hyannis, Onset, Orleans, Pocasset, Sagamore, Sandwich, and Woods Hole, Massachusetts, Universal Transverse Mercator grid, Polyconic projection, zone 19 NAD, 1:25,000

Figure 1-4. Distribution of areal recharge and return flow on the Sagamore and Monomoy flow lenses, Cape Cod, Massachusetts.

Pumping

Pumping wells were simulated by the WEL Package (McDonald and Harbaugh, 1988), which is a specified-flux boundary condition. Two general groups of pumping scenarios were simulated in the steady-state models: (1) a set of current pumping conditions approximating ground-water withdrawal for the years 2003–04 and (2) a set of future pumping conditions approximating ground-water withdrawals in the year 2020. Pumping data were compiled from MDEP records for the period 1995-2000 and used to estimate current (2003) average pumping rates. Water use for the year 2020 was estimated from Massachusetts Department of Conservation and Recreation (MDCR, formerly the Department of Environmental Management) water-use projections and with information from local communities (Joseph Cerutti, Massachusetts Department of Environmental Protection, written commun., 2003). Pumping rates at individual wells for current and future pumping scenarios are summarized in table 1-3 (at back of appendix).

The communities of central and western Cape Cod currently (2003) operate a total of 156 production wells, 97 wells in the Sagamore flow lens and 59 in the Monomoy flow lens (fig. 1-5). Falmouth also withdraws drinking water from Long Pond, which is simulated as both a pond and source of pumped ground water (fig. 1-5). In the Sagamore flow lens, the midpoint elevations of the well screens range from about 28 ft above to 62 ft below NGVD 29; the wells are simulated within the model from layers 3 to 14. The midpoint elevations of wells in the Monomoy flow lens range from about 7 ft above to 83 ft below NGVD 29, within model layers 7 to 16. A total of 175 wells, including present and proposed sites, are projected to be in operation by the year 2020, 112 in the Sagamore flow lens and 63 in the Sagamore and Monomoy flow lens, respectively.

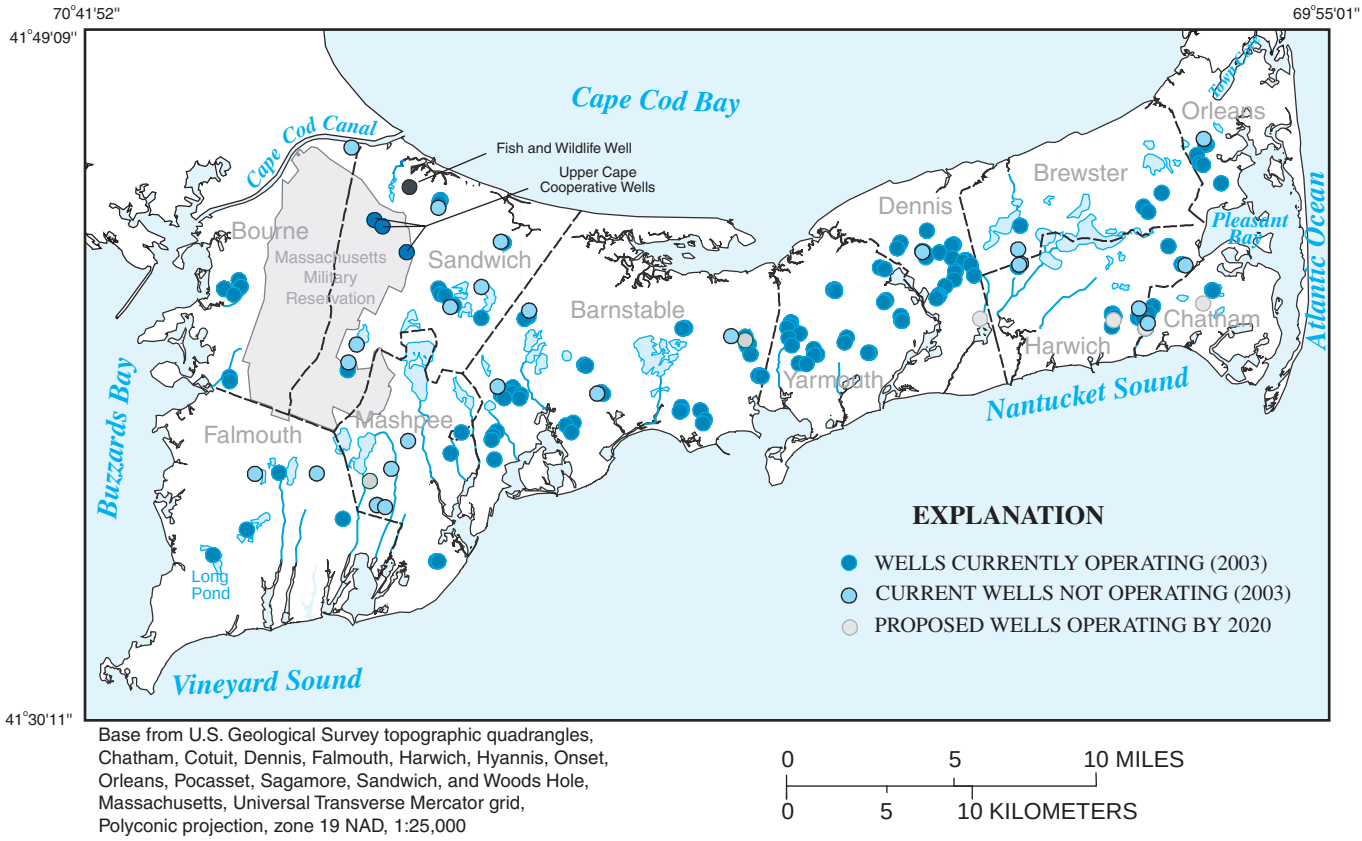

Figure 1-5. Locations of pumped wells, municipal boundaries, Sagamore and Monomoy flow lenses, Cape Cod, Massachusetts.

Current (2003) Pumping

About 17.4 Mgal/d of water are withdrawn from the Sagamore flow lens annually and about 8.1 Mgal/d from the Monomoy flow lens. The largest ground-water withdrawals in the Sagamore flow lens (6.3 Mgal/d) are in Barnstable (fig. 1-6*A*) and the smallest (0.8 Mgal/d) are in Mashpee. The MMR withdraws about 0.1 Mgal/d from the aquifer. Ground-water withdrawal by communities on the Monomoy flow lens range from 1.2 Mgal/d in Orleans to 2.7 Mgal/d in Dennis. Yarmouth withdraws about 6.8 Mgal/d and 0.4 Mgal/d from the Sagamore and Monomoy flow lenses, respectively.

Two separate scenarios were simulated for current (2003) conditions in the Sagamore flow lens: with and without operation of the Upper Cape Cooperative (UCC) wells in Sandwich (fig. 1-5). The UCC wells were installed in 2002 to compensate for the loss of potable water owing to ground-water contamination emanating from the MMR (fig. 1-5). The wells were installed on the MMR within Sandwich (fig. 1-5) and are pumped seasonally to supply water to Bourne, Falmouth, Mashpee, and Sandwich during periods of high-water demand. An annual average of 1.7 Mgal/d of water is currently withdrawn from the three wells (fig. 1-6*B*). The pumping rates shown in figure 1-6*A* represent pumping with operation of the Upper Cape Cooperative wells. When the wells operate, pumping in the surrounding communities decreases by an amount equal to the volume of water withdrawn at the UCC wells.

The only nonmunicipal well simulated in the model is a well at the Massachusetts Department of Fisheries and Wildlife (MDFW) fish hatchery in Sandwich in the Sagamore flow lens (fig. 1-5); the well is pumped at 1 Mgal/d in the models. Other nonmunicipal wells, which include private-supply wells and irrigation wells for golf courses, account for a small portion of total pumping and are not included in the models. Also, water withdrawn from these wells is returned to the aquifer as increased recharge at or near the wells; as a result, the net withdrawal of water is near zero. The baseline scenario includes operation of the UCC wells. The alternative current (2003) pumping scenario, referred to as variant 2 on figure 1-6*B*, includes no pumping from the UCC wells.

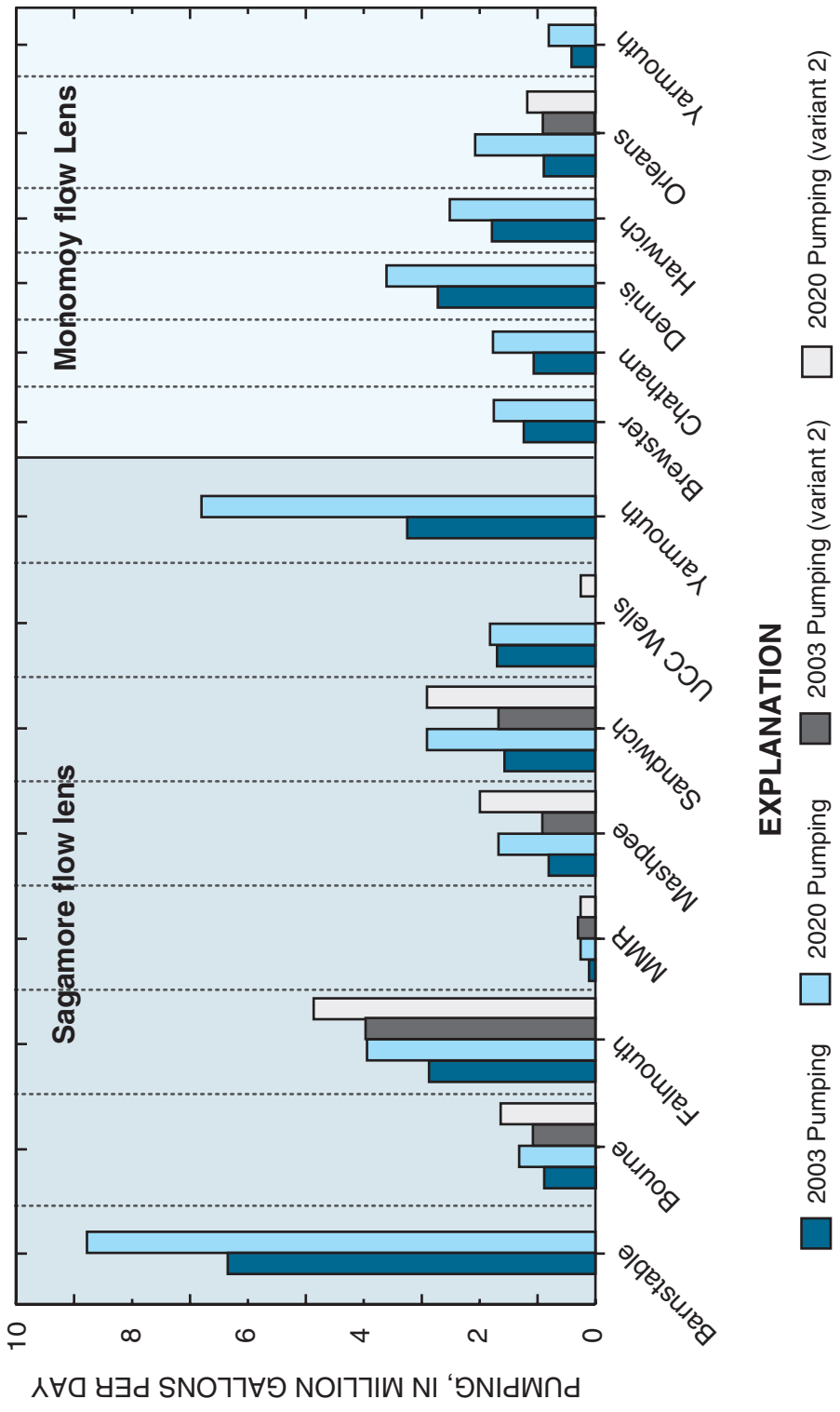

Figure 1-6. Average ground-water withdrawals by town for current (2003) and future (2020) pumping scenarios, Cape Cod, Massachusetts.

Additional pumping stresses on the Sagamore flow lens include those associated with extraction-treatment-reinjection remediation (ETR) systems on the MMR. When all of the systems are installed, about 12.8 Mgal/d of water will be withdrawn, treated, and returned to the aquifer, either as subsurface injection or as artificial recharge (Mike Goydas, Jacobs Engineering Group, written commun., 2003). Following treatment, pumped water is returned to the aquifer near the extraction wells to maintain a hydraulic mass balance; the ETR systems are designed to minimize regional effects on water levels and hydraulic gradients. A version of the Sagamore model that incorporates these additional stresses was developed to determine the effects of these stresses on areas contributing recharge to production wells in the region; because no substantial effects were observed, these model-simulation results are not included in this report.

Future (2020) Pumping

Future (2020) pumping scenarios were developed by personnel at the MDEP Drinking Water Program (Joseph Cerutti, Massachusetts Department of Environmental Protection, written commun., 2003) by using MDCR water-demand projections and additional information from local communities regarding buildout and population projections. The 2020 pumping scenarios include increased pumping rates in existing wells, the addition of new wells and, in some communities, existing wells being taken out of service (fig. 1-5). Total projected future (2020) pumping were 27.4 Mgal/d from the Sagamore flow lens and 11.6 Mgal/d from the Monomoy flow lens; these rates represent increases of about 56 percent and 43 percent, respectively, over current (2003) withdrawals. In 2020, Barnstable is projected to withdraw about 8.7 Mgal/d, an increase of about 40 percent over current pumping. The largest increases in 2020 pumping, as compared to current pumping, are predicted to be in Yarmouth, which has projected pumping that is more than double the current withdrawals. Projected 2020 pumping also is more than double current withdrawals in Orleans on the Monomoy flow lens (fig. 1-6*A*).

Two separate scenarios are simulated for future conditions: (1) with and without pumping of the UCC wells in the Sagamore flow lens, as described previously, and (2) with and without the transfer of pumped ground water from Orleans on the Monomoy flow lens to Eastham on an adjacent flow lens outside of the study area. About 0.9 Mgal/d of water is projected to be transferred; this amount accounts for about 40 percent of total 2020 withdrawals for Orleans (fig. 1-6*B*). The baseline scenario includes both the UCC wells and the transfer of water from Orleans to Eastham. The alternative scenario, referred to as variant 2 on figure 1-6*B*, includes no pumping from the UCC wells and no transfer of water from Orleans to Eastham.

Wastewater

Most ground water withdrawn for public supply is returned to the aquifer as wastewater return flow. A consumptive loss of about 15 percent is assumed for Cape Cod (Masterson and Barlow, 1997). An amount equal to 85 percent of generated wastewater for each town is returned to the aquifer as enhanced recharge (by means of the RCH Package) in residential areas (fig. 1-4). In Falmouth, Barnstable, and on the MMR, water also is returned to the aquifer as enhanced recharge at centralized waste-disposal facilities (WDFs) (fig. 1-4). In these cases, waste-disposal volumes at WDFs were compiled from each facility; the difference between the volumes discharged at the WDFs and the total amount of available wastewater was returned uniformly in residential areas as septic-system return flow. Current (2003) pumping and measured discharges at the WDFs were used to estimate the portion of generated waste water discharged at the WDFs and the portion returned as disseminated septic-system discharge in nonsewered, residential areas for simulated current and future (2020) conditions.

Calibration to Measured Water Levels and Streamflows

Initial input parameters for the steady-state models were adjusted within ranges of reasonable values to best-fit hydrologic conditions measured in the aquifer, including measured water levels and streamflows. A deterministic, or trial-and-error, approach was used in the model-calibration process. Parameters adjusted during model calibration included recharge, horizontal and vertical hydraulic conductivity, and leakances at coastal and stream boundaries. The input values discussed in the preceding sections represent the final values produced during the calibration process.

Steady-state models simulate average hydrologic conditions, and water-level observations that are representative of long-term average conditions are needed for model calibration. Water-level observations were available from a number of sources, including a network of long-term monitoring wells maintained by the Cape Cod Commission (CCC) and water-level measurements made at ponds by the Association for the Preservation of Cape Cod (APCC). The USGS cooperates with these organizations and compiles water-level measurements in a Web-accessible database (http://waterdata.usgs.gov). In addition to USGS water-level measurements, water-level measurements also were obtained from local water suppliers, private consulting firms, and the MMR Installation Restoration Program (IRP), managed by AFCEE, and the IAGWS, managed by the National Guard Bureau (NGB).

Available water-level measurements from the region were compiled into a geographic-information system (GIS) database that was queried to produce a subset of measurements that were reasonably representative of long-term average water levels. There are a total of 424 water-level-calibration sites in the Sagamore flow lens, including 409 wells and 15 ponds, and a total of 71 sites—47 wells and 24 ponds in the Monomoy flow lens (fig. 1-7). These sites consist of the following groups: (1) long-term monitoring wells and ponds with at least 20 years of historical record, (2) sites where synoptic water-level measurements were made in March 1993 by USGS, (3) sites where synoptic water-level measurements were made in June and July 2000 and June and July 2001 in and around the MMR by IRP and IAGWS contractors, and (4) sporadic measurements from other sources made during the summers of 2000 or 2001 (fig. 1-7). Comparisons of measurements made at long-term monitoring wells during the summers of 2000 and 2001 to historical averages showed that the mean difference was about 0.1 ft; this small difference indicates that these periods were generally representative of long-term average conditions. Measurements in March 1993 were also close to long-term average conditions in the region (Savoie, 1994).

Long-term average streamflow values can greatly assist in model calibration. The USGS operated a continuous stream-gaging station on the Herring River in Harwich (site 1105880) during the period 1966-88 and has operated long-term stations on the Quashnet River in Mashpee since 1988 (site 11058837). In addition, USGS operated a continuous streamflow station on Mill Creek in Sandwich (site 110587880) for the period 2000–03; this period corresponds to a period of generally average hydrologic conditions as indicated by water levels in long-term monitoring wells (fig. 1-7). Measurements of streamflow also have been made at various partial-record sites on Cape Cod. Streamflow data were collected at 28 partial-record sites on western Cape Cod by USGS in 1993 (Savoie, 1994). Streamflow data also have been collected from the Coonamessett and Quashnet Rivers on western Cape Cod as part of the MMR IRP. To augment the limited streamflow data available for calibration of steady-state models, streamflows were measured as part of this investigation at 20 sites in the Sagamore flow lens and 8 sites in the Monomoy flow lens (fig. 1-7).

Streamflow data collected in May 2002 at the current and former stream-gaging stations (Quashnet River, Mill Creek, and Herring River) were in close agreement with long-term mean and median streamflow estimates; this agreement indicates that streamflows measured at the additional 28 partial-record sites likely are reasonable estimates of long-term average conditions. Streamflow measured in May 2002 at the current long-term station on the Quashnet River was 15.3 ft^3/s, which was close to the long-term mean and median values of 15.8 and 15.3 ft^3/s, respectively. Measured streamflow in the Herring River in May 2002 was 7.7 ft^3/s, similar to long-term mean and median values of 9.9 and 8.6 ft^3/s, respectively. In Mill Creek, at the outlet of Lower Shawme Pond, the measured streamflow of 6.3 ft^3/s was similar to the mean and median streamflows of 6.4 ft^3/s. The stream flows measured in May 2002 were used to estimate seepages along stream reaches; the differences between measured streamflows at upstream and downstream sites were assumed to represent ground-water discharge or seepage into the stream segment between the sites.

During the model-calibration process, specified fluxes equal to flows measured in May 2002 from pond outlets were removed from each pond that drains into a stream by using the WEL package. Adjustments to model inputs were made by using estimated average pond levels as calibration targets; the final calibrated pond stage was used to establish a boundary elevation in the stream node representing the outlet, as described in the "Hydrologic Boundaries" section. This approach ensures that these pond outflows are accounted for in the calibrated steady-state model and that long-term-average pond outflows are reasonably reproduced. The method allows for the simulation of pond outflows under steady-state conditions.

Prior to model calibration, the sensitivities of simulated water levels to model-input parameters were calculated using the SEN Process in MODFLOW-2000 (Hill and others, 2000). This information can streamline the calibration process by identifying the parameters that most affect model calibration as well as those parameters that do not have important effects on simulation results. A version of the Monomoy flow model was developed that defined model inputs as parameters. Initial K values were constant within each model layer, but a fining-down sequence was incorporated into the model; K values decreased from 300 ft in layer 1 to 10 ft/d in layer 20. The composite-scaled sensitivities of simulated water levels to horizontal and vertical K and boundary leakances were calculated (fig. 1-8); because these sensitivities are dimensionless, they can be compared for input parameters with different measurement units. The measured water levels discussed previously were used in the analysis. Simulated water levels were most sensitive to the horizontal K of the upper model layers (fig. 1-8); the sensitivities of simulated water levels to K generally decreased with depth within the model. The simulated water levels were moderately sensitive to leakances at discharge boundaries. Simulated water levels were less sensitive to vertical K (fig. 1-8). This finding indicates indicting that anisotropy values generally are not important in model calibration and have little effect on simulation results.

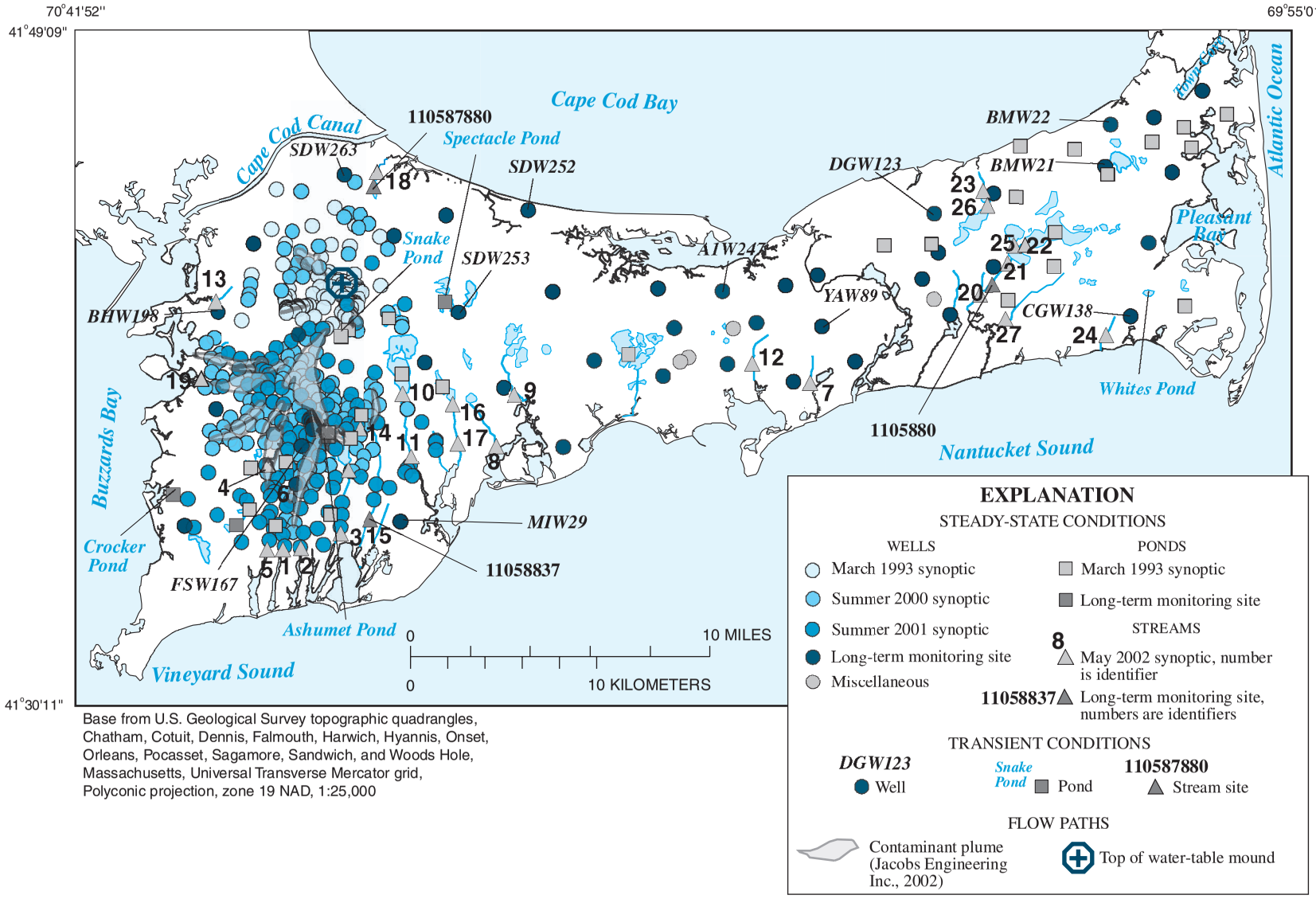

Base from U.S. Geological Survey topographic quadrangles, Chatham, Cotuit, Dennis, Falmouth, Harwich, Hyannis, Onset, Orleans, Pocasset, Sagamore, Sandwich, and Woods Hole, Massachusetts, Universal Transverse Mercator grid, Polyconic projection, zone 19 NAD, 1:25,000

Figure 1-7. Locations of wells, streamflow sites, and contaminant plumes used for calibration of Sagamore and Monomoy flow models, Cape Cod, Massachusetts.

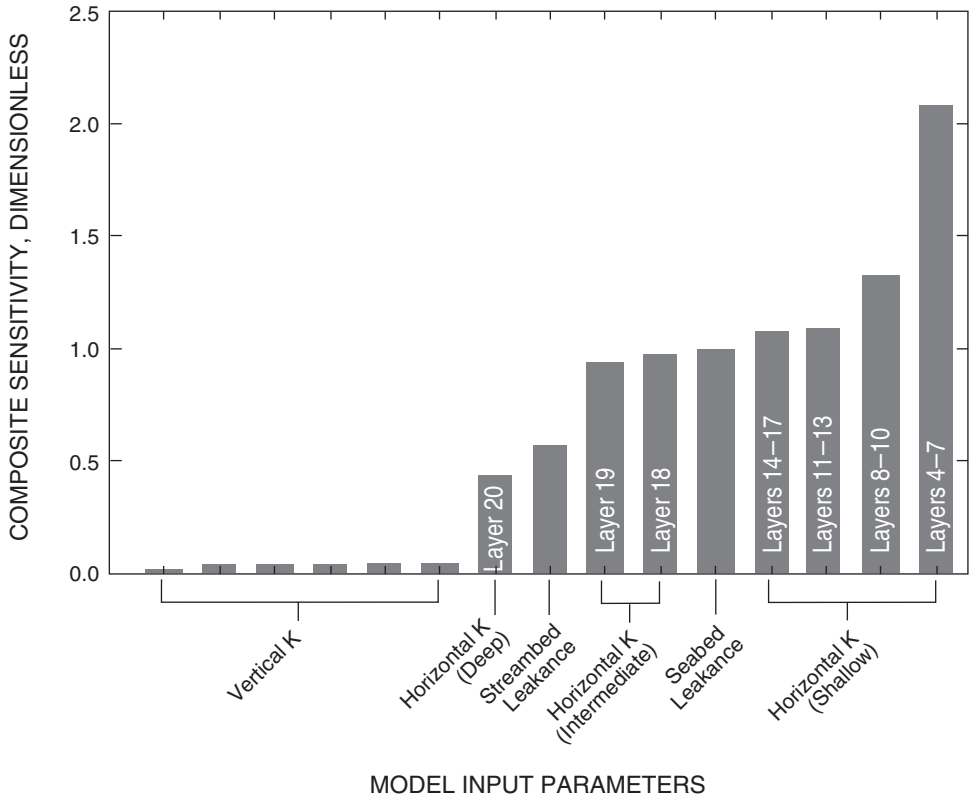

Figure 1-8. Composite sensitivities for steady-state model-input parameters for the Monomoy flow model, Cape Cod, Massachusetts. (K refers to hydraulic conductivity.)

The degree of fit between simulated and measured water levels and flows was used to determine if the models were reasonably calibrated and suitable for predictions of hydrologic conditions. Simulated steady-state water levels were in reasonable agreement with long-term average water levels in the aquifer (fig. 1-9*A*). The absolute mean residual (AMR) is the average of the absolute differences between measured values and their simulated equivalents and is used to quantify the degree of fit between simulated and measured water levels. The AMRs for the Sagamore and the Monomoy flow models were 1.42 ft and 1.72 ft, respectively. These values correspond to 2.0 and 4.9 percent of the total head gradient for the Sagamore and Monomoy flow lenses, respectively; a value of 5.0 percent or less generally is considered a reasonable model fit. The model residuals are randomly distributed around zero (fig. 1-9*B*); this result indicates that the models generally are unbiased. The largest residuals (greater than 5 ft) in the Sagamore flow model are for cells along the Buzzards Bay and Sandwich Moraines (fig. 1-10). These are areas with steep hydraulic gradients (fig. 5), where discrete water levels are difficult to match; however, the steady-state Sagamore model adequately represents hydraulic-gradient directions and total gradient magnitudes in the area. Residuals in the remainder of the model domains showed no discernible spatial trends (fig. 1-10).

The model-calculated and measured streamflows are shown in figure 1-9*C*. Simulated streamflows are in good agreement with long-term average flows at the three USGS stream-gaging stations (fig. 1-9*D*). These measured streamflows are good indicators of long-term average flows and were given a higher priority during model calibration than measurements at partial-record sites. Simulated stream seepages, which represent ground-water discharge into a stream reach, also are in good agreement with seepages estimated from differences between flows measured at partial-record sites in May 2002 (fig. 1-9*C*). These measurements were given a lower priority than the long-term average measurements, although streamflows measured in May 2002 at the three long-term sites were close to long-term averages and the partial-record measurements from May 2002 probably are reasonable indicators of long-term average flows. Flows measured during a rainy period in March 1993 are likely higher than average, but are included for comparison. The largest difference between simulated and measured seepages, which represent the base inflow from the ground-water system into the stream reaches, from May 2002 is for site 5 in the Coonamessett River (figs. 1-7 and 1-9*C*). The simulated seepage is higher than seepage estimated from May 2002 flow measurements (at sites 5 and 6, fig. 1-9*C*). However, model-calculated seepages were similar to seepages estimated from March 1993 measurements (site 5 on fig. 1-9*C*).

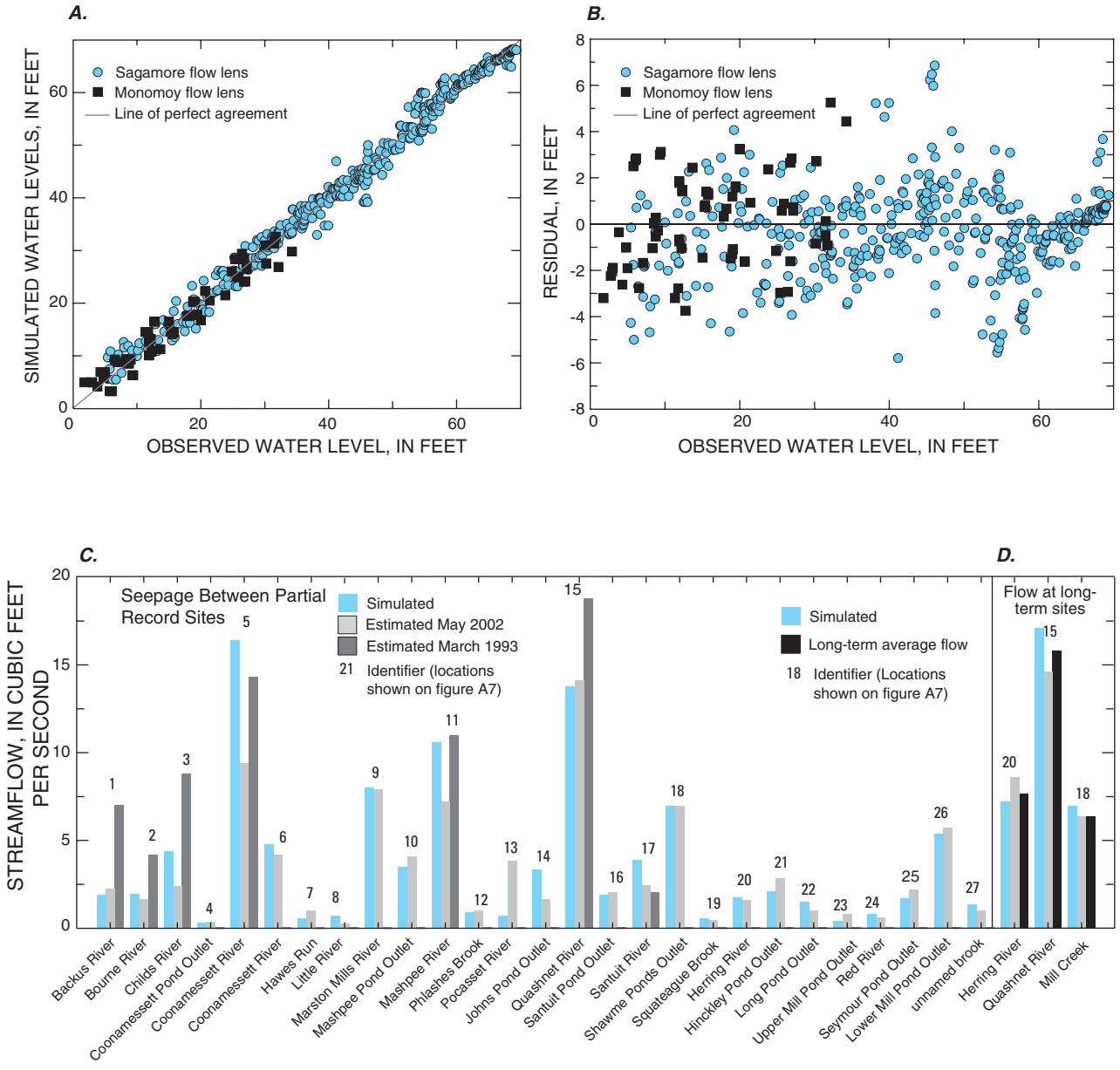

Figure 1-9. *A*, Comparison of simulated and observed water levels; *B*, residual (observed–simulated) water levels as a function of observed water levels; *C*, comparison of simulated and estimated streamflow between partial record sites; and *D*, comparison of simulated and observed streamflows at long-term sites for the Sagamore and Monomoy flow models, Cape Cod, Massachusetts.

Transient Models

Whereas steady-state models represent hydrologic conditions under constant hydraulic stresses, transient models incorporate time-varying stresses and can be used to evaluate the effects of temporal changes in recharge and pumping on the hydrologic system. Transient models use the same model inputs to represent aquifer characteristics—including K and aquifer geometries—as do steady-state models, but require additional information. These additional input parameters include confined and unconfined storage properties of the aquifer sediments, changing recharge and pumping inputs over the time scale of interest, and, in some cases, adjustments to simulated hydrologic boundaries.

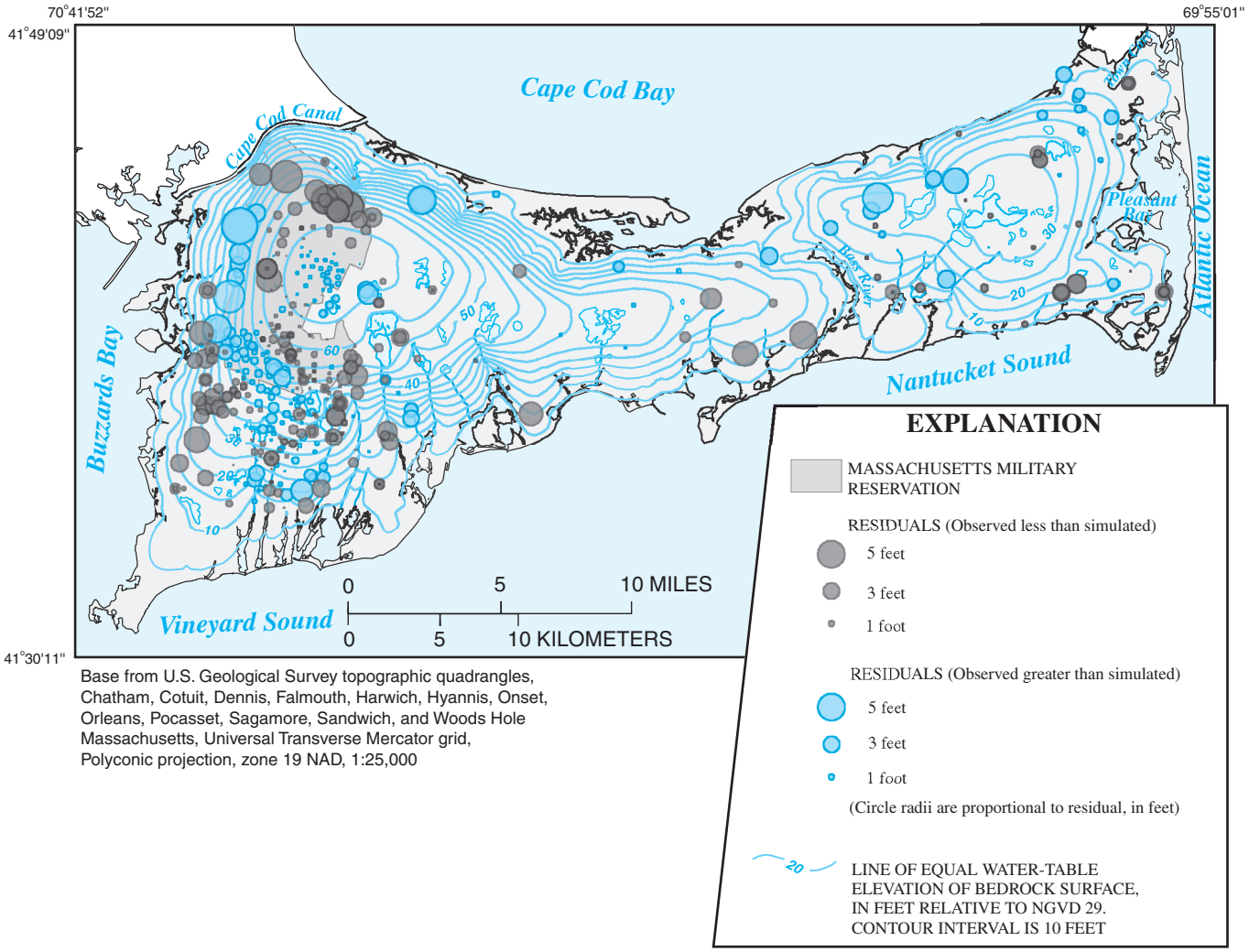

Figure 1-10. Spatial distribution of residuals (observed–simulated) for the Sagamore and Monomoy flow models, Cape Cod, Massachusetts

Discretization of Time

Hydrologic stresses were evaluated over two time scales: (1) a monthly time scale simulating variations in hydrologic stresses during an average year and (2) a multiyear time scale simulating variations in recharge for a 55-year period (based on recharge form 1941 to 1995) and average seasonal variations in pumping. The monthly time scale allows for the simulation of average monthly conditions and the multiyear time scale allows for the simulation of long-term hydrologic events such as extended periods of droughts and periods of above average recharge. In transient models, time is discretized into stress periods and time steps. Stress periods refer to periods of time in which specified model stresses, such as pumping and recharge, are constant; changing stresses over periods of time are simulated by using sequential stress periods with changing stresses from one stress period to the next. Stress periods are further divided into time steps, which are units of time for which water levels and flows are calculated.

In the transient models representing average monthly variations in hydrologic stresses, conditions over an average year were simulated by dividing the annual hydrologic cycle into 12 monthly stress periods, representing average pumping and recharge during each month. Each stress period consisted of daily time steps; the number of time steps was equal to the number of days in each month. The water levels produced by the steady-state models were used as initial conditions for each transient simulation. The total simulation length was 5 years (or 60 stress periods) to ensure that enough time had elapsed in the simulation to achieve a state of dynamic equilibrium, defined as a condition in which simulated water levels and flows do not

change year to year for a given stress period and time step. The final year of simulated time (12 stress periods) was used to represent hydrologic conditions over an average year.

In the transient models representing multiyear variations in seasonal recharge, and average seasonal variations in pumping, hydrologic conditions over the 55-year period (based on recharge during the period 1941–55) were simulated by dividing the time period into 110 stress periods; these stress periods represented in-season and off-season conditions during those 55 years. The in-season period covered the period of generally higher water withdrawals and lower recharge rates and the off-season period covered the period of lower water withdrawals and higher recharge rates. The in-season stress periods represent average stresses for the months of May–September and the off-season stress periods represent average stresses for the months of October–April. In-season and off-season stress periods were 153 and 212 days in length, respectively. Each time step represented approximately 1 month. The in-season stress period was divided into five equal time steps, each 30.6 days in length, and the off-season stress period was divided into seven equal time steps, each about 30.2 days in length.

Modifications to Hydrologic Boundaries

The only hydrologic boundary conditions that were modified to facilitate transient modeling were those used to simulate streamflow from ponds. An approach was used that explicitly accounts for the relation between pond levels and the resulting surface-water outflow at pond outlets; this approach is similar to the method used in a previous study to simulate streamflows on western Cape Cod (Walter and Masterson, 2003). During initial calibration of the steady-state models, specified fluxes equal to the flows measured at pond outlets in May 2002 were removed from the ponds, by using the WEL Package (McDonald and Harbaugh, 1988, fig. 1-9*C*). The models then were calibrated using pond stages as calibration targets. Next, the STR Package (Prudic, 1989) was used to represent pond outlets as stream reaches; leakances were set to a high value (1×10^6 ft^2/d) to represent negligible resistance to flow between the pond and pond outlets. The model-calculated pond levels from the initial calibration runs for the cells that included the locations of pond outlets were then specified as the elevations of the stream stages. The tops and bottoms of the streambeds were set to values of 0.1 ft and 0.2 ft below the stream-stage altitudes, respectively, to represent the structure controlling flow from the pond outlets. This method reproduced the total amount of water pumped from the pond cells as discharge to the pond outlets and resulted in steady-state flows that are in close agreement with measured flows at the pond outlets (fig. 1-9*C*). Both the final steady-state and transient models use this method to simulate pond outlets.

The benefit of this approach is that it allows transient pond-level fluctuations to affect the simulated surface-water outflow to the adjoining stream, as is observed in the aquifer. As pond levels increase in response to higher simulated seasonal recharge rates, the flow from the ponds to the streams also increases. As pond levels decrease because of decreased recharge, the surface-water outflow from the pond decreases until the pond level drops below the specified altitude of the streambed bottom, at which time surface outflow from the pond stops.

Storage Characteristics

The storage characteristics of the aquifer, which quantify the volume of water the aquifer releases for a given decline in head, consists of two components: specific yield (Sy) and specific storage (Ss). Specific yield, which is a function of sediment porosity and moisture-retention characteristics, is unconfined storage and represents gravity-driven dewatering of the aquifer at a declining water table. Specific yields can not exceed sediment porosity, which is about 0.39 on Cape Cod (Garabedian and others, 1985). Specific storage is a function of the compressibility of the aquifer and, to a much lesser extent, of water; a measure of confined storage, specific storage represents a release of water because of compression of the aquifer. In unconfined aquifers, such as Cape Cod, specific yield typically is orders of magnitude larger than specific storage and is the most important storage parameter.

Specific yields for glacial sediments from southeastern New England typically range from 0.2 to 0.3, whereas specific storage typically is less than 0.00001; most numerical models of the region use specific yields between 0.24 and 0.30 (Barlow and Dickerman, 2000; Moench, 1994; Masterson and Barlow, 1997; Walter and others, 1997). A specific yield of 0.25 and a specific storage of 1.5×10^{-5} was used in the numerical models to simulate storage in the aquifer sediments; these values are consistent with storage values of 0.26 and 1.3×10^{-5} reported by Moench (2001) and are within the range of reasonable values. Ponds have porosities of 1 and, therefore, have a high unconfined storage and low confined storage; confined storage in ponds is controlled only by the compressibility of water, which is small. The specific yield and specific storage of simulated ponds were specified as 1.0 and 1.5×10^{-9}, respectively.

The storage characteristics of the aquifer control, in part, the degree to which water levels fluctuate in the aquifer and in ponds in response to given changes in recharge. Model-calculated water-level fluctuations in well BHW198, a long-term monitoring well in Bourne (fig. 1-7), are shown in figure 1-11 for different specific yields. The simulated water levels during an average year for specific yields of 0.2, 0.25, and 0.3 were 2.2, 1.9, and 1.6 ft, respectively (fig. 1-11*A*). The measured range in water levels was 1.8 ft, which is best matched by a specific yield of 0.25. Over a multiyear time scale, the water levels for specific yields of 0.2, 0.25, and 0.3 were 8.53, 7.29, and, 6.04 ft respectively; the measured range was about 5.7 ft (fig. 1-11*B*).

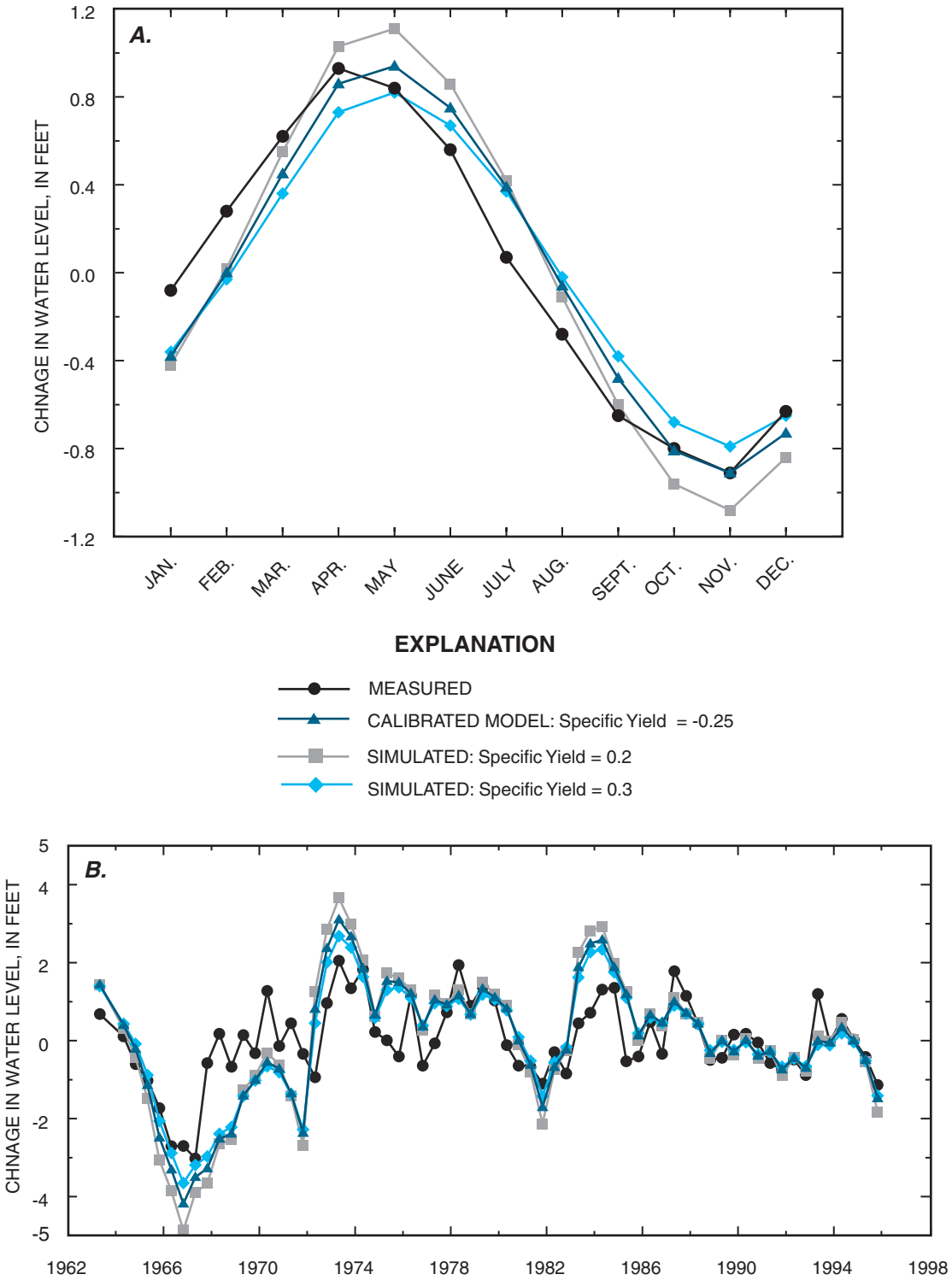

Figure 1-11. Sensitivity of water levels at well BHW198, Bourne, Massachusetts, to specific yield for *A*, monthly time scales; and *B*, multiyear time scales.

Recharge

The record of precipitation at Hatchville, MA (fig. 1), measured over a period of 55 years (1941–95), was used to estimate monthly and annual average recharge rates for the region. Measured precipitation at Hatchville has varied from a high of 74 in/yr in 1972 to a low of 26 in/yr in 1965 (fig. 6). Annual and monthly average recharge rates were estimated by applying analytical results from a recent investigation in a nearby basin. Barlow and Dickerman (2000) developed relations between measured precipitation and recharge estimated from base-flow measurements over a 20-year period in the Hunt River Basin, RI, which is underlain by glacial sediments similar to those on western Cape Cod. Ratios of precipitation to recharge for each month from the Hunt River Basin were applied to the long-term precipitation data from Hatchville, MA, on Cape Cod and used to estimate monthly and annual recharge. These monthly recharge estimates were used to determine average monthly and seasonal recharge rates on Cape Cod for use in the transient models.

The method used to estimate recharge rates or western Cape Cod did not use local streamflow measurements; the underlying assumption is that the study area and the reference basin in Rhode Island have similar hydrogeologic settings. Although there are uncertainties in the recharge estimates, the method does incorporate major elements of the precipitation record from western Cape Cod, including major droughts in the mid-1960s and early-1980s, and is a good approximation of general recharge values and trends. Therefore, the analysis does effectively illustrate concepts related to the effects of transient recharge on hydrologic conditions in the aquifer. The results of the transient-modeling analysis are intended to illustrate the general effects of time-varying recharge and pumping on the water levels and streamflows and how these effects may vary within different areas of the aquifer. The simulation results for a particular year should not be considered accurate estimates of hydrologic conditions for that specific year.

Average Monthly Recharge

Recharge onto aquifer, ponds, and wetlands were varied monthly. Average estimated monthly recharge rates onto aquifer sediments at Hatchville, MA, varied from 0.9 in. in September to 3.9 in. in March (fig. 1-12*A*). The average monthly estimates were normalized to an annual average of 27.25 in/yr, which proportionally adjusted each monthly value—by an increase of about 10 percent—to yield the same value as the annual average; this adjustment was done to assure that the transient and steady-state models were consistent. Recharge, as a percentage of precipitation, ranged from 90 percent in March to 22 percent in July.

Although ponds are areas of net recharge under steady-state conditions, they become net sinks when surface evaporation exceeds precipitation. Potential evapotranspiration (PET) rates were estimated from long-term atmospheric data from the Providence, RI area by using the Jensen-Haise Equation (Jensen and Haise, 1963), which is based on measurements of temperature and integrated solar radiation. Monthly recharge rates onto pond surfaces were determined by taking the differences between measured precipitation and average monthly PET estimates. The estimated recharge rates onto pond surfaces ranged from a net loss of 2.9 in. in June to a net gain of 4.5 in. in November (fig. 1-12*A*). There were a total of 20.5 in. of off-season recharge onto pond surfaces and a total in-season water loss of 4.7 in., yielding a net annual recharge of 15.8 in., which is consistent with the steady-state models.

Wetlands are assumed to be areas of no net recharge under steady-state conditions. However, wetlands are areas of net recharge during the winter months and areas of net water loss during the growing season (Motts and O'Brien, 1981). The highest PET from wetlands occurs in July and August when wetland plant growth is highest (O'Brien, 1977). Wetland recharge rates range from a net loss of 7.5 in. in both July and August to a net gain of 4.5 in. in November (fig. 1-12*A*). Wetlands are assumed to be similar to other surface-water bodies, so recharge onto wetlands during off-season months (October–May) was assumed to be the same as recharge onto ponds (fig. 1-12*A*). Hall and others (1972) reported an in-season water loss of about 20 in. from wetlands in New England for the period June–August. The fractions of PET for the in-season months (May–September) to total in-season PET (Motts and O'Brien, 1981) was used to estimate in-season monthly wetland recharge rates; a total in-season PET of 20.5 in. was used in the analysis. This value is consistent with reported values (Hall and others, 1972 and Motts and O'Brien, 1981) and yields a net recharge of 0, which is consistent with the steady-state models.

Additional simulations in which wetland recharge was the same as recharge onto ponds for all months (net positive recharge of 16 in.), wetlands were areas with a net water loss of 8 in., and wetland recharge had a constant rate of zero were done to test the sensitivity of water levels to wetland recharge. Marston Mills Pond is in an area with various large wetlands (fig. 1-4). Pond water levels calculated by the calibrated transient model had a total range of 0.8 ft; this simulation incorporates monthly changes in recharge that have a net annual recharge of zero. For simulations in which wetlands had a net positive recharge and a constant recharge of zero, the simulated pond has a water-level range of 0.8; the water-level range for simulations with a net negative recharge rate was 1.0 ft. The simulation results indicate that transient representations of wetland recharge do not substantially affect transient water levels.

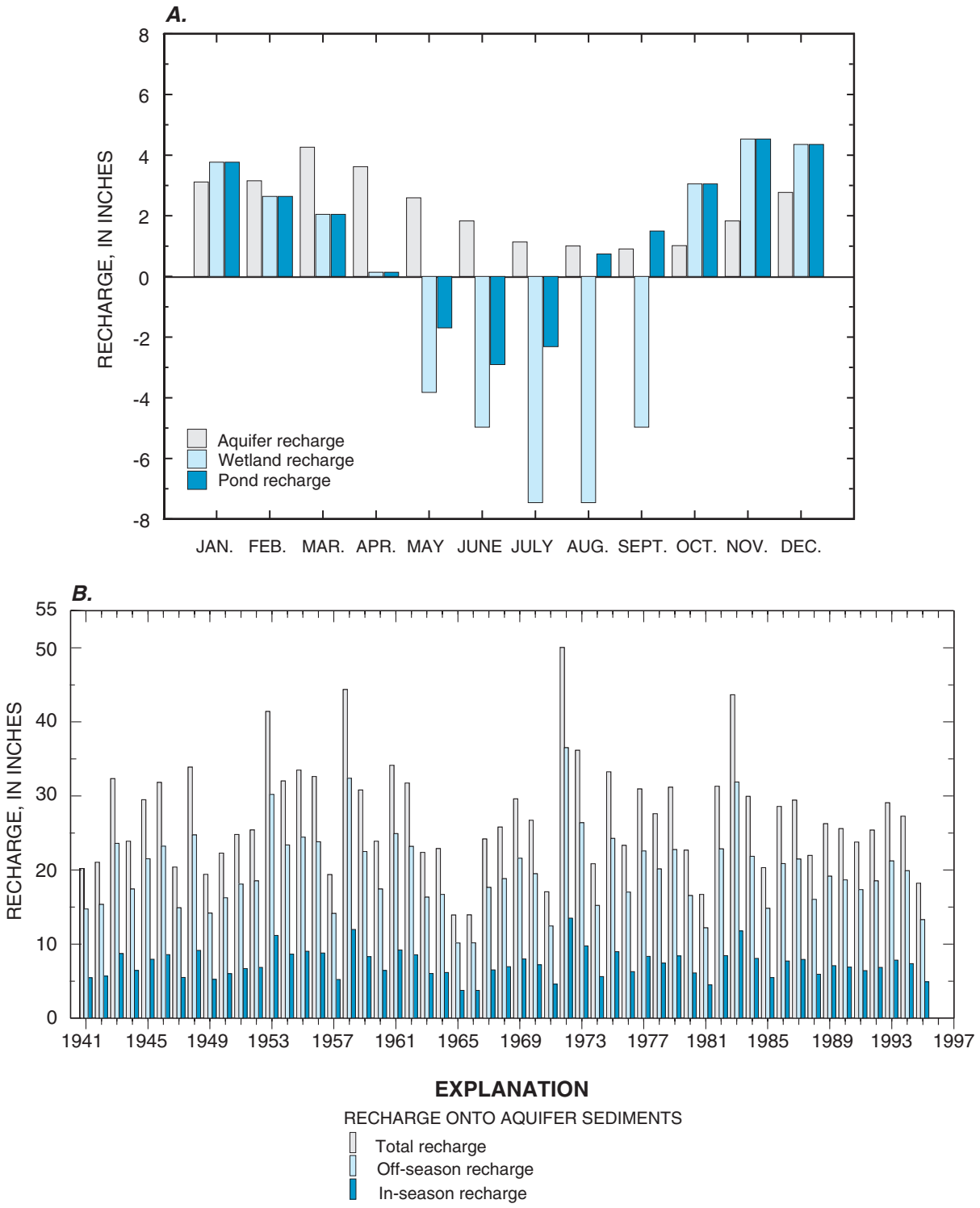

Figure 1-12. Estimated recharge to aquifer sediments, ponds, and wetlands in the Sagamore and Monomoy flow models, Cape Cod, Massachusetts, *A*, by month; and *B*, seasonally for the period 1941–95.

Annual and Seasonal Recharge

The precipitation record from Hatchville, MA (fig. 2) and the ratio of recharge to precipitation in an average year were used to estimate annual recharge for a 55-year period (1941–95). The estimated annual recharge rates, which had a long-term average of 24.6 in/yr, were normalized to an average of 27.25 in/yr to be consistent with the steady-state regional model. Annual recharge onto aquifer sediments ranged from 13.9 in. in 1965 to 50.0 in. in 1972 (fig. 1-12*B*). Estimates of recharge rates for the in-season (May–September) and off-season (October–April) periods represent 73 and 27 percent, respectively, of total annual recharge. These ratios were used to partition in-season and off-season recharge onto aquifer sediments for each of the 55 years. Off-season recharge ranged from 10.2 to 36.5 in. and in-season recharge ranged from 3.8 to 13.5 in. (fig. 1-12*B*).

Off-season pond recharge was indexed to annual recharge variations by using the ratio of average off-season pond recharge to average total annual recharge (0.75). This method was used to estimate off-season pond recharge and resulted in a long-term average that is the same as off-season pond recharge for an average year. In-season pond recharge was estimated by subtracting the difference between off-season and in-season pond recharge in an average year from the off-season recharge estimated for each of the 55 years; this method resulted in average in-season pond recharge for the 55 years that is the same as that for an average year. Off-season pond recharge ranged from 10.4 in. in 1965 to 37.5 in. in 1972; in-season pond recharge ranged from -14.8 in. to 12.3 in. in the same years.

Wetlands were assigned the same off-season recharge as ponds. In-season recharge was estimated by subtracting the difference between in-season and off-season wetland recharge in an average year from the off-season wetland recharge estimated for each of the 55 years. This method resulted in average in-season and off-season recharge rates that are consistent with the steady-state models. The lowest off-season and in-season wetland recharge rates were 14.8 and -38.7 in., respectively, in 1965; the highest off-season and in-season wetland recharge rates were 37.5 and -11.6, respectively, in 1972.

Simulated water levels at Marston Mills Pond had a total range of 6.7 ft if wetland recharge varied seasonally but had a net recharge of zero over the 55-year period simulated in the model. For simulations in which wetlands had a net positive recharge and a net negative recharge, water levels ranged from 7.3 and 6.8 ft, respectively, over the same period; the total water-level range was 7.2 ft in simulations in which wetland recharge were simulated as a constant value of zero. The simulation results suggest that seasonal wetland recharge does not have large effects on simulated water levels over multiyear time scales.

Pumping

Pumping increases because the demand for potable water increases during the summer months. Transient simulations incorporate temporal changes in pumping and simulate the effects of these changing stresses on the hydrologic system. Pumping records and demand projections used to estimate average steady-state pumping were used to estimate average monthly pumping and average seasonal pumping for current (2003) and future (2020) conditions.

Average Monthly Pumping

Monthly pumping data compiled from MDEP records for the period 1995–2000 were used to estimate average monthly pumping. For existing wells with adequate pumping records, the simulated average monthly data for current (2003) pumping was estimated directly from the data. In some cases, average pumping rates were available, but there was an incomplete record of monthly pumping. In these cases, the ratios of town-wide pumping for each month to total annual pumping for the town were used to estimate monthly pumping at the well from the average pumping rate. Current pumping from the Sagamore flow lens ranged from 34.6 Mgal/d in July to 10.2 Mgal/d in January (fig. 1-13*A*). From the Monomoy flow lens, monthly pumping ranged from 16.5 Mgal/d in July to 4.7 Mgal/d in March (fig. 1-13*B*).

Future (2020) monthly pumping rates were estimated from the projected steady-state pumping rates developed by MDEP. Monthly pumping rates for existing wells with adequate monthly pumping data were estimated from the ratios of average current (2003) pumping for each month to total annual pumping. For new or existing wells without adequate monthly pumping data, future monthly pumping rates were estimated from the ratios of town-wide pumping for each month to total annual pumping for the town. Future pumping from the Sagamore flow lens ranged from 52.9 Mgal/d in July to 16.4 Mgal/d in March (fig. 1-13*A*). Monthly pumping for future (2020) conditions from the Monomoy flow lens ranged from 25.4 Mgal/d in July to 7.1 Mgal/d in March (fig. 1-13*B*).

Wastewater return flow was estimated for each month on the basis of the total monthly pumping rates for each town. Wastewater was returned to the aquifer as enhanced recharge within residential areas (fig. 1-4). In towns with waste-disposal facilities, the fraction of total generated waste water that is currently discharged at the facilities and the estimated monthly pumping were used to determine the monthly estimated discharge at the plants; the remaining waste water was discharged as septic system return flow in residential areas. The same approach was used to estimate monthly wastewater return flow for future pumping.

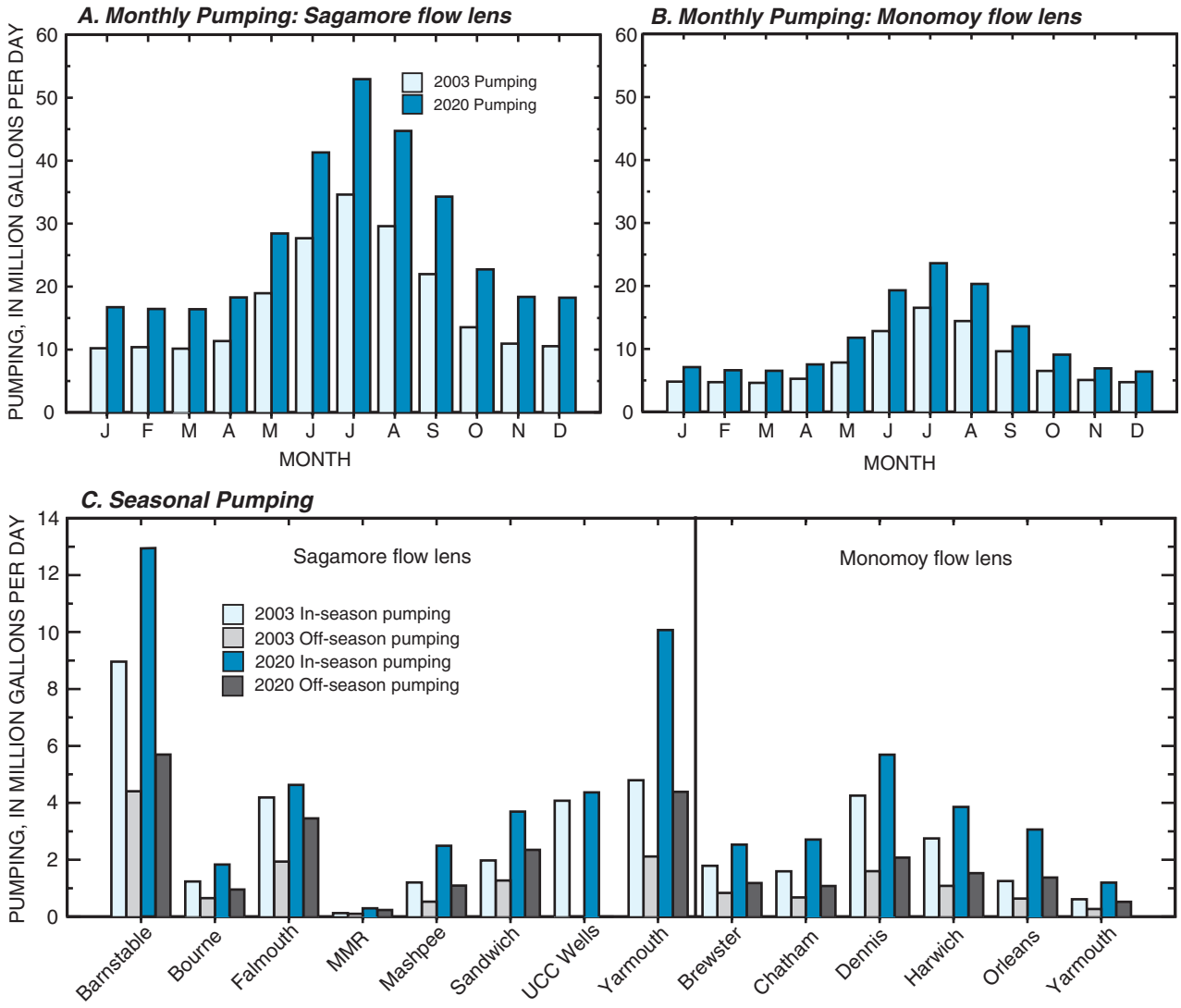

Figure 1-13. Average ground-water withdrawals by month for current (2003) and proposed (2020) pumping conditions for *A*, the Sagamore flow lens; *B*, the Monomoy flow lens; and *C*, in-season and off-season ground-water withdrawals by town for current and future pumping scenarios, Cape Cod, Massachusetts.

Seasonal Pumping

Seasonal pumping rates were determined from the estimated monthly pumping rates for current (2003) and future (2020) conditions. Off-season pumping rates represent the average pumping rate for the period October–April; in-season pumping rates are the average of monthly pumping for the months of May–September. From the Sagamore flow lens, current off-season pumping ranged from 4.4 Mgal/d for Barnstable to 0.7 Mgal/d for Bourne; in-season pumping in those towns was 9.0 and 1.2 Mgal/d, respectively. Off-season and in-season pumping for the MMR was 0.1 and 0.3 Mgal/d, respectively. Dennis had the largest current seasonal pumping from the Monomoy flow lens: 4.3 Mgal/d during the in-season time period and 1.6 Mgal/d during the off-season time period (fig. 1-13*C*). In-season and off-season pumping was the same during the 55-year period simulated in the models.

The largest increase in seasonal pumping for the year 2020 on the Sagamore flow lens was in Yarmouth, which had an increase of 5.3 Mgal/d, more than double current in-season pumping. In-season pumping also more than doubled for Orleans on the Monomoy flow lens (fig. 1-13C). Wastewater return flow for in-season and off-season stress periods for both current (2003) and future (2020) pumping was estimated from pumping rates and discharged in residential areas as enhanced recharge; in-season and off-season discharge rates at WDFs were estimated by using the methods described in the preceding section “Average Monthly Pumping.”

Comparison to Measured Water Levels and Flows

Simulated changes in water levels and streamflows through time were compared to those measured in long-term monitoring wells and at streamflow sites to assess the capacity of the models to predict the effects of changing stresses on the hydrologic system. Water levels in a network of wells and ponds are monitored by the CCC, the USGS, and by the APCC (fig. 1-7); water-level data have been collected at some wells since 1963. Data are compiled and stored by USGS in a database that is Web-accessible (http://waterdata.usgs.gov).

Simulated water levels are based on current (2003) pumping and are used in comparisons to measured water levels. Measured monthly or seasonal average water levels, however, are calculated for the entire period of record for each well or pond and the averages likely include values from periods of time with different pumping regimes. Available data were not sufficient to incorporate historical pumping into the models in a reasonable manner. Pumping accounts for about 6 percent of ground-water flow in the aquifers; changes in pumped volumes during the periods of record, which range from 20 to 35 years, likely are less than 5 percent of ground-water flow. In addition, most pumping historically has been concentrated in urbanized areas and many observation wells are in areas where water levels likely have not been appreciably affected by pumping. Whereas pumping may lower water levels in some areas, model simulations indicate that the temporal variability of water levels, as expressed as deviations from the average water level, does not change appreciably because of pumping. For these reasons, the comparison of simulated and measured fluctuations in water levels through time is assumed to be a reasonable means of verifying the transient models.

Monthly Conditions

Average monthly water levels were estimated from historical data for wells that had at least 20 measurements for each month for the period of record. Average monthly water levels were normalized to the annual average for the period of record to express the water levels as a departure from average; this process allows for a more direct comparison between the simulated and measured variability of water levels over time. Measured water levels generally are highest in April–June and lowest in October–December (fig. 1-14). The data indicate that minimum and maximum water levels lag about 2 months behind the minimum and maximum recharge in September and March of a typical year, respectively (fig. 1-12). Water levels in the wells during an average year fluctuate between 1.2 and 1.8 ft (fig. 1-14). Simulated water levels also were highest in April–June and lowest in October–December; this result indicates that the model adequately simulates the timing of monthly head fluctuations and the temporal relation between changes in recharge and water levels. Simulated water-level fluctuations during an average year range from 1.4 to 2.1, which is similar to fluctuations measured in the wells (fig. 1-14).

Suitable records of data were available to estimate average monthly water-level changes for four ponds: Ashumet Pond, Crocker Pond, Spectacle Pond, and Snake Pond (fig. 1-7). Averages were calculated for months with 20 or more measurements. Average water levels for the winter months could not be estimated at Spectacle and Snake Ponds owing to limited data (fewer than three measurements). Ponds stages generally were highest in May and lowest in November. Simulated water levels also were highest in May and lowest in November–December. Ponds generally had smaller ranges in water levels during an average year. The total change in water levels during an average year ranged from 0.6 ft to 1.2 ft. The total simulated change in water levels during an average year ranged from 0.9 ft to 1.5 ft (fig. 1-15). The data indicate that the models reasonably represent changes in pond stages over an average annual hydrologic cycle.

Streamflow data from the three USGS stations on Cape Cod were used to estimate average monthly flows. Comparisons of model-calculated streamflow fluctuations to measured streamflow fluctuations are summarized in figure 1-16. Minimum streamflows occur in the fall (September–November) and the highest streamflows occur in the spring (April–May). Simulated streamflows were lowest in August–October and highest in April (fig. 1-16*A*-*C*). The total range in monthly average measured streamflows at Herring River, Quashnet River, and Mill Creek/Shawme Pond outlet were 8.6, 7.1, and 1.4 ft^3/s, respectively. The simulated ranges during an average year at the same sites were 8.0, 7.5, and 1.6 ft^3/s, respectively, similar to the measured ranges. The data indicate that the transient models reasonably represent the magnitude and timing of variations in streamflows in an average year. The models accurately represent the annual range in streamflow at the Herring River, but generally predict the annual minimum and maximum streamflows about a month earlier than those estimated from streamflow data (fig. 1-16*C*). Comparisons of simulated streamflow at the midpoint of each month to the statistical distribution of measured values for each month over the period of record are presented in figure 1-16*D*-*F*.

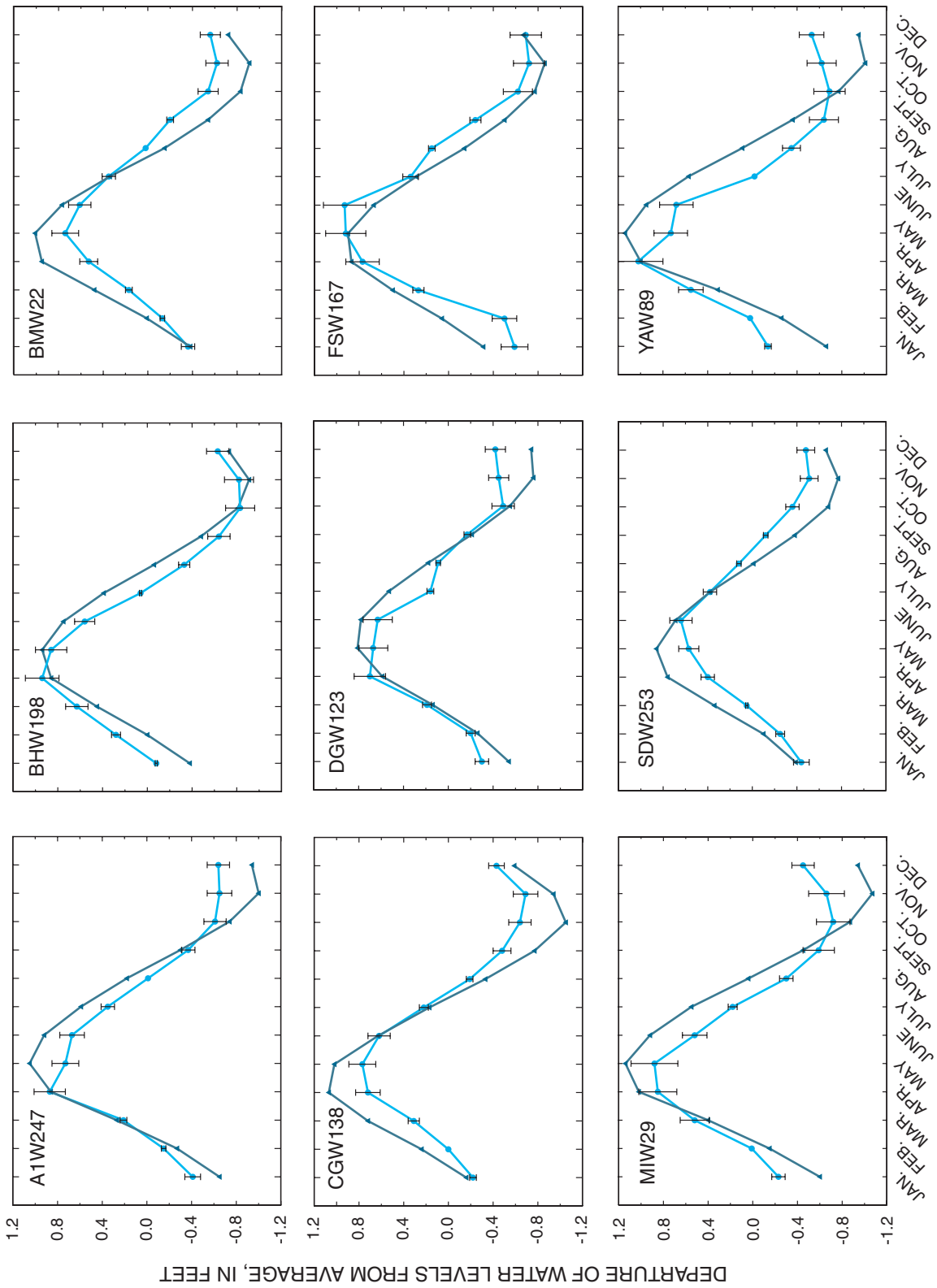

Figure 1-14. Comparisons of monthly simulated and observed water-level changes relative to averages at wells in the Sagamore and Monomoy flow models, Cape Cod, Massachusetts.

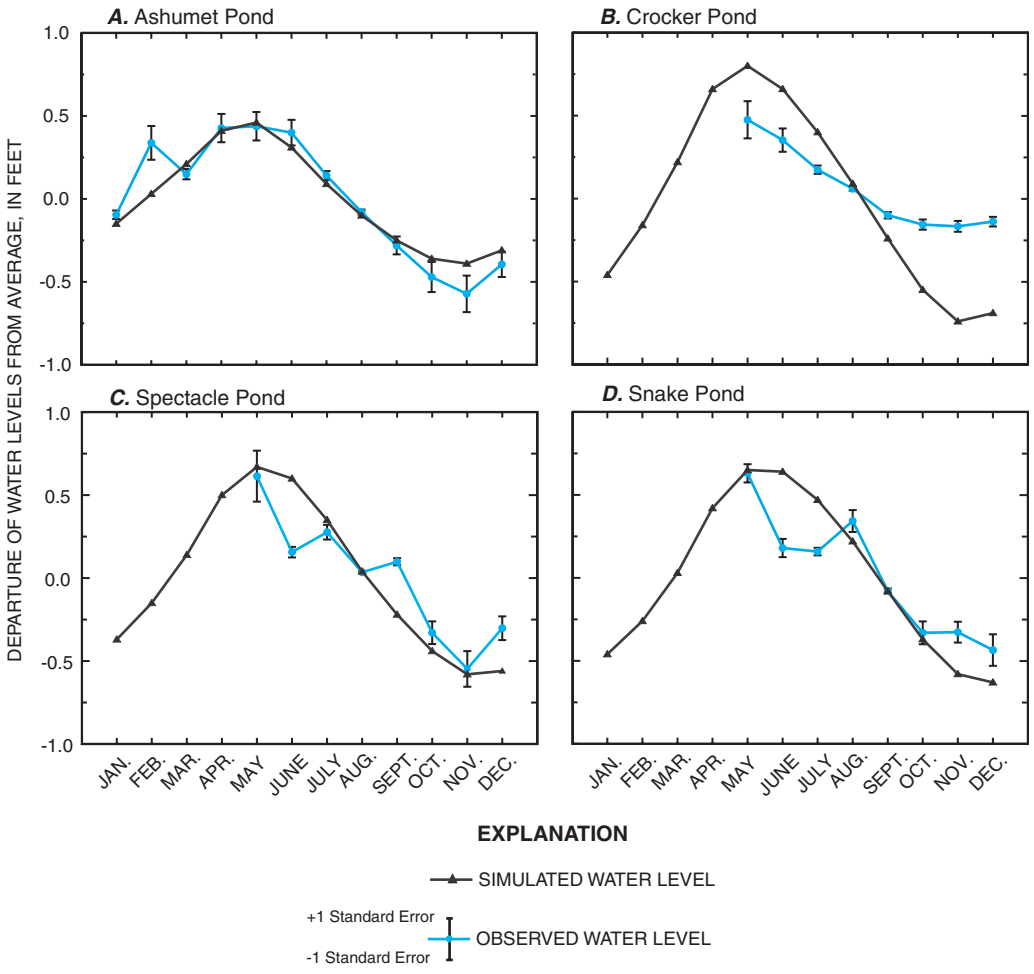

Figure 1-15. Comparisons of monthly simulated and observed water-level changes relative to averages at ponds in the Sagamore and Monomoy flow models, Cape Cod, Massachusetts.

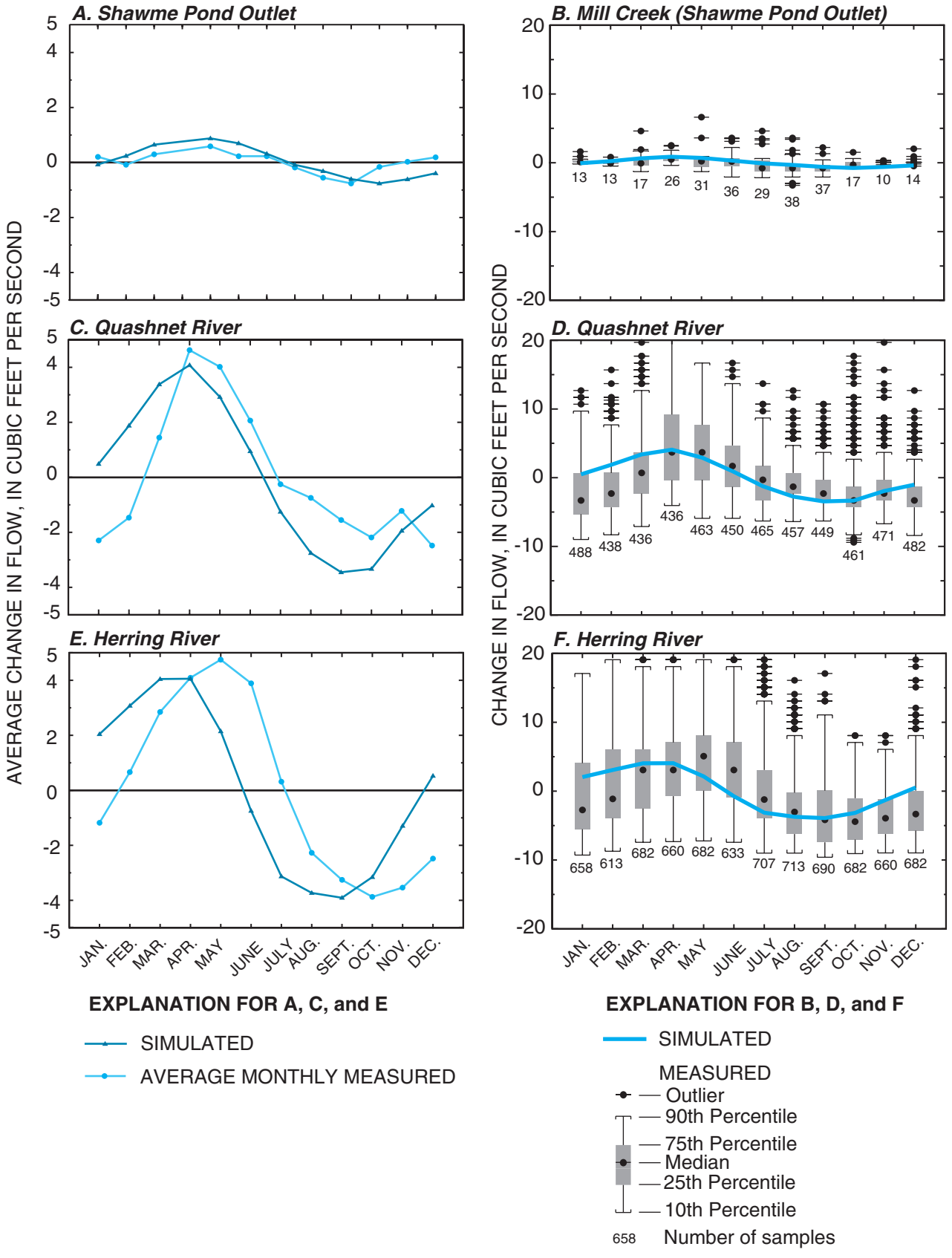

Figure 1-16. Comparisons of average monthly simulated and measured streamflow changes relative to averages at three monitoring sites in the Sagamore and Monomoy flow models, Cape Cod, Massachusetts.

Annual and Seasonal Conditions

Historical water levels were used to estimate seasonal averages for the period 1963–95 and for comparison with simulated water-level changes during that period. This 33-year record includes periods of low water levels in the mid-1960s and the early 1980s as a well as a period of high water levels in the early 1970s. Average seasonal water levels were normalized to the annual average for the period of record to express the water levels as a departure from average; this allows for a more direct comparison between the simulated and measured variability of water levels over time. These patterns in water levels reflect periods of lower and higher than average recharge (fig. 1-12*B*). Measured changes in water levels, relative to long-term-average water levels, were lowest in 1966–67 and generally highest in 1973–74; the highest water levels in two of the wells were measured in 1984. Wells with no data earlier than 1976 had minimum water levels in 1981–82 (fig. 1-17). The fact that recharge rates were lowest in 1965–66 indicates a time lag on the order of months to a year in the response of water levels to changes in recharge. Simulated water levels also were lowest in 1966–67 and highest in 1973–74 (fig. 1-17); thus, the models reasonably simulate the temporal relation between recharge and water levels in the aquifer. Water-level changes over multiyear time scales were larger than the monthly changes within an average year. The total change in measured water levels in wells ranged from 1.8 (SDW252) to 8.8 ft (A1W247) (fig. 1-17); the total simulated change in water levels range from 3.9 to 9.4 ft. The data indicate that the model-predicted changes in water levels for the period 1963–95 are in general agreement with measured changes. The models closely match measured water-level changes during some periods of time, but overestimate or underestimate water levels at other times. This result likely is due to previously discussed assumptions about the simulated recharge rate and the inability to represent recharge accurately over the entire period of simulation. However, the data does indicate that the models reasonably represent major features in the recharge record, such as droughts in the mid-1960s and early 1980s (fig. 1-17).

Historical water-level data were used to estimate the variability of pond stages for the period 1971–95 in five ponds (fig. 1-18). The water levels in the ponds were lowest in 1991–92 and highest at various times from 1973 to 1984; a period of low water levels in early 1980s was associated with a significant drought (fig. 1-12). The total range in measured water levels over the period of record ranged was 2.1 ft to 6.6 ft (fig. 1-18). The lowest simulated pond stages were in 1981; this period corresponds to the period of low recharge and measured pond stages in the early 1980s (fig. 1-12). The total change in simulated water levels over the period of record ranged from 2.6 ft to 5.1 ft. The data show that the models reasonably represent the response of the hydrologic system, as evidenced by pond stages, to changes in recharge.

Historical streamflow data from the Herring River (from 1966–88) and the Quashnet River (from 1988–95) (fig. 1-7) were used to estimate streamflow variability for the period 1966–95 (fig. 1-19). Seasonally averaged streamflows in the Herring River ranged between about 10 ft^3/s above to 10 ft^3/s below the average flow for the period of record (1966–88). The total ranges in measured and simulated streamflows in the Herring River were 17.7 and 15.5 ft^3/s, respectively. Extended (multiyear) periods of lower than average flows, both measured and simulated, occurred in the mid-1960s and in the early and later 1980s; periods of higher than average flows, both measured and simulated, occurred in the early 1970s and mid-1980s (fig. 1-19*A*). These temporal trends are similar to those observed for ground-water (fig. 1-17). Both measured and simulated streamflows in the Quashnet River, relative to average flow, were lowest in 1995; the highest measured and simulated flows were in the period 1993–94. The total measured and simulated fluctuations in streamflow at the site, relative to average flow, were 6.9 and 7.1 ft^3/s, respectively (fig. 1-19*B*). The data indicate that the models reasonably simulate streamflow over a multiyear time scale and accurately represent the stream-flow response to time-varying stresses.

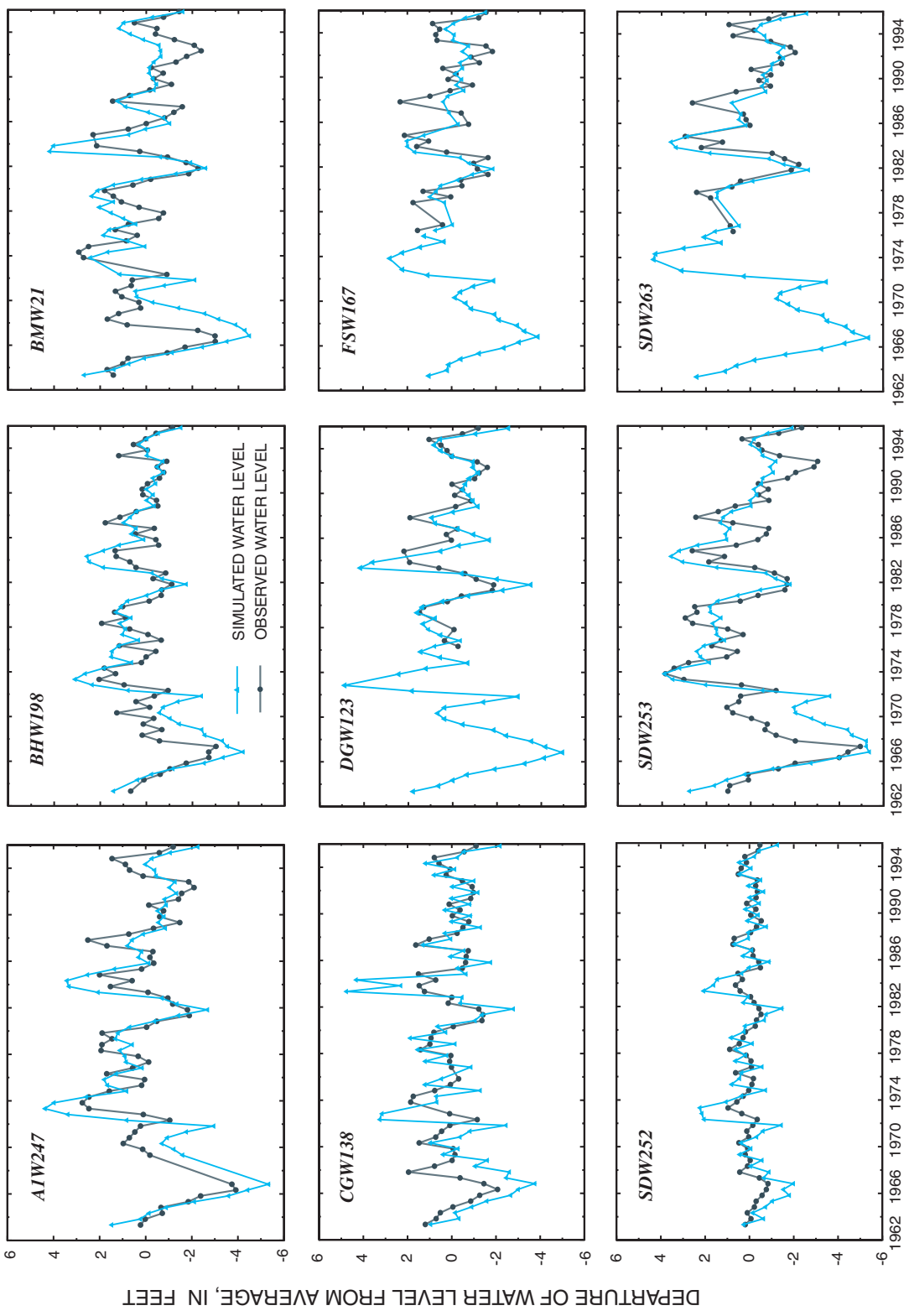

Figure 1-17. Comparisons of seasonal simulated and observed water-level changes relative to averages at wells over multiyear time scales in the Sagamore and Monomoy flow models, Cape Cod, Massachusetts.

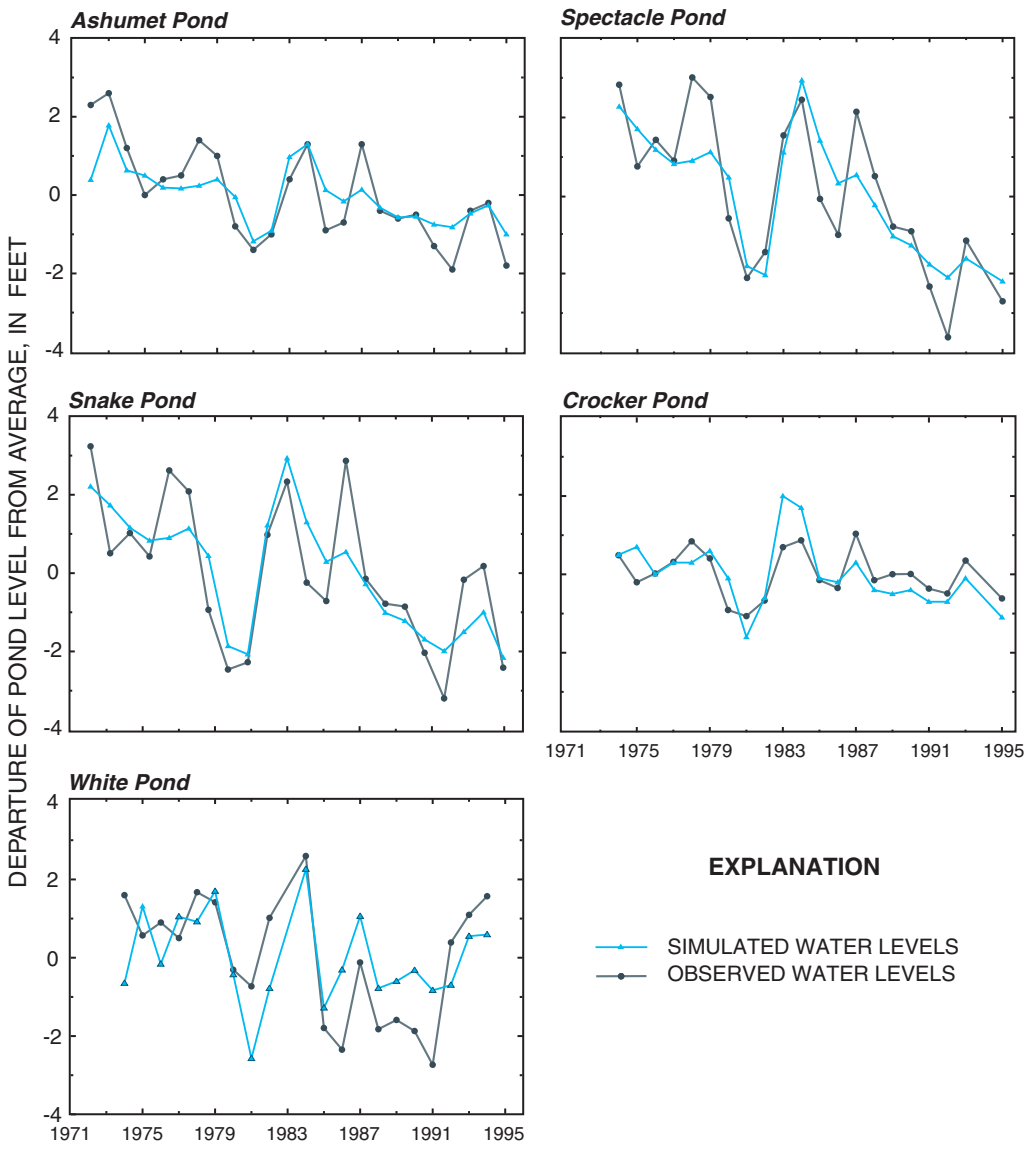

Figure 1-18. Comparisons of seasonal simulated and observed water-level changes relative to averages at ponds over multiyear time scales in the Sagamore and Monomoy flow models, Cape Cod, Massachusetts.

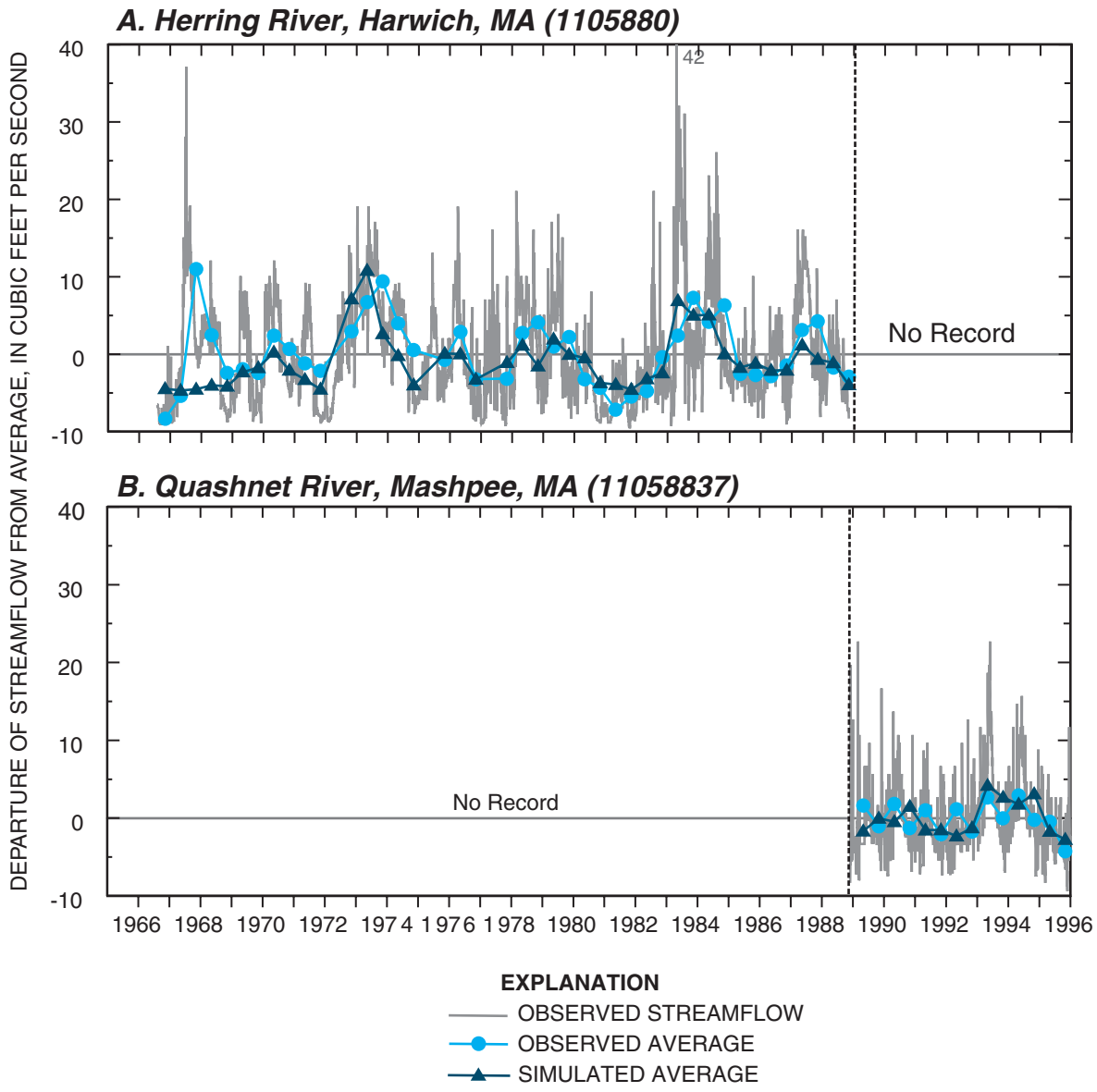

Figure 1-19. Comparisons of seasonal simulated and observed streamflow changes relative to averages at streamflow sites in the Sagamore and Monomoy flow models, Cape Cod, Massachusetts.

References Cited

Barlow, P.M., and Dickerman, D.C., 2000, Numerical simulation and conjunctive-management models of the Hunt-Annaquatucket-Pettaquamscutt stream-aquifer system, Rhode Island: U.S. Geological Survey Professional Paper 1636, 79 p.

Barlow, P.M., 1994, Particle-tracking analysis of contributing areas of public-supply wells in simple and complex flow systems, Cape Cod, Massachusetts: U.S. Geological Survey Water-Supply Paper 2434, 66 p.

Barlow, P.M. and Hess, K. M., 1993, Simulated hydrologic responses of the Quashnet River stream-aquifer system to proposed ground-water withdrawals: U.S. Geological Survey Water-Resources Investigations Report 93-4064, 52 p.

DeSimone, L.A., Water, D.A., Eggleston, J.R., and Nimiroski, M.T., 2002, Simulation of ground water flow and evaluation of water-management alternatives in the upper Charles River Basin, eastern Massachusetts: U.S. Geological Survey Water-Resources Investigation Report 02-4234, 94 p.

Farnsworth, R.K., Thompson, E.S., and Peck, E.L., 1982, Evaporation atlas for the contiguous 48 United States; National Oceanic and Atmospheric Administration Technical Report NWS 33, 26 p.

Freeze, A.R., and Cherry, J.A., 1979, Groundwater: Englewood Cliffs, NJ, Prentice Hall, Inc., p. 37.

Garabedian, S.P., LeBlanc, D.R., Gelhar, L.W., and Celia, M.A., 1985, Large-scale natural-gradient tracer test in sand and gravel, Cape Cod, Massachusetts—2. Analysis of spatial moments for a nonreactive tracer: Water Resources Research, v. 27, no. 5, p. 911–924.

Guswa, J.H., and LeBlanc, D.R., 1985, Digital models of ground-water flow in the Cape Cod aquifer system, Massachusetts: U.S. Geological Survey Water-Supply Paper 2209, 112 p.

Hall, F.R., Rutherford, R.J., and Byers, G.L.,1972, The Influence of a New England Wetland on Water Quantity and Quality: Durham, NH, Water Resources Research Center, University of New Hampshire, 7 p.

Hansen, B.P., and Lapham, W.W., 1990, Geohydrology and simulated ground-water flow, Plymouth–Carver Aquifer, southeastern Massachusetts: U.S. Geological Survey Water-Resources Investigation Report 90-4204, 82 p., 2 pls.

Harbaugh, A.W., Banta, E.R., Hill, M.C., and McDonald, M.G., 2000, MODFLOW-2000, The U.S. Geological Survey modular ground-water model—User guide to modularization concepts and the ground-water flow process: U.S. Geological Survey Open-File Report 00-92, 121 p.

Hill, M.C., Banta, E.R, Harbaugh, A.W., and Anderman, E.R., 2000, MODFLOW-2000, The U.S Geological Survey modular ground-water model—User guide to the observation, sensitivity, and parameter-estimation processes and three post-processing programs: U.S. Geological Survey Open-File Report 00-184, 209 p.

Hsieh, P.A., and Freckelton, J.R., 1993, Documentation of a computer program to simulate horizontal-flow barriers using the U.S. Geological Survey's modular three-dimensional finite-difference ground-water-flow model: U.S. Geological Survey Open-File Report 92-477, 32 p.

Jensen, M.E., and Haise, H.D., 1963, Estimating evapotranspiration from solar radiation: Proceedings of the American Society of Civil Engineering, Journal of Irrigation and Drainage, v. 89, no. IR4, p. 15–41.

Leahy, P.P., and Martin, Mary, 1993, Geohydrology and simulation of ground-water flow in the Northern Atlantic Coastal Plain Aquifer system: U.S. Geological Survey Professional Paper 1404-K, p. 81.

LeBlanc D.R., Garabedian, S.P., Hess, K.M., Gellar, L.W. Quadri, R.D., Stollenwerk, K.G., and Wood, W.W., 1991, Large-scale natural-gradient tracer test in sand and gravel, Cape Cod, Massachusetts—l. Experimental design and tracer movement: Water Resources Research, v. 27, no. 5, p. 895–910.

LeBlanc, D.R., Guswa, J.H., Frimpter, M.H., and Londquist, C.J., 1986, Ground-water resources of Cape Cod, Massachusetts: U.S. Geological Survey Hydrologic Atlas 692, 4 pls.

Massachusetts Department of Fisheries and Wildlife, 1993, Pond maps for southeastern Massachusetts: Publication No. 17363-106-1M, May 1993, 85 p.

Masterson J.P., 2004, Simulated interaction between freshwater and saltwater and effects of ground-water pumping and sea-level change, lower Cape Cod Aquifer System, Massachusetts: U.S. Geological Survey Scientific Investigations Report 2004-5014, 68 p.

Masterson, J.P., and Barlow, P.M., 1997, Effects of simulated ground-water pumping and recharge on ground-water flow in Cape Cod, Martha's Vineyard, and Nantucket Island Basins, Massachusetts: U.S. Geological Survey Water-Supply Paper 2447, 78 p.

Masterson, J.P., and Walter, D.A., 2000, Delineation of ground-water recharge areas, western Cape Cod, Massachusetts: U.S. Geological Survey Water-Resources Investigation Report 00-4000, 1 pl.

Masterson, J.P., Walter, D.A., and Savoie, Jennifer, 1997, Use of particle tracking to improve numerical model calibration and to analyze ground-water flow and contaminant migration, Massachusetts Military Reservation, western Cape Cod, Massachusetts: U.S. Geological Survey Water-Supply Paper 2482, 50 p.

McCobb, T.D., and LeBlanc, D.R., 2002, Detection of fresh ground water and a contaminant plume beneath Red Brook Harbor, Cape Cod, Massachusetts, 2000: U.S. Geological Survey Water-Resources Investiagiton Report 02-4166, 36 p.

McDonald, M.G., and Harbaugh, A.W., 1988, A modular three-dimensional finite-difference ground-water-flow model: U.S. Geological Survey Techniques of Water-Resources Investigations, book 6, chap A1, 586 p.

Moench, A.F., 2001, Specific yield as determined by type-curve analysis of aquifer-test data: Ground Water, v. 32, no. 6, p. 949–957.

Motts, W.S. and O'Brien, A.L., 1981, Geology and hydrology of wetlands in Massachusetts: Amherst, MA, Water Resources Research Center, University of Massachusetts, 18 p.

Nicholson, R.S., and Watt, M.K.,1997, Simulation of ground-water flow in the unconfined aquifer system of Toms River, Metedeconk River, and Kettle Creek Basins, New Jersey: U.S. Geological Survey Water-Resources Investigations Report 97-4066, 99 p.

O'Brien, A.L., 1977, Hydrology of two small wetland basins in eastern Massachusetts: American Water Resources Association Water Resources Bulletin, v. 13, no. 2, p. 325–340.

Orzol, L.L., 1997, User's guide for MODTOOLS—Computer programs for translating data of MODFLOW and MODPATH into Geographic Information Systems files: U.S. Geological Survey Open-File Report 94-464, 86 p.

Pollock, D.W., 1994, User's guide for MODPATH/MODPATH-PLOT, version 3—A particle tracking post-processing package for MODFLOW, the U.S. Geological Survey finite-difference ground-water flow model: U.S. Geological Survey Open-File Report 94-464, 234 p.

Prudic, D.E., 1989, Documentation of a computer program to simulate stream-aquifer relations using a modular, finite-difference, ground-water flow model: U.S. Geological Survey Open-File Report 88-729, 113 p.

Reilly, T.E., and Goodman, A.S., 1985, Quantitative analysis of saltwater-freshwater relationships in ground-water systems—A historical perspective: Journal of Hydrology, v. 80, p. 125–160.

Savoie, J.G., 1994, Altitude and configuration of the water table, western Cape Cod, Massachusetts, March 1993: U.S. Geological Survey Open-File Report 94-462, 1 sheet, scale 1:50,000.

Walter, D.A., and Masterson, J.P., 2003, Simulation of advective flow under steady-state and transient recharge conditions, Camp Edwards, Massachusetts Military Reservation, Cape Cod, Massachusetts: U.S. Geological Survey Water-Resources Investigations Report 03-4053, 51 p.

Walter, D.A., Masterson, J.P., and Barlow, P.M., 1997, Hydrogeology and analysis of ground-water-flow system, Sagamore Marsh Area, southeastern Massachusetts: U.S. Geological Survey Water-Resources Investigations Report 94-4200, 41 p.

Table 1-3

Table 1-3. Current (2003) and future (2020) ground-water withdrawals for the Sagamore and Monomoy flow models and location of wells in model coordinates (layer, row, and column), Cape Cod, Massachusetts.

[**Data source:** BFD, Barnstable Fire Department; BWC, Barnstable Water Company; CFD, Cotuit Fire Department; COWD, Centerville–Osterville Water Department; MMR, Massachusetts Military Reservation; UCC, Upper Cape Cooperative Wells. MADEP, Massachusetts Department of Environmental Protection; ft, foot; Mgal/d, million gallons per day]

Sagamore flow model										
Town	MADEP number	Data source	Model			Screen midpoint elevation (ft)	Current (2003) no UCC wells (Mgal/d)	Current (2003) with UCC wells (Mgal/d)	Projected (2020) no UCC wells (Mgal/d)	Projected (2020) with UCC wells (Mgal/d)
			Layer	Row	Column					
Barnstable	4020002-02G	COWD	11	127	207	-35.09	0.120	0.120	0.052	0.052
Barnstable	4020004-10G	BWC	9	97	282	-10.14	.143	.143	.280	.280
Barnstable	4020002-08G	COWD	9	121	253	-16.67	.158	.158	.095	.095
Barnstable	4020002-04G	COWD	11	120	253	-31.66	.071	.071	.062	.062
Barnstable	4020002-07G	COWD	10	122	252	-24.34	.050	.050	.075	.075
Barnstable	4020002-16G	COWD	10	81	187	-26.23	.442	.442	.363	.363
Barnstable	4020002-13G	COWD	7	82	186	8.93	.277	.277	.261	.261
Barnstable	4020002-06G	COWD	9	128	204	-19.14	.118	.118	.069	.069
Barnstable	4020003-02G	CFD	7	132	172	1.18	.119	.119	.121	.121
Barnstable	4020003-04G	CFD	9	134	172	-12.5	.081	.081	.001	.001
Barnstable	4020003-03G	CFD	10	142	173	-20.86	.054	.054	.085	.085
Barnstable	4020002-14G	COWD	9	114	181	-11.92	.111	.111	.069	.069
Barnstable	4020002-15G	COWD	8	112	181	-1.99	.109	.109	.061	.061
Barnstable	4020002-17G	COWD	9	114	178	-18.82	.293	.293	.201	.201
Barnstable	4020002-18G	COWD	11	116	177	-35.06	.018	.018	.261	.261
Barnstable	4020002-19G	COWD	10	115	176	-28.07	.012	.012	.261	.261
Barnstable	4020002-11G	COWD	9	116	184	-10.13	.291	.291	.261	.261
Barnstable	4020002-12G	COWD	7	115	184	3.76	.078	.078	.125	.125
Barnstable	4020004-03G	BWC	12	127	262	-47.78	.251	.251	.549	.549
Barnstable	4020002-03G	COWD	11	114	219	-34.5	.076	.076	.097	.097
Barnstable	4020002-05G	COWD	10	114	218	-20.93	.142	.142	.173	.173
Barnstable	4020004-07G	BWC	10	107	286	-25.14	.162	.162	.244	.244
Barnstable	4020004-07Ga	BWC	13	107	286	-59.14	.162	.162	.244	.244
Barnstable	4020004-02G	BWC	11	107	287	-39.27	.487	.487	.511	.511
Barnstable	4020004-11G	BWC	11	107	286	-38.34	.535	.535	.509	.509
Barnstable	4020004-04G	BWC	8	94	281	-9.31	.179	.179	.170	.170
Barnstable	4020004-05G	BWC	8	93	282	-7.16	.145	.145	.153	.153
Barnstable	4020004-08G	BWC	8	91	280	-.1	.000	.000	.000	.000
Barnstable	4020004-09G	BWC	8	90	280	-6.3	.046	.046	.168	.168
Barnstable	4020002-01G	COWD	11	131	206	-30.6	.006	.006	.261	.261
Barnstable	4020002-09G	COWD	8	102	211	-2.99	.137	.137	.157	.157
Barnstable	4020002-10G	COWD	7	102	212	6.36	.143	.143	.144	.144
Barnstable	4020000-02G	BFD	10	90	274	-20.52	.000	.000	.320	.320
Barnstable	4020000-01G	BFD	8	79	262	-6.84	.000	.000	.000	.000
Barnstable	4020002-21G	COWD	9	111	174	-17.32	.000	.000	.261	.261
Barnstable	4020002-20G	COWD	9	79	188	-17.32	.000	.000	.261	.261
Barnstable	4020002-22G	COWD	9	114	217	-17.32	.000	.000	.261	.261
Barnstable	4020000-03G	BFD	11	86	254	-36.7	.273	.273	.200	.200
Barnstable	4020000-04G	BFD	13	86	253	-52.05	.242	.242	.200	.200
Barnstable	4020003-06G	CFD	13	131	159	-53.07	.085	.085	.208	.208

Table 1-3. Current (2003) and future (2020) ground-water withdrawals for the Sagamore and Monomoy flow models and location of wells in model coordinates (layer, row, and column), Cape Cod, Massachusetts.—Continued

[**Data source:** BFD, Barnstable Fire Department; BWC, Barnstable Water Company; CFD, Cotuit Fire Department; COWD, Centerville–Osterville Water Department; MMR, Massachusetts Military Reservation; UCC, Upper Cape Cooperative Wells. MADEP, Massachusetts Department of Environmental Protection; ft, foot; Mgal/d, million gallons per day]

Sagamore flow model										
Town	MADEP number	Data source	Model			Screen midpoint elevation (ft)	Current (2003) no UCC wells (Mgal/d)	Current (2003) with UCC wells (Mgal/d)	Projected (2020) no UCC wells (Mgal/d)	Projected (2020) with UCC wells (Mgal/d)
			Layer	Row	Column					
Barnstable	4020004-06G	BWC	13	125	263	-54.92	0.487	0.487	0.451	0.451
Barnstable	4020004-01G	BWC	10	121	261	-25.47	.000	.000	.000	.000
Barnstable	4020003-05G	CFD	9	130	174	-15.1	.096	.096	.117	.117
Barnstable	4020004-12G	BWC	18	121	261	-149.47	.103	.103	.355	.355
Bourne	4036003-01G	Bourne	10	9	112	-23.51	.000	.000	.162	.130
Bourne	4036000-03G	Bourne	11	69	64	-34.31	.139	.108	.205	.165
Bourne	4036000-04G	Bourne	9	66	64	-15.69	.154	.124	.198	.160
Bourne	4036000-01G	Bourne	11	69	57	-37.41	.079	.071	.096	.077
Bourne	4036000-01Gc	Bourne	9	69	57	-19.41	.079	.071	.096	.077
Bourne	4036000-01Gb	Bourne	9	69	57	-16.41	.079	.071	.096	.077
Bourne	4036000-01Ga	Bourne	10	69	57	-21.41	.079	.071	.096	.077
Bourne	4036000-02G	Bourne	9	107	60	-13.58	.106	.075	.187	.151
Bourne	4036000-05G	Bourne	8	109	60	-2.29	.152	.117	.223	.179
Bourne	4036000-06G	Bourne	12	72	61	-46.63	.222	.186	.284	.228
Falmouth	4096000-01G	Falmouth	8	148	97	-4.76	.000	.000	1.111	.770
Falmouth	4096000-03G	Falmouth	9	148	81	-12.4	.674	.213	.753	.750
Falmouth	4096000-02G	Falmouth	10	168	108	-21.96	.496	.035	.666	.591
Falmouth	4096000-01S	Falmouth	7	183	53	5	2.468	2.468	.997	.641
Falmouth	4096000-04G	Falmouth	10	172	67	-23.88	.334	.160	.314	.314
Falmouth	4096000-0AG	Falmouth	8	149	70	-5.22	.000	.000	1.023	.879
MMR	4096001-01G	MMR	5	104	110	24.78	.304	.112	.260	.260
Mashpee	4172039-06G	Mashpee	9	146	129	-18	.000	.000	.226	.205
Mashpee	4172039-0FG	Mashpee	8	135	136	-8.7	.000	.000	.238	.212
Mashpee	4172039-0CG	Mashpee	8	128	130	-4.24	.000	.000	.141	.000
Mashpee	4172039-0AG	Mashpee	9	163	126	-18.58	.000	.000	.228	.205
Mashpee	4172039-04G	Mashpee	9	140	154	-17.04	.137	.121	.204	.204
Mashpee	4172039-02G	Mashpee	12	186	148	-40.44	.302	.268	.251	.217
Mashpee	4172039-03G	Mashpee	12	186	149	-45.15	.361	.328	.250	.215
Mashpee	4172039-0GG	Mashpee	9	162	123	-18.16	.000	.000	.238	.212
Mashpee	4172039-05G	Mashpee	8	162	123	-.19	.109	.081	.226	.205
Mashpee	4172039-01G	Mashpee	5	152	120	28.71	.010	.010	.000	.000
Sandwich	4261000-07G	Sandwich	10	50	177	-25.34	.199	.185	.261	.261
Sandwich	4261000-0BG	Sandwich	11	35	149	-33.02	.000	.000	.161	.161
Sandwich	4261000-02G	Sandwich	10	32	150	-22.76	.089	.080	.100	.100
Sandwich	4261000-03G	Sandwich	10	32	150	-23.31	.103	.094	.110	.110
Sandwich	4261000-05G	Sandwich	6	93	114	16.44	.000	.000	.100	.100
Sandwich	4261000-0EG	Sandwich	8	49	176	.00	.000	.000	.161	.161
Sandwich	4261000-04G	Sandwich	5	72	150	23.22	.048	.035	.201	.201
Sandwich	4261000-06G	Sandwich	6	72	152	13.09	.417	.404	.221	.221
Sandwich	4261000-08G	Sandwich	9	82	167	-14.5	.152	.138	.151	.151

Table 1-3. Current (2003) and future (2020) ground-water withdrawals for the Sagamore and Monomoy flow models and location of wells in model coordinates (layer, row, and column), Cape Cod, Massachusetts.—Continued

[**Data source:** BFD, Barnstable Fire Department; BWC, Barnstable Water Company; CFD, Cotuit Fire Department; COWD, Centerville–Osterville Water Department; MMR, Massachusetts Military Reservation; UCC, Upper Cape Cooperative Wells. MADEP, Massachusetts Department of Environmental Protection; ft, foot; Mgal/d, million gallons per day]

Sagamore flow model										
Town	MADEP number	Data source	Model			Screen midpoint elevation (ft)	Current (2003) no UCC wells (Mgal/d)	Current (2003) with UCC wells (Mgal/d)	Projected (2020) no UCC wells (Mgal/d)	Projected (2020) with UCC wells (Mgal/d)
			Layer	Row	Column					
Sandwich	4261000-0CG	Sandwich	8	77	154	-2.45	0.000	0.000	0.261	0.261
Sandwich	4261000-0DG	Sandwich	5	101	110	24.2	.000	.000	.171	.171
Sandwich	4261000-10G	Sandwich	7	69	149	8.36	.245	.231	.261	.261
Sandwich	4261000-11G	Sandwich	7	76	156	9.61	.163	.150	.171	.171
Sandwich	4261000-09G	Sandwich	11	33	149	-35.79	.260	.247	.321	.321
Sandwich	4261000-0AG	Sandwich	7	69	167	5.09	.000	.000	.261	.261
UCC	4261024-01G	UCC	9	54	135	-16.2	.000	.566	.253	.613
UCC	4261024-02G	UCC	12	43	125	-49.94	.000	.566	.000	.603
UCC	4261024-03G	UCC	14	40	122	-6.63	.000	.566	.000	.603
Yarmouth	4351000-13G	Yarmouth	9	95	309	-19.41	.122	.122	.259	.259
Yarmouth	4351000-18G	Yarmouth	10	98	309	-27.55	.110	.110	.209	.209
Yarmouth	4351000-19G	Yarmouth	11	98	311	-32.6	.107	.107	.202	.202
Yarmouth	4351000-11G	Yarmouth	10	90	323	-22.93	.138	.138	.290	.290
Yarmouth	4351000-12G	Yarmouth	10	92	322	-25.5	.123	.123	.257	.257
Yarmouth	4351000-20G	Yarmouth	10	90	299	-28.5	.132	.132	.321	.321
Yarmouth	4351000-02G	Yarmouth	9	85	299	-16.6	.058	.058	.106	.106
Yarmouth	4351000-02Ga	Yarmouth	11	86	298	-31.6	.058	.058	.106	.106
Yarmouth	4351000-03G	Yarmouth	7	85	299	4.45	.082	.082	.140	.140
Yarmouth	4351000-03Ga	Yarmouth	9	85	299	-13.72	.082	.082	.140	.140
Yarmouth	4351000-04G	Yarmouth	6	84	300	12.3	.094	.094	.189	.189
Yarmouth	4351000-04Ga	Yarmouth	8	84	300	-8.5	.094	.094	.189	.189
Yarmouth	4351000-14G	Yarmouth	10	101	303	-28	.092	.092	.235	.235
Yarmouth	4351000-17G	Yarmouth	12	102	306	-48.5	.136	.136	.308	.308
Yarmouth	4351000-24G	Yarmouth	10	94	300	-23.69	.089	.089	.249	.249
Yarmouth	4351000-06G	Yarmouth	12	97	333	-42	.174	.174	.243	.243
Yarmouth	4351000-05G	Yarmouth	12	97	333	-49.9	.175	.175	.250	.250
Yarmouth	4351000-23G	Yarmouth	12	89	303	-45.28	.118	.118	.401	.401
Yarmouth	4351000-15G	Yarmouth	13	74	340	-53.7	.110	.110	.346	.346
Yarmouth	4351000-16G	Yarmouth	12	75	339	-46.6	.098	.098	.449	.449
Yarmouth	4351000-07G	Yarmouth	11	83	347	-37.1	.091	.091	.225	.225
Yarmouth	4351000-08G	Yarmouth	11	83	347	-37.2	.102	.102	.238	.238
Yarmouth	4351000-09G	Yarmouth	11	83	347	-32.8	.095	.095	.211	.211
Yarmouth	4351000-10G	Yarmouth	11	81	346	-37	.269	.269	.554	.554
Yarmouth	4351000-01Ga	Yarmouth	9	70	318	-15.9	.120	.120	.160	.160
Yarmouth	4351000-01G	Yarmouth	9	70	318	-12.6	.120	.120	.160	.160
Yarmouth	4351000-01Gb	Yarmouth	10	70	318	-27.99	.120	.120	.160	.160
Yarmouth	4351000-01Gc	Yarmouth	10	70	318	-24.76	.120	.120	.160	.160

Table 1-3. Current (2003) and future (2020) ground-water withdrawals for the Sagamore and Monomoy flow models and location of wells in model coordinaets (layer, row, and column), Cape Cod, Massachusetts.—Continued

[**Data source:** BFD, Barnstable Fire Department; BWC, Barnstable Water Company; CFD, Cotuit Fire Department; COWD, Centerville–Osterville Water Department; MMR, Massachusetts Military Reservation; UCC, Upper Cape Cooperative Wells. MADEP, Massachusetts Department of Environmental Protection; ft, foot; Mgal/d, million gallons per day]

Monomoy Flow Model									
Town	MADEP number	Source	Model			Screen midpoint elevation (ft)	Current (2003) wells (Mgal/d)	Projected (2020) with interbasin transfer (Mgal/d)	Projected (2020) no interbasin transfer (Mgal/d)
			Layer	Row	Column				
Brewster	4041000-01G	Brewster	10	74	147	-27.23	0.291	0.461	0.461
Brewster	4041000-02G	Brewster	10	77	149	-23.33	.290	.471	.471
Brewster	4041000-0BG	Brewster	15	93	94	-78.82	.000	.471	.471
Brewster	4041000-04G	Brewster	13	82	95	-51.25	.331	.040	.040
Brewster	4041000-03G	Brewster	10	68	155	-28	.319	.301	.301
Chatham	4055000-07G	Chatham	14	117	151	-67.8	.152	.286	.286
Chatham	4055000-04G	Chatham	15	116	173	-77.08	.000	.000	.000
Chatham	4055000-0CG	Chatham	11	124	149	-38.36	.000	.299	.299
Chatham	4055000-01G	Chatham	9	126	148	-14.85	.074	.063	.063
Chatham	4055000-02G	Chatham	9	126	148	-13.6	.154	.000	.000
Chatham	4055000-03G	Chatham	12	126	148	-42.17	.058	.290	.290
Chatham	4055000-06G	Chatham	13	120	149	-57.6	.223	.293	.293
Chatham	4055000-05G	Chatham	12	110	176	-49	.127	.230	.230
Chatham	4055000-08G	Chatham	16	110	177	-83.25	.274	.299	.299
Dennis	4075000-11G	Dennis	8	99	73	-.99	.215	.253	.253
Dennis	4075000-08G	Dennis	8	98	70	-1.94	.145	.149	.149
Dennis	4075000-09G	Dennis	7	97	71	7.35	.074	.079	.079
Dennis	4075000-15G	Dennis	9	91	66	-10.2	.144	.149	.149
Dennis	4075000-16G	Dennis	9	91	65	-12	.159	.200	.200
Dennis	4075000-14G	Dennis	11	122	77	-36.86	.001	.000	.000
Dennis	4075000-20G	Dennis	15	92	42	-78	.054	.240	.240
Dennis	4075000-10G	Dennis	9	94	60	-16.72	.142	.230	.230
Dennis	4075000-18G	Dennis	15	85	55	-79	.215	.252	.252
Dennis	4075000-01G	Dennis	8	114	59	-7.93	.038	.043	.043
Dennis	4075000-01Ga	Dennis	8	113	59	-8.02	.038	.043	.043
Dennis	4075000-01Gb	Dennis	9	113	59	-14.6	.038	.043	.043
Dennis	4075000-01Gc	Dennis	9	112	60	-15.09	.038	.043	.043
Dennis	4075000-01Gd	Dennis	9	112	60	-15	.038	.043	.043
Dennis	4075000-05G	Dennis	7	94	54	5.95	.066	.069	.069
Dennis	4075000-07G	Dennis	8	93	53	-1	.032	.050	.050
Dennis	4075000-12G	Dennis	9	96	54	-18	.104	.140	.140
Dennis	4075000-02G	Dennis	8	102	67	-6.08	.106	.149	.149
Dennis	4075000-03G	Dennis	8	102	67	-4.42	.059	.060	.060
Dennis	4075000-04G	Dennis	9	102	67	-14.55	.072	.120	.120
Dennis	4075000-13G	Dennis	9	104	75	-16.57	.258	.252	.252
Dennis	4075000-21G	Dennis	11	105	66	-36.69	.205	.251	.251
Dennis	4075000-22G	Dennis	18	94	53	-129.15	.000	.250	.250
Dennis	4075000-06G	Dennis	8	108	63	-5	.111	.099	.099
Dennis	4075000-19G	Dennis	14	90	43	-67	.214	.252	.252
Dennis	4075000-17G	Dennis	9	96	65	-12.61	.142	.120	.120

Table 1-3. Current (2003) and future (2020) ground-water withdrawals for the Sagamore and Monomoy flow models and location of wells in model coordinaets (layer, row, and column), Cape Cod, Massachusetts.—Continued

[**Data source:** BFD, Barnstable Fire Department; BWC, Barnstable Water Company; CFD, Cotuit Fire Department; COWD, Centerville–Osterville Water Department; MMR, Massachusetts Military Reservation; UCC, Upper Cape Cooperative Wells. MADEP, Massachusetts Department of Environmental Protection; ft, foot; Mgal/d, million gallons per day]

Monomoy Flow Model									
Town	MADEP number	Source	Model			Screen midpoint elevation (ft)	Current (2003) wells (Mgal/d)	Projected (2020) with interbasin transfer (Mgal/d)	Projected (2020) no interbasin transfer (Mgal/d)
			Layer	Row	Column				
Harwich	4126000-10G	Harwich	10	99	165	-24.5	0.177	0.148	0.148
Harwich	4126000-04G	Harwich	13	126	134	-58.84	.214	.208	.208
Harwich	4126000-01G	Harwich	9	120	134	-13.71	.186	.175	.175
Harwich	4126000-02G	Harwich	10	120	134	-22.02	.092	.104	.104
Harwich	4126000-03G	Harwich	7	121	135	2.98	.166	.142	.142
Harwich	4126000-05G	Harwich	10	123	134	-20.06	.004	.000	.000
Harwich	4126000-06G	Harwich	8	122	145	-9.61	.168	.169	.169
Harwich	4126000-07G	Harwich	9	121	145	-19.36	.163	.176	.176
Harwich	4126000-08G	Harwich	8	122	147	-7.75	.195	.182	.182
Harwich	4126000-09G	Harwich	10	99	163	-26.26	.148	.123	.123
Harwich	4126000-12G	Harwich	9	91	158	-19.82	.073	.187	.187
Harwich	4126000-0AG	Harwich	10	99	95	-25.97	.000	.171	.171
Harwich	4126000-0CG	Harwich	10	118	145	-25.97	.000	.182	.182
Harwich	4126000-0GG	Harwich	10	99	165	-25.97	.000	.182	.182
Harwich	4126000-11G	Harwich	15	100	94	-75.76	.192	.182	.182
Harwich	4126000-0AA	Harwich	10	99	94	-25.97	.000	.171	.171
Orleans	4224000-04G	Orleans	11	56	171	-32.5	.085	.103	.284
Orleans	4224000-05G	Orleans	11	56	173	-32	.081	.144	.178
Orleans	4224000-06G	Orleans	11	52	170	-34	.072	.066	.372
Orleans	4224000-01G	Orleans	9	49	175	-13	.003	.000	.109
Orleans	4224000-01Ga	Orleans	12	49	175	-46	.003	.000	.109
Orleans	4224000-02G	Orleans	11	48	174	-32	.140	.105	.178
Orleans	4224000-03G	Orleans	11	48	174	-38.9	.255	.264	.273
Orleans	4224000-08G	Orleans	12	45	173	-45.13	.000	.153	.191
Orleans	4224000-07G	Orleans	16	64	180	-80.13	.255	.344	.383
Yarmouth	4351000-21G	Yarmouth	12	101	37	-44.1	.199	.369	.369
Yarmouth	4351000-22G	Yarmouth	12	100	35	-46.7	.213	.435	.435